AD NUMBER
AD017397
CLASSIFICATION CHANGES
TO: unclassified
FROM: confidential
LIMITATION CHANGES
TO: Approved for public release, distribution unlimited
FROM: Distribution authorized to U.S. Gov't. agencies and their contractors; Administrative/Operational Use; 30 SEP 1953. Other requests shall be referred to Office of Naval Research, Arlington, VA.
AUTHORITY
ONR ltr, 1 Dec 1955; ONR ltr, 9 Nov 1977

CONFIDENTIAL

MECHANICAL ENGINEERING DEPARTMENT
INTERNAL FLOW RESEARCH
REPORT 1-13

HYDRODYNAMIC SPEED REDUCERS FOR SHIP DRIVE

Contract Nonr 24832
Office of Naval Research

Mechanical Engineering Department

Internal Flow Research

Report 1 - 13

HYDRODYNAMIC SPEED REDUCERS

For

SHIP DRIVE

Part A - The General Problem of Hydrodynamic Speed Reducers for Ships with Particular Attention to Increased Ratios of Transmission.

G. F. Wislicenus

Part B - Experimental Investigation and Theoretical Analysis of an Axial Flow Primary Stage for Hydrodynamic Speed Reducers.

W. G. Rose

Approved

George F. Wislicenus
Research Contract Director.

Performed under Contract Nonr 24832 with the Office of Naval Research.

ACKNOWLEDGMENT

The Investigators are indebted to the Undersea Warfare Branch of the Office of Naval Research for continued support and encouragement through many years. Particular recognition is due to Mr. Henry W. Boehly of that office who was connected with and sponsored the reported investigations through their entire duration.

TABLE OF CONTENTS

HYDRODYANMIC SPEED REDUCERS FOR SHIP DRIVE

Part A

THE GENERAL PROBLEM OF HYDRODYNAMIC SPEED REDUCERS FOR SHIPS WITH PARTICULAR ATTENTION TO INCREASED RATIOS OF TRANSMISSION

Part B

EXPERIMENTAL INVESTIGATION AND THEORETICAL ANALYSIS OF AN AXIAL FLOW PRIMARY STAGE

CHAPTER I

Objectives and Summary of Results of the Reported Investigation.

THE OBJECTIVE of the Investigation Reported here was to Establish the Essential Characteristics of Hydrodynamic Speed Reducers for Ships so as to serve as basis for a decision on the use of this type of speed reducer in place of mechanical or electrical reduction gears.

* * * *

In view of the known, successful application of hydrodynamic speed reducers or "Transformers" of the Foettinger type in the German Navy prior and during the first world war, the foregoing objective may be divided into two parts:

1. The establishment of the essential design characteristics of the original Foettinger Transformers; and

2. In view of the known limitations in Ratio of Speed Reduction of the original transformers (to about 5 to 1), the investigation of ways and means for increasing the ratio of speed reduction to values suitable for modern Naval applications. A tentative goal selected was a ratio of 15 to 1.

* * * *

THE GENERAL RESULT of the reported investigation is that Hydrodynamic Speed Reducers offer a practically useful way of speed reduction under conditions where mechanical reduction gears are found to be unsatisfactory. The Efficiencies of hydrodynamic speed reducers vary from about 90% at ratios of transmission of 5 to 1 or less to about 82 to 85% at ratios of transmission of 15 to 1 or more. (see Figure 1). The size and weight of hydrodynamic transmissions appear to compare rather favorably with all other types of power transmission,particularly at high powers and high ship speeds.

* * * *

SPECIFIC RESULTS may be summed-up as follows:

1. The Original Design of a Foettinger Transformer for a Ratio of Transmission of 4.6 to 1 has been reconstructed (Chapter III). It could be designed and built by a competently-staffed shipyard, or hydraulic turbine or pump builder . Its power-size-speed relation is given by equation (1) on page 15 . Its efficiency is represented by area "1" in Figure 1.

2. The Original Design could be used up to transmission ratios of about 7.5 to 1 by changing the primary runner only (Chapter V). Its efficiency is estimated to lie between 87% and 88.5% (see Area "2" in Figure 1). Its power-size-speed relation is also represented by equation (1) on page 15.

3. At Ratios of Transmission above 10 to 1 some definite departures from the design principles of the original Foettinger Transformers are necessary (Chapter IV).

4. A Separate Primary Pump (or pumps) and Secondary Turbine offers a definite possibility of achieving ratios of speed reduction of over 15 to 1 (Chapter VI). An efficiency of transmission of 83% appears possible (assuming 91% pump efficiency, 93% turbine efficiency, and 1.5 to 2% losses in the connecting pipe lines). The secondary turbine is very small as expressed by equation (12) on page 52, but the space and weight problems of the pipe connection with the primary pump(s) cannot be estimated without a complete layout of its overall arrangement. The separate primary and secondary elements offer the possibility of efficient cruising conditions with a reduced number of primary elements operating at full speed. This type of hydrodynamic transmission requires development and manufacturing facilities as are available primarily in the steam and gas turbine field.

5. By means of an Axial-Flow Primary Runner transmission ratios in the neighborhood of 15 to 1 are obtainable (chapter VII). The transition from the axial flow primary runner to the first stage secondary runner was investigated experimentally (Part B of this report) and was found to involve losses between 1 and 2 percent. Without compromising the design of the axial flow primary runner it appears that overall efficiencies of 83 to 85 percent appear possible (see Area "3" in Figure 1). The necessary secondary turbine design was analysed (Chapters IV and VII) and was found to be feasible. This type of transmission requires development and manufacturing facilities as found only in the steam and gas turbine field. The development of transformers of this type is believed to be comparable in magnitude to that of a new gas turbine unit for ship drive. The power-size-speed relationship for a transformer with axial-flow primary runner is given by equation (14) on page 64.

6. By using Counter-Rotating Secondary Elements it appears possible to meet the demands for greater ratios of speed reduction than currently available (Chapter VIII). This demand stems from the need of avoiding all cavitation at the external propelling mechanism, and is difficult to meet with mechanical reduction gears at maximum ship speed because of the resulting size of the reduction gears and accompanying problems.

7. For extraordinarily large powers (e.g. for short bursts of high power for large vessels) the hydrodynamic transmission may offer the only possible solution of speed reduction, considering that its power increases with the fifth power of its linear dimensions. The use of mercury in place of water (assumed here) will reduce the linear dimensions for the same power and speed by a factor of about 0.60, but probably without any substantial saving in weight.

8. The obtainable efficiencies of transmission as a function of the ratio of speed reduction are summarized in Figure 1. It is seen that recent developments of hydrodynamic "Torque Converters" exemplified by the Lysholm-Smith Converter fall in efficiency below the curve of probable values given in that diagram. This is believed to be due to the different intended use of these more recent Converters for variable speed ratios, and to the smaller dimensions of these torque converters. This indicates that present day torque converter developments are not applicable to ship drive without considerable modification and development.

Also slightly below the estimated average curve falls the efficiency of two Foettinger transformers in series. Here attention is called to the interesting possibility of using one transformer of moderate transmission ratio (say 7 to 1) between the low-pressure steam turbine and the propeller shaft, and another (small) transformer between the low-pressure and the high-pressure steam turbines. The latter transmits of course only the power of the high-pressure turbine so that its losses apply to only about half of the total power transmitted. The overall efficiency of transmission may in this case be equivalent to about 84% with attractive (high) speeds available for the high-pressure turbine.

CONFIDENTIAL

1. The Original Foettinger Transformers (Chapt.III)
2. Foettinger Transformer with Primary Radial Flow Runner of Increase Specific Speed (Chapt. V)
3. Transformer with Axial-Flow Primary Runner (Chapt. VII)

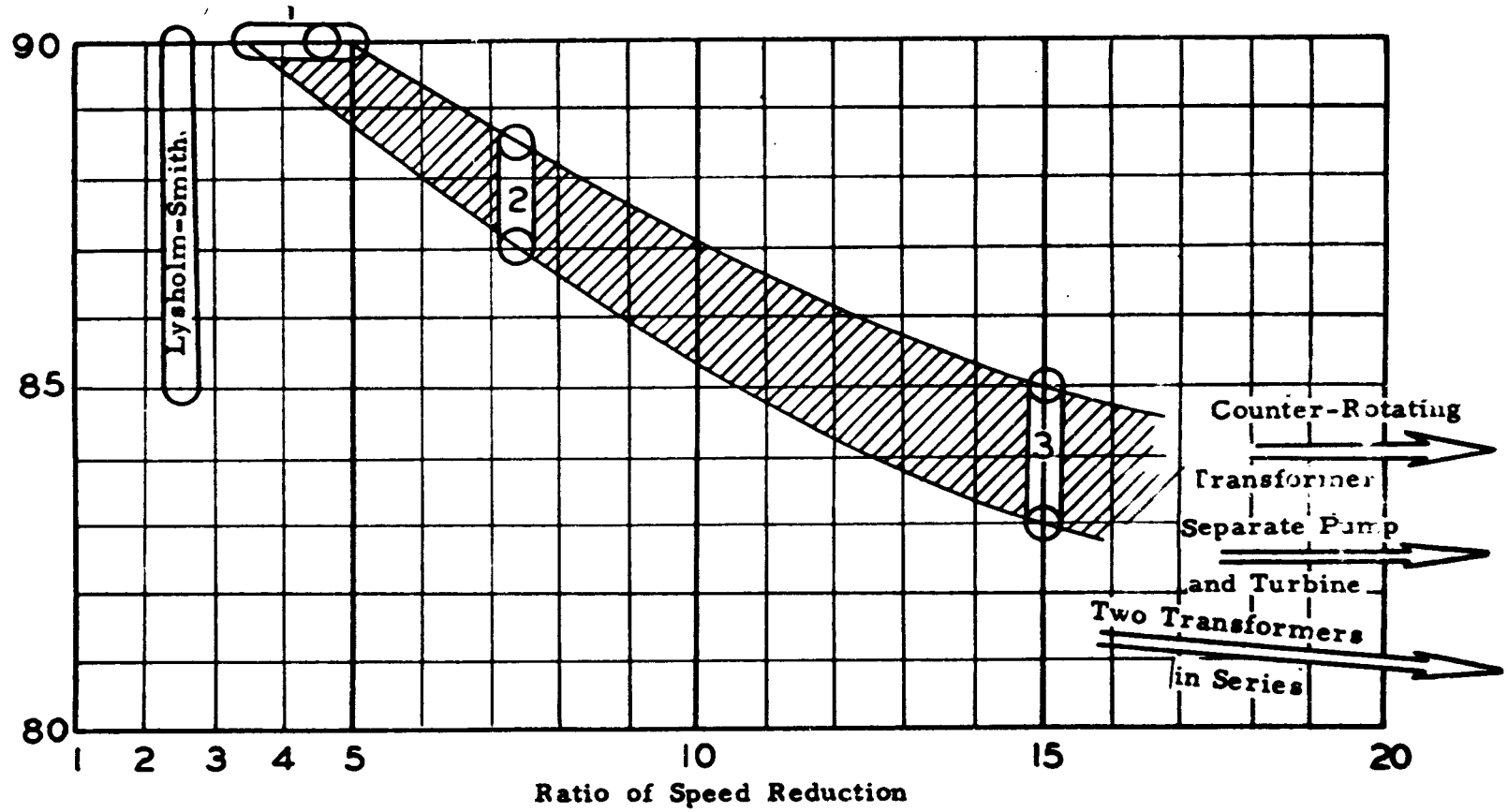

Efficiency of Hydrodynamic Speed Reducers versus Ratio of Speed Reduction

CHAPTER II

INTRODUCTION

This Chapter attempts to describe briefly the principles of the "Foettinger transformers" for ship drive and to evaluate these principles in the light of more recent developments of hydraulic torque converters and of the requirements of modern ship propulsion. It is hoped to clarify in this manner the scope and principle objectives of the present investigation.

A "Foettinger transformer" is a hydrodynamic transmission in which a "primary" pump impeller supplies a combination of "secondary" turbine vane systems with a stream of water (or light oil). Both the primary pump runner and the secondary turbine systems are located in one and the same casing and in close proximity to each other (see Figure 2, showing the forward operation and the reverse operation circuits of a transformer in section).

The original development of Foettinger transformers was prompted by the need of operating the propeller shafts of ships at a substantially lower speed than that of steam turbines for ship drive. It appears that prior and during the First World War the German Navy was not in possession of adequate designs for mechanical reduction gears. Under these conditions the Foettinger transformer offered an attractive solution for this problem at the moderate speeds of early steam turbines.

As mentioned in the summary, hydraulic speed reducers of the Foettinger type achieved efficiencies in the vicinity of 90% at ratios of speed reduction between 4 and 5 to 1. This was rather remarkable, particularly at a time when hydraulic turbines had barely reached 90% efficiency, whereas centrifugal pumps were commonly used with efficiencies in the vicinity of 80%. The principal method by which this efficiency was achieved consisted of utilizing the fluid velocities at the discharge of the primary or pump runner directly as the entrance velocities to the first stage of the secondary (i.e., turbine) element. Thereby the flow losses in the stationary parts of a centrifugal pump and in most of the stationary parts of the turbine were eliminated. It should be clear from this description that the relationship between the primary pump runner and the first secondary turbine runner, in particular with regard to their respective discharge and inlet velocities, is a controlling element in the design and the early success of Foettinger transformers.

Since 1920 Foettinger transformers have no longer been used as reduction gears for ships, principally because of the development of successful mechanical reduction gears with higher efficiencies and, in particular, with higher ratios of speed reduction than obtainable with the

Foettinger principles of design. On the other hand it was recognized that hydraulic speed reducers can be used successfully to change the unfavorable torque speed characteristics of certain prime-movers, particularly internal combustion engines, to the more favorable torque speed characteristics of a turbine, which is the secondary part of the hydraulic transmission. As a consequence, most developments in the field of hydraulic speed reducers or "torque converters" that took place since 1920 were not so much concerned with maximum overall efficiency at one particular ratio of transmission as with the problem of obtaining reasonably high efficiencies over a range of transmission ratios. This leads to the achievement of a high torque increase as a consequence of a reduction in the secondary speed corresponding to an increased load on the secondary or power output element of the transformer. One of the most successful general developments along these lines is probably that known under the name Lysholm-Smith which is produced in this country by the Twin-Disc Corporation and others. The available designs of this type have their maximum efficiency at speed reduction ratios between 2 and 3 to 1 and the largest units readily available today fall in the general range of 1,000 h.p. at primary speeds commonly used for stationary internal combustion engines of that power. It is, therefore, clear that the use of this type of hydraulic speed reducers for ships would require appreciable development. Nevertheless, this line of approach should be seriously considered as one in which industrial experience is now available in this country. The Lysholm-Smith type of converter will not be further considered in this report only because design information on this type of speed reducer is available and, therefore, does not need to be introduced here.

Whereas modern developments of hydraulic torque converters serve primarily a different objective than is essential for the application to ship drive, it is equally clear that the early ship transformers of the Foettinger type cannot either be used directly for this purpose, primarily because their ratio of transmission is completely insufficient when used in connection with modern steam turbines. The lowest ratios of transmission that appear to have any useful application for ship drive by means of steam or gas turbines seem to lie between 12 to 1 and 15 to 1, with higher ratios of speed reduction being definitely desirable. It has, therefore, been the principal objective of the present investigation to find whether speed reduction ratios of not less than 12 to 1 are obtainable with hydrodynamic speed reducers and, in particular, whether such reduction ratios seem possible without undue sacrifices in efficiency.

If one were to return to the most basic elements of a hydrodynamic transmission, namely a centrifugal pump and a separate hydraulic turbine, connected with the former only by two pipelines, there would be no reason for limiting the ratio of transmission since the speed of the turbine for given hydrodynamic conditions could be arbitrarily reduced by employing a large number of turbine stages in series. This arrangement will indeed be considered below as a possible and perhaps a practical one. However, the efficiency of this type of an arrangement is

necessarily that of the product of the best possible pump and turbine efficiency which lies today, if we allow for hydrodynamic flow losses between the two units, only slightly above 80%. This figure demands pump as well as turbine efficiencies in the neighborhood of 91% or 92% which are obtainable today but are not likely to be exceeded substantially in the foreseeable future.

Besides the efficiency problem just mentioned, the separate units for the primary and secondary elements of the hydraulic speed reducer necessarily involve more space and weight than a unit that combines the secondary and primary element into one compact arrangement, as is characteristic for the original Foettinger transformers. Since this hydrodynamic combination was also the key for the high efficiencies obtained with the early Foettinger transformers, it is natural to maintain this feature for a new development contemplated at this time.

As mentioned before the combination of the primary and secondary elements into one closely connected unit makes the discharge velocity configuration of the primary element directly responsible for the inlet velocity conditions to the first stage of the secondary or turbine runner. It becomes immediately evident that a great difference in the rotational speed between the primary and the secondary runner introduces here a problem inherent in this closely coupled arrangement; meaning that for essentially the same fluid velocities the peripheral velocities of hydrodynamic runners cannot be varied arbitrarily without encountering conditions that may be quite detrimental to the efficiency of the machine concerned. Therefore, the problem of increasing the difference in speed between the primary and secondary runner without spoiling the hydrodynamic connection between these elements constitutes the principal consideration for the development of Foettinger type speed reducers with increased ratios of transmission.

The following report will attempt to solve this problem by establishing first on the basis of an actual design the hydrodynamic features and characteristics of the original Foettinger transformers that served so well at transmission ratios in the neighborhood of 4 or 5 to 1. The design of this type of transformer will be presented in sufficient detail to permit the construction of such a machine in the case transmission ratios in the range mentioned would be desirable. More important is to firmly establish the early Foettinger designs as basis for further developments in this field, as it must be admitted that these early designs represent in this field an achievement not surpassed and hardly reached in present days.

Following the establishment of this background the problem of increased speed reduction ratio will be examined in a general manner but yet in sufficient detail to permit an intelligent choice between the various lines of procedure that appear to be open.

Amongst these lines of procedure particular attention will then be focused on the use of a primary or pump element of the highest speed possible under given operating conditions. Such a pump runner is known to be necessarily of the axial-flow type. Considering that axial-flow machinery has received extraordinary attention in recent years due to the need of efficient axial-flow compressors for gas turbines, it is to be expected that these advancements can be used effectively, and on the basis of presently available engineering talent and know-how, to advance the art of hydraulic speed reducer design. For this reason, an experimental investigation was initiated to examine some basic problems involved in the application of axial-flow runners as primary elements for hydraulic speed reducers. The results of this experimental investigation and their theoretical analysis are presented in detail in Part B of this report. In Part A these results will be used to examine the hydrodynamic design characteristics of an entire speed reducing unit employing this type of a primary element. It was found, and will be shown here, that a compact hydrodynamic speed reducer with an axial-flow primary runner can be designed to achieve a ratio of transmission of 15 to 1 at an overall efficiency estimated to be not less than 83%. The success of this development will be contingent on the availability of adequate engineering talent for this development, and on a realistic appreciation of its magnitude.

Besides investigating the extreme case of an axial-flow primary stage, the question was considered as to how far the ratio of speed reduction could be increased without departing from the principle of accelerated relative flow in the primary runner. Adherence to this principle makes it necessary to maintain a radial flow impeller for this part of the transformer. It was found under these conditions the "specific speed" of the primary runner could be increased by a factor of approximately 1.6 as compared with the primary runner of the original Foettinger transformer discussed. In this fashion, the ratio of speed reduction is increased to a value slightly above 7 to 1. A design for a primary element of these characteristics is presented in Chapter V.

Consideration was also given to a multi-stage axial flow turbine as secondary element supplied by one or more separate centrifugal pumps driven by the prime mover(s). No detailed design studies were made beyond a numerical evaluation of the probable size and weight of such a unit in comparison with other types of hydrodynamic speed reducers. It was found that weight and size would be comparable between this and other types to the extent that the flexibility of arrangement inherent in separate pumps and turbines may in some cases outweigh any slight disadvantage in weight and size. Of particular interest appears to be the possibility of changing the number of primary elements between full speed and part load (cruising) operation in such a manner that the cruising steam turbine unit can operate at all times at full speed and, therefore, at maximum efficiency.

Connected with the development of hydrodynamic speed reducers for ships are of course other problems, such as the problem of reversing, the advantages that may be derived from using counter-rotating secondary elements in connection with counter-rotating propellers or jet pump runners, the problem of cooling the working fluid, and the like. Important as these problems are, they will be only briefly outlined in this report since it was deemed necessary to focus greater attention on the PRINCIPLES involved in achieving the goal set forth for this investigation, i.e., the achievement of increased ratios of speed reduction by means of hydrodynamic transformers of minimum size and the best possible overall efficiency for the speed reduction elected.

Forward Operation Circuit

2335 mm Profile Diameter
600 mm Profile Width (Axial)

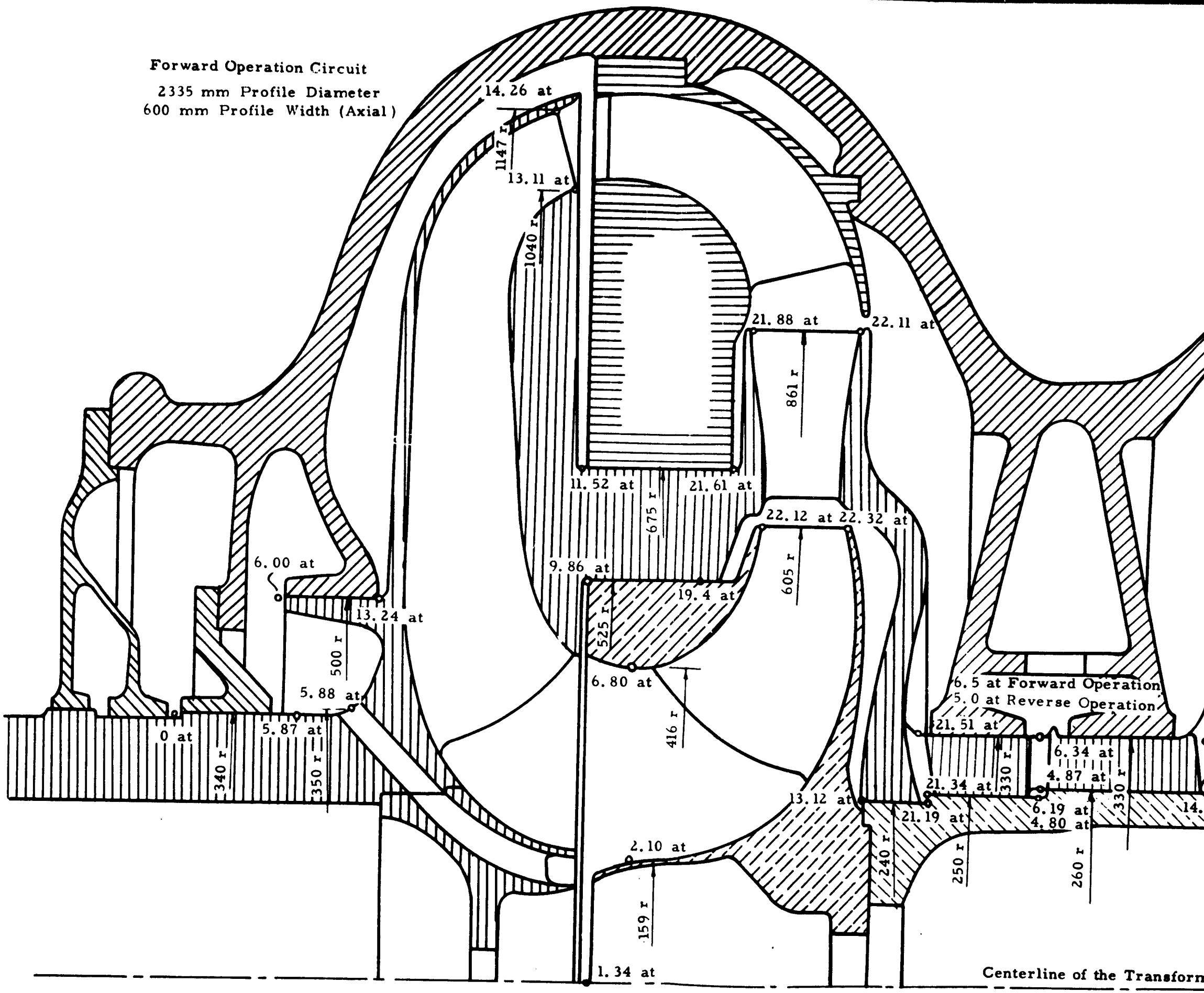

Foettinger Transformer for a Ratio of Speed Reduction of 4.6 to 1

Reverse Operation Circuit

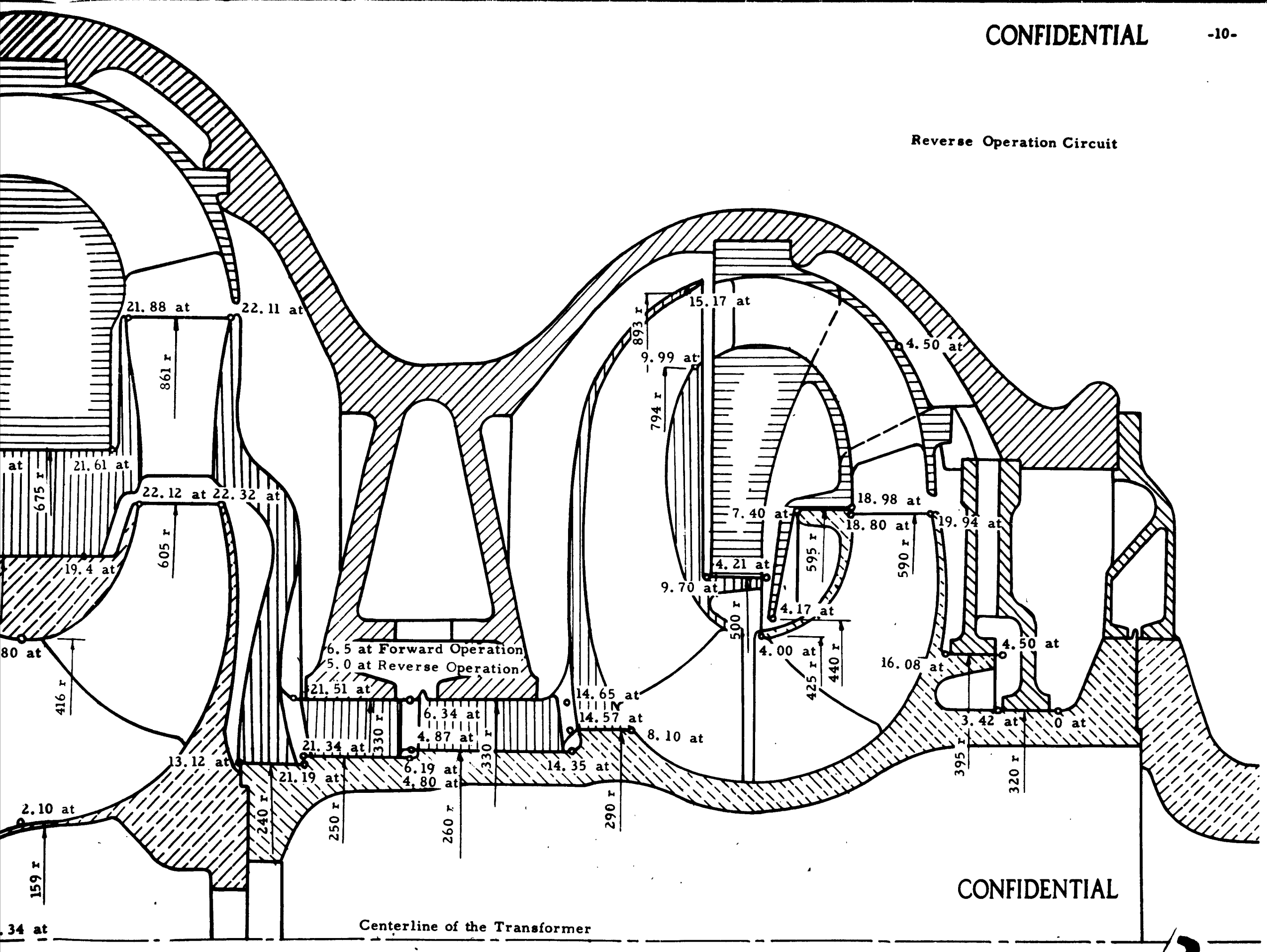

CONFIDENTIAL

Foettinger Transformer for a Ratio of Speed Reduction of 4.6 to 1

Figure 2

12

CHAPTER III

THE DESIGN OF A FOETTINGER TRANSFORMER WITH THE SPEED REDUCTION RATIO OF 4.6 TO 1

The design of a Foettinger transformer presented in this Chapter has been developed primarily on the basis of data received from Dr. Wilhelm Spannhake. Dr. Spannhake was chief engineer of transformer developments at the Vulcan Works in Germany at the time the development of this type of hydrodynamic reduction was at its height. The design considered here was one of the latest of this period of development.

Dr. Spannhake was anxious to make it clear that the design on which he furnished us with all available data should not be regarded today as an optimum for the operating conditions selected. In particular, Dr. Spannhake felt that the through-flow velocities (meridional velocities) should perhaps be increased in relation to the peripheral components of the fluid velocities in order to obtain more gradually curved vanes and perhaps a smaller profile diameter of the entire unit. Nevertheless, it was felt that before such changes could be considered the original design should be re-established to the best of our ability since it did represent the result of competent and extensive work in this field over a fair number of years.

A radial or "meridional" section through the transformer is shown in Figure 2, with details of construction left somewhat diagrammatic. The dimensions given are in millimeters. After careful consideration it was concluded that for forward operation (i.e., when operating with the left part of the transformer shown in Figure 2), this transformer transmitted 20,800 h.p. at a primary speed of 1200 rpm.

Besides the general design principle of Foettinger transformers mentioned before, namely that the primary (pump) runner discharges directly in the first stage of the secondary (turbine) runner, the design presented here and indeed most Foettinger transformers developed in these days incorporated the following important design principles:

a. The flow relative to any of the vane systems in the transformer (circuit for forward operation) is accelerated. The reason for this design principle must still be regarded as valid. The design principle of accelerated relative fluid motions was carried out, wherever possible, to include details of the flow as produced by either the curvature of the enclosing shroud walls, or by the effect of pressure differences across the vanes. Obviously, the last requirement could not be satisfied in all details but the departures from this principle (accelerated fluid motions) were probably quite small in all parts of the transformer. The bulk of the fluid motions was indeed rather strongly accelerated.

b. The meridional fluid motions were derived by assuming a potential flow for this component. For the design study presented here the potential flow was rather accurately evaluated for the inlet to the primary runner and the velocity diagrams at the inlet to the primary runner vanes were derived on that basis. In other parts of the transformer the effect of the curvature of the meridional flow was only approximated but it is believed that the velocity diagrams and resulting vane shapes come rather close to those intended by the original designers.

c. The flow-energy losses in the various parts of the transformer were regarded as proportional to the square of the velocities relative to the vane systems considered. This necessarily involves an attempt to minimize all relative velocities for given operating conditions.

Figure 3 shows the best possible estimate of the velocity vector diagrams pertaining to various points in the transformer. The subscripts given with the velocities correspond to the points marked in the profile shown in Figure 4. In Figure 3 the various velocity vector diagrams are located relative to each other in such a manner that the peripheral runner velocities (U) are placed at a distance from the "center line" which is proportional to their true distance from the center line in the actual machine. Thereby the ends of all peripheral velocities (U) fall on two straight lines, one for all peripheral velocities of either of the two secondary runners. The velocity diagrams were verified by comparison with the pressure values given in the cross-section of the transformer shown in Fig. 2. (measured in atmospheres).

In the following the various elements of this particular transformer will be discussed in some detail beginning with the primary runner. The consideration will be limited to the circuit for foreward operations as its design characteristics are obviously the most significant for future developments.

* * * *

THE VELOCITY VECTOR DIAGRAMS OF THE PRIMARY RUNNER are shown in Figure 5 for its discharge diameter and for three points along the inlet edges of the runner vanes. For the discharge velocity diagram it is of interest to note that, considering the peripheral velocity of the runner itself as unity, the average radial (meridional) velocity is 0.255, and the peripheral component of the absolute fluid velocity leaving the primary runner is 0.47.

It will be seen that the fluid enters the primary runner with a considerable rotational component in the direction of the primary runner motion. This inlet flow follows the law of a free, i.e. potential vortex, its peripheral component being therefore inversely proportional to the distance from the axis of rotation. The meridional component of the flow entering the runner was assumed to satisfy a potential flow distribution as mentioned before. CONFIDENTIAL

It will be noticed that the relative velocity w_1 at the maximum diameter of the inlet edge of the runner vane is not larger than the relative velocity w_5 at the discharge of the primary runner, whereas all other relative velocities at the inlet of the runner are decidedly smaller than that at its discharge. The principle of accelerated relative flow is therefore maintained even throughout the primary runner where it is obviously most difficult to satisfy this condition. It will be noticed that the positive rotation of the absolute flow at the inlet to the primary runner contributes strongly towards meeting this condition.

The relative velocity w_5^* is a ficticious relative velocity that would exist if the flow were following the direction of the discharge edges of the vane exactly, whereas w_5 is the true relative velocity at that diameter.

From the velocity vector diagram shown in Figure 5, one can derive the vane shape by drawing, according to Prasil, a CONFORMAL representation of the vane shape as appearing in surfaces of revolution following the direction of the meridional flow through the runner. In Figure 6 the conformal representation of the lower side of the primary runner vane is shown for the two shroud surfaces and one meridional stream surface between the outer and the inner shroud. In passing, it may be mentioned that this conformal representation is characterized by maintaining, as the name implies, all angles between lines drawn on the true surfaces of revolution and on the plane on which the representation is drawn. The points 1, 2, 3, etc., shown on the two shrouds in the meridional section through the impeller, Figure 7, mark concentric circles drawn on these shrouds and the intermediate stream surface. These circles are transformed into the horizontal lines of equal numbers in the conformal mapping shown in Figure 6. The vertical lines in Figure 6 are marked by angles, and correspond to the intersection of the shroud surfaces and the intermediate stream surface with radial planes drawn under the angles given. The distances between the circles, 1, 2, 3, etc., are chosen so that the fields formed by two successive circles and two successive sections with radial planes have, in the mean, equal dimensions in peripheral and radial directions. The corresponding net work in the conformal plane is obviously a network of squares, serving to transform the lines drawn in the conformal plane on to the surfaces in space.

From the conformal mapping, it is possible to locate points of the vane surface falling into radial planes, thereby obtaining radial sections through the vane surface. For the lower surface of the vane, these sections are shown in Figure 7 (shaded on one side) which are marked by the angle by which this section is displaced from the location of the discharge edge of the vane. By choosing a suitable vane thickness it is obviously possible to determine in this fashion the entire vane surface and therefrom derive all necessary information for its construction. The method used here is described in some detail in the last chapter of Reference 3.

An end view of the lower surface of the vane so derived is shown in Figure 8. The vane shape derived here is believed to be compatible with twelve runner vanes although the number of these vanes cannot be exactly derived from the information available.

* * * *

The small VANELESS SPACE between the primary runner discharge and the first stage secondary runner inlet is proportioned in such a fashion that the meridional velocity component remains constant whereas the peripheral component of the absolute fluid velocity obviously diminishes according to the law of constant angular momentum. Investigations at this University that will be described in Chapter VII and Part B have served to confirm the soundness of this old design principle and to extend its validity.

* * * *

THE FIRST STAGE OF THE SECONDARY RUNNER is shown in Figure 9. To the right of the vane section is shown an estimate of the velocity distributions on the high pressure and on the low pressure sides of these vanes, indicating that even on the low pressure side the regions of retarded relative fluid motion are probably quite small.

The vane shape was derived by assuming the relationship between the peripheral component (V_u) of the absolute flow and the distance from the axis of rotation which is shown by a thin, broken line in Figure 9. Obviously the rate of change of this component (in connection with the distance from the axis) marks the change in angular momentum and thereby establishes a measur for the local blade loading or pressure difference between the two sides of the blades. Using the cross section between the vanes to determine the average local velocity between two successive vanes, and a potential velocity distribution between two successive vanes to determine the relation between the mean, the maximum, and the minimum velocity in one cross section between the vanes, it is possible to arrive at a reasonably consistent picture of the velocity characteristics for the vane shape selected.

* * * *

THE DESIGN OF THE STATIONARY VANE SYSTEM between the first stage and the second stage of the secondary runner again involves curvature of the meridional stream as well as changes in the peripheral component of the flow as did the design of the primary runner. Therefore, one again uses the method of conformal mapping as described there. In Figure 10 the circles drawn on the inner and outer shroud surfaces of the stationary vane system are marked with numbers from zero to seven. These circles are transformed into the horizontal straight lines marked by the same numbers in the conformal representation shown in Figures 11 and 12. These circles are spaced so as to go together with radial sections drawn at three degree intervals.

THE SECOND STAGE OF THE SECONDARY RUNNER is also shown as a meridional section in Figure 10 and is again treated by the method of conformal mapping as shown in Figure 13. However this time the conformal plane uses a network of radial lines and concentric circles because this form of representation comes far closer to the predominantly radial arrangement of this runner than would be a representation in a plane with rectangular coordinates as used before. The discharge velocity diagrams of this runner are not shown in Figure 3 because they would be likely to interfere with those for the inlet of the primary runner in that illustration. However it is obvious that the discharge has to be foreward in the direction of the runner motion in order to produce the positive prerotation, that was previously described as essential for giving the desired velocity distribution at the inlet to the primary runner.

It is apparent that the vanes of the second stage of the secondary runner come very close to being plane radial vanes as used commonly in hydraulic couplings. Nevertheless there is conclusive evidence that departures from the plane radial shape were actually used in the original Foettinger designs .

There is no clear evidence as to the number of vanes used in this radial flow turbine stage. However it appears that the circumferential spacing of the vanes at their tips was somewhat greater than the width of the passage as shown in the same region of the meridional section in Figure 10. This would lead one to believe that the number of vanes in the second stage of the secondary runner was intended to be somewhere between 35 to 40 giving a lift coefficient of the vanes somewhere in the neighborhood of unity.

* * * *

THE SIZE OF THE FOETTINGER TRANSFORMER just described is given in Figure 2 for a power input of 20,800 h.p. at a primary speed of 1200 rpm and a secondary speed of 260 rpm. The outside diameter of this unit appears to be approximately 2560 millimetres or 8.40 ft. On that basis one can immediately write down the following equation for the power of a transformer of this type based merely on the fact that this power changes with the fifth power of the linear dimensions and the third power of the speed of rotation, assuming that all proportions of the machine remain similar and all velocities are changed proportionally to each other:

$$HP = 2.80 \times 10^{-8} \times D_o^5 \times n_{II}^3 \qquad (1)$$

In this equation D_o it is the outside diameter of the casing in ft., n_{II} the secondary speed in rpm, and HP the (primary) horse-power. This as well as similar relations for other transformers given in this report are based on WATER as working fluid.

Subsequently we shall derive similar expressions for the sizes of other torque converters and by their constants shall be able to compare various types of transformers regarding their size for equal operating conditions. It should be noted that the suggested relation contains the secondary speed as being most likely decisive for the outside diameter of the transformer.

* * * *

For the REVERSE OPERATION CIRCUIT the velocity diamgrams are shown in figure 14. From these diagrams the vane shapes of the respective vane systems can readily be developed by methods similar to those previously described. However the quality of these vanes is not nearly as important due to the lesser importance of efficiency for reverse operation. For the same reason the proportions of the reversing circuit have been chosen considerably smaller than those of the circuit for foreward operation and in the design shown in Figure 2 the reversing circuit has only one stationary and one secondary runner vane system. It is of interest to observe that older transformers than the one shown in that illustration were designed with two-stage secondary runners for the reversing circuit which apparently was later found to be unnecessary.

It is of course known that reversing was accomplished by emptying the foreward operation circuit and filling the reverse operation circuit. During either form of operation water was constantly bled from the transformer and returned to the operating circuit by means of an external pump in order to remove the heat developed in the operating circuit due to its flow losses. It has been reported that this cooling circuit was used as a preheating stage for the condensate before returning same to the feed pumps of the main boilers, thereby recovering a small percentage of the hydrodynamic losses of the transformer. It is claimed however that the efficiencies quoted before had been obtained without taking account of this recovery, nor charging, on the other hand, the power needed for the transformer circulating pump against its power consumption. In any practical application the auxiliary circuits and pumps as well as details of the mechanical arrangement would of course be of considerable importance. It is however not the intent of the present study to describe these mechanical details or auxiliaries in detail.

* * * *

Figure 15 shows a pictorial view of the lower half of the transformer casing with its rotor suspended above it. The casing shows the inlets and discharge openings to and from the transformers circuits, specifically:

a. The inlet into the reverse operation circuit;

b. The discharge from the reverse operating circuit;

c. The discharge from the foreward operation circuit;

d. The inlet to the foreward operation circuit, which passes through the secondary shaft seals.

The rotor suspended above the casing shows the foreward circuit parts to the right and the reverse circuit parts to the left. Visible are particularly the (axial) inlet openings to the last (radial) stage of the secondary runner, and the radial discharge from the first stage of the secondary runner of the foreward operation circuit.

* * * *

THE DESIGN DRAWINGS presented in this chapter are neither sufficiently accurate nor sufficiently complete to serve directly as vane layouts for the four principal vane systems of this transformer. In other words, it will be necessary to reconstruct and complete the designs of these elements on the basis of the velocity diagrams and other considerations presented in this chapter in order to obtain the precision and reliability necessary for the construction of such a unit. On the other hand, it is believed that the vane layouts presented here will serve as guides for the final design work, and are believed to be sufficiently accurate to represent the intentions and principles of the original design.

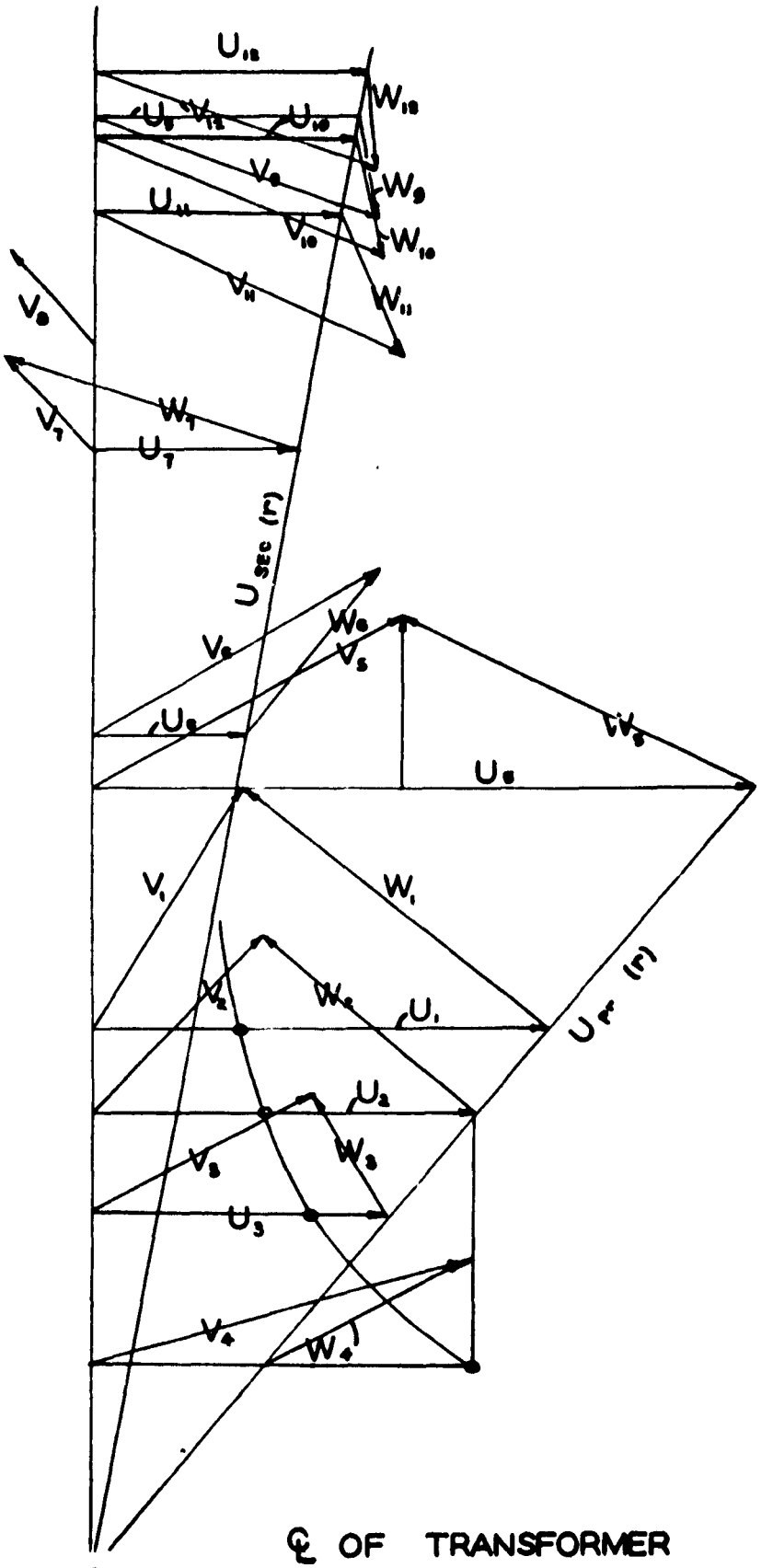

Velocity Vector Diagrams for Transformer with Ratio of Speed Reduction of 4.6 to 1

Figure 3 CONFIDENTIAL

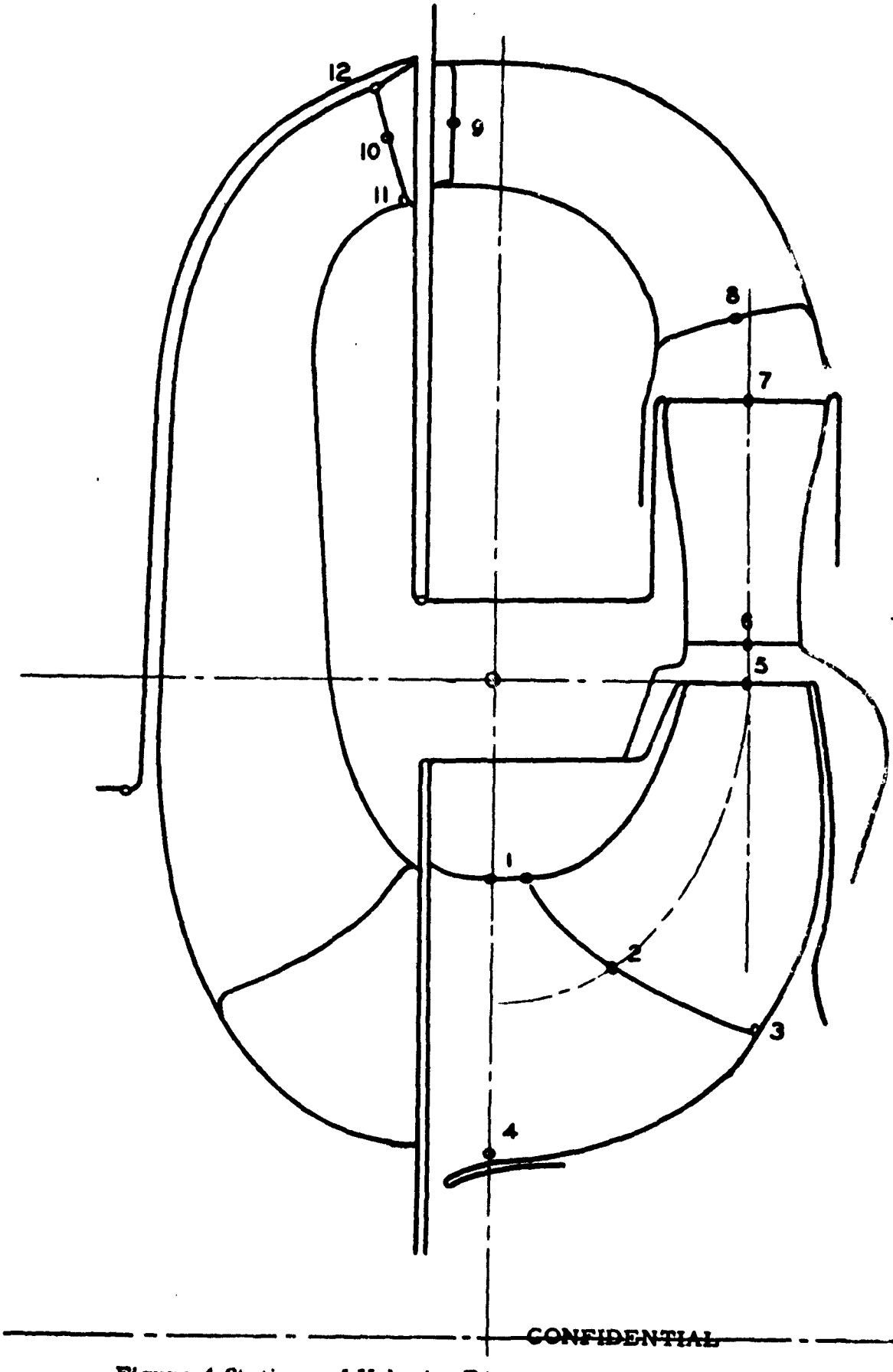

Figure 4 Stations of Velocity Diagrams in the Transformer

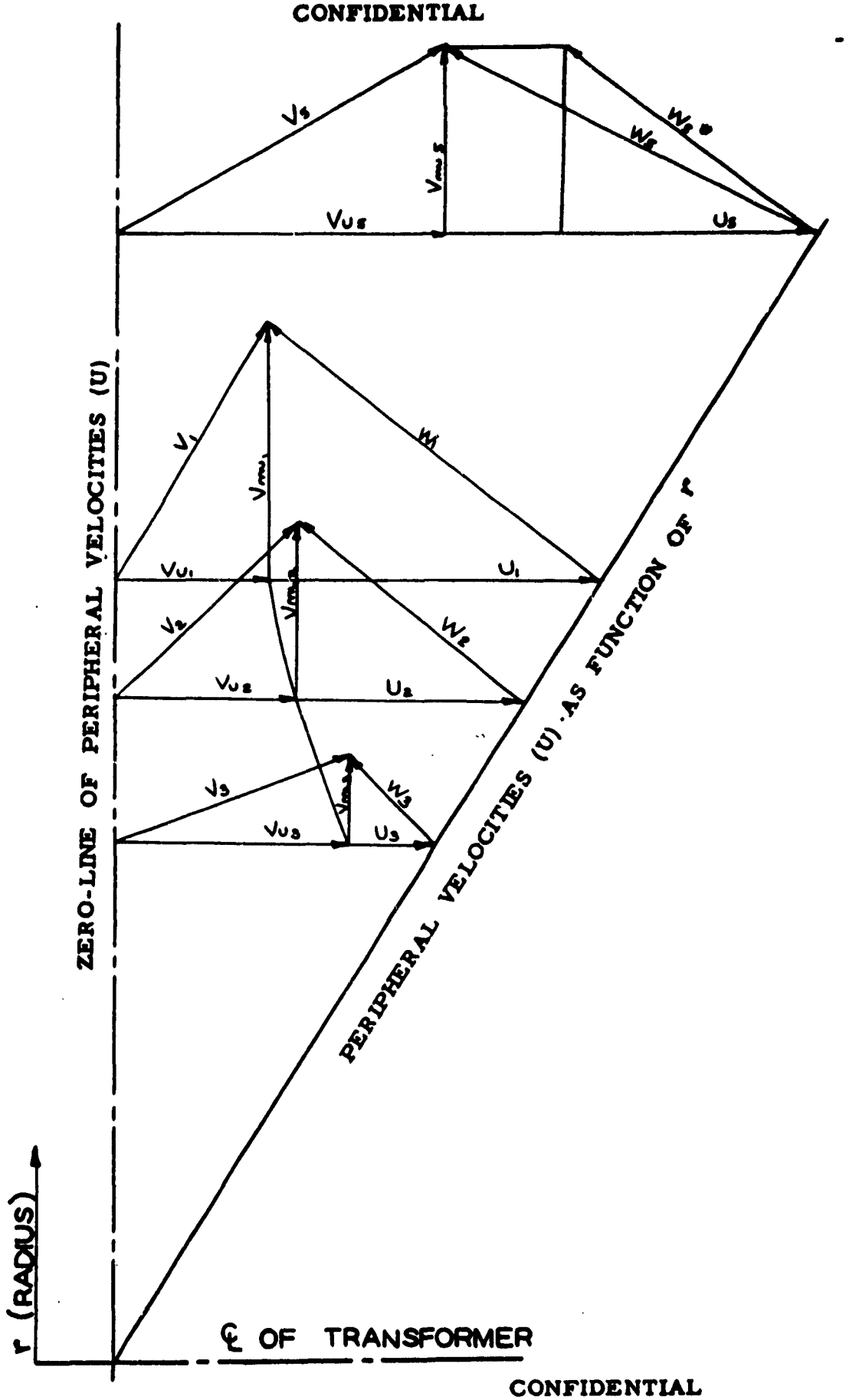

FIGURE 5

Velocity Diagrams of Primary Runner for a Speed Reduction Ratio of 4.6 to 1

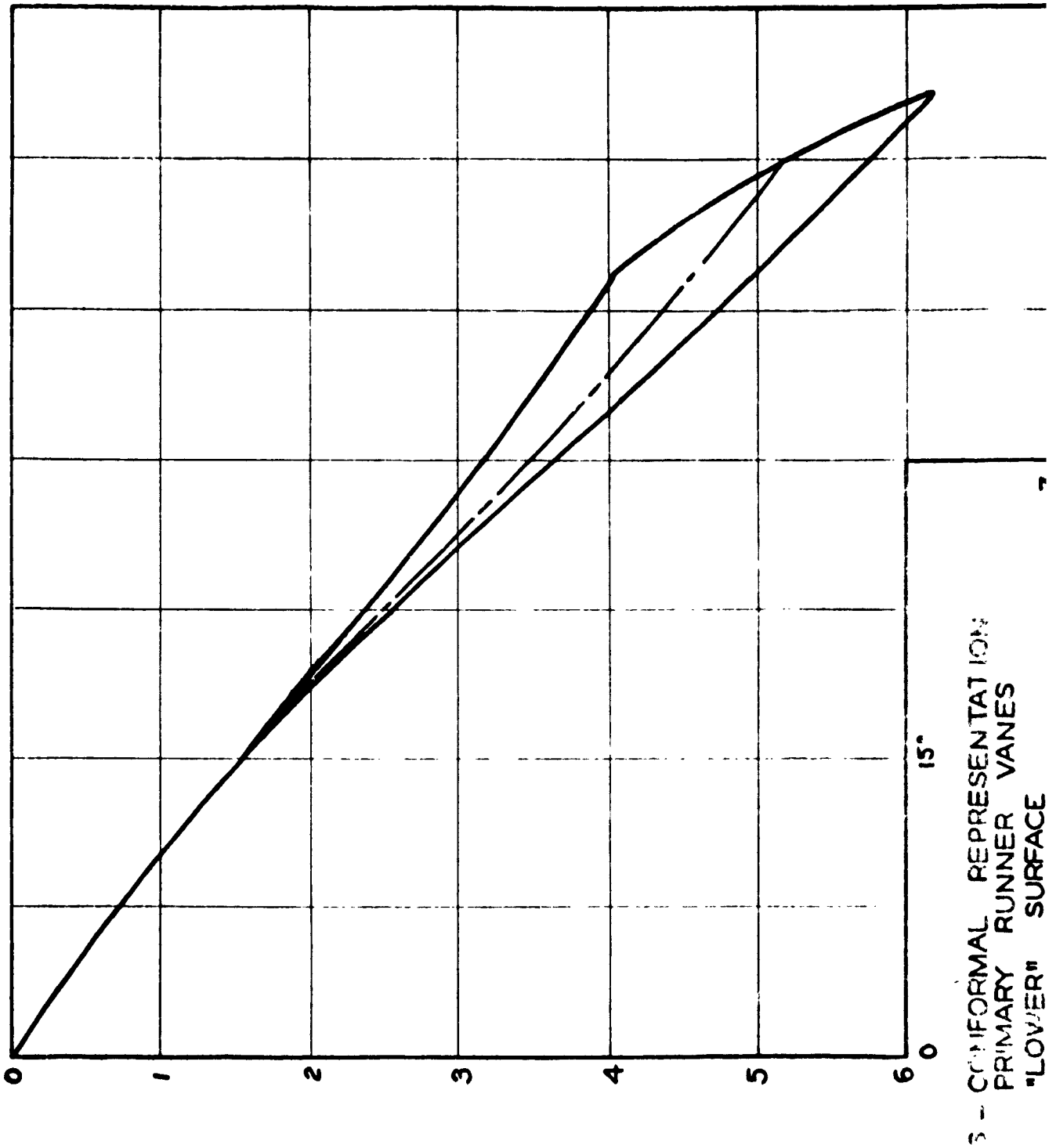

FIGURE 3 – CONFORMAL REPRESENTATION
PRIMARY RUNNER VANES
"LOWER" SURFACE

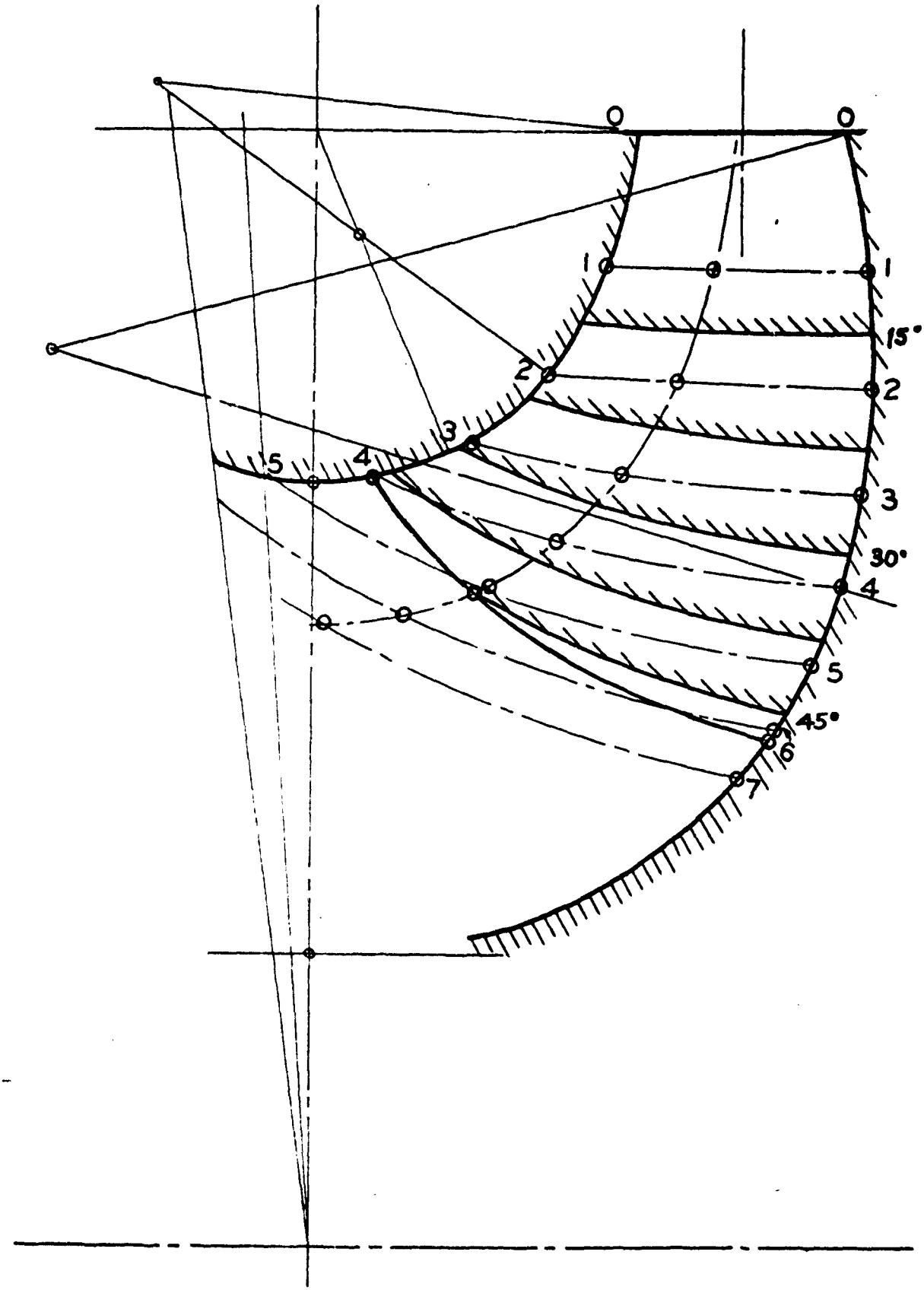

FIGURE 7 CONFIDENTIAL

Meridional Section of Primary Runner

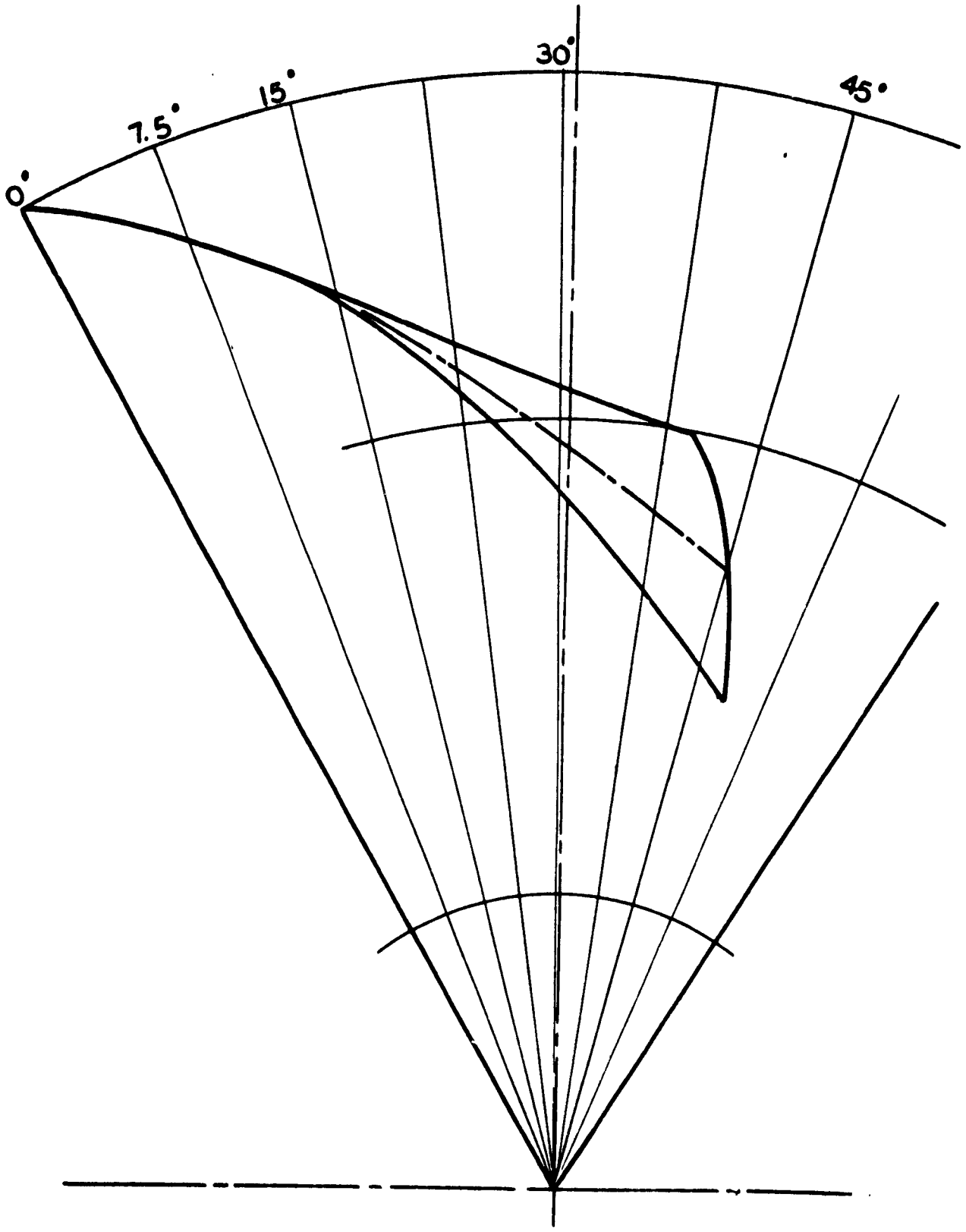

Lower Vane Surface of Primary Runner

FIGURE 8

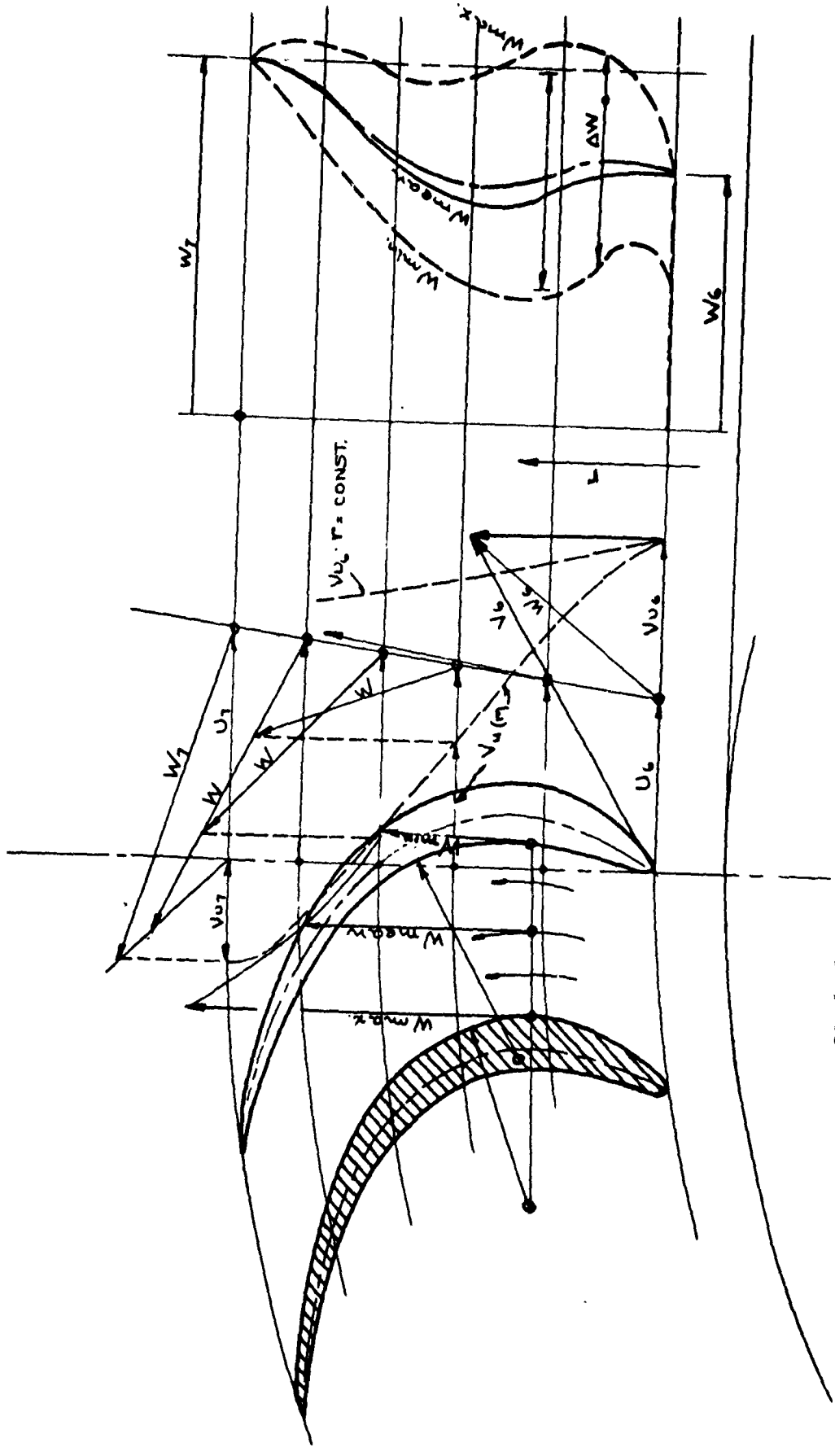

Blade Layout First Stage of the Secondary Runner

FIGURE 9

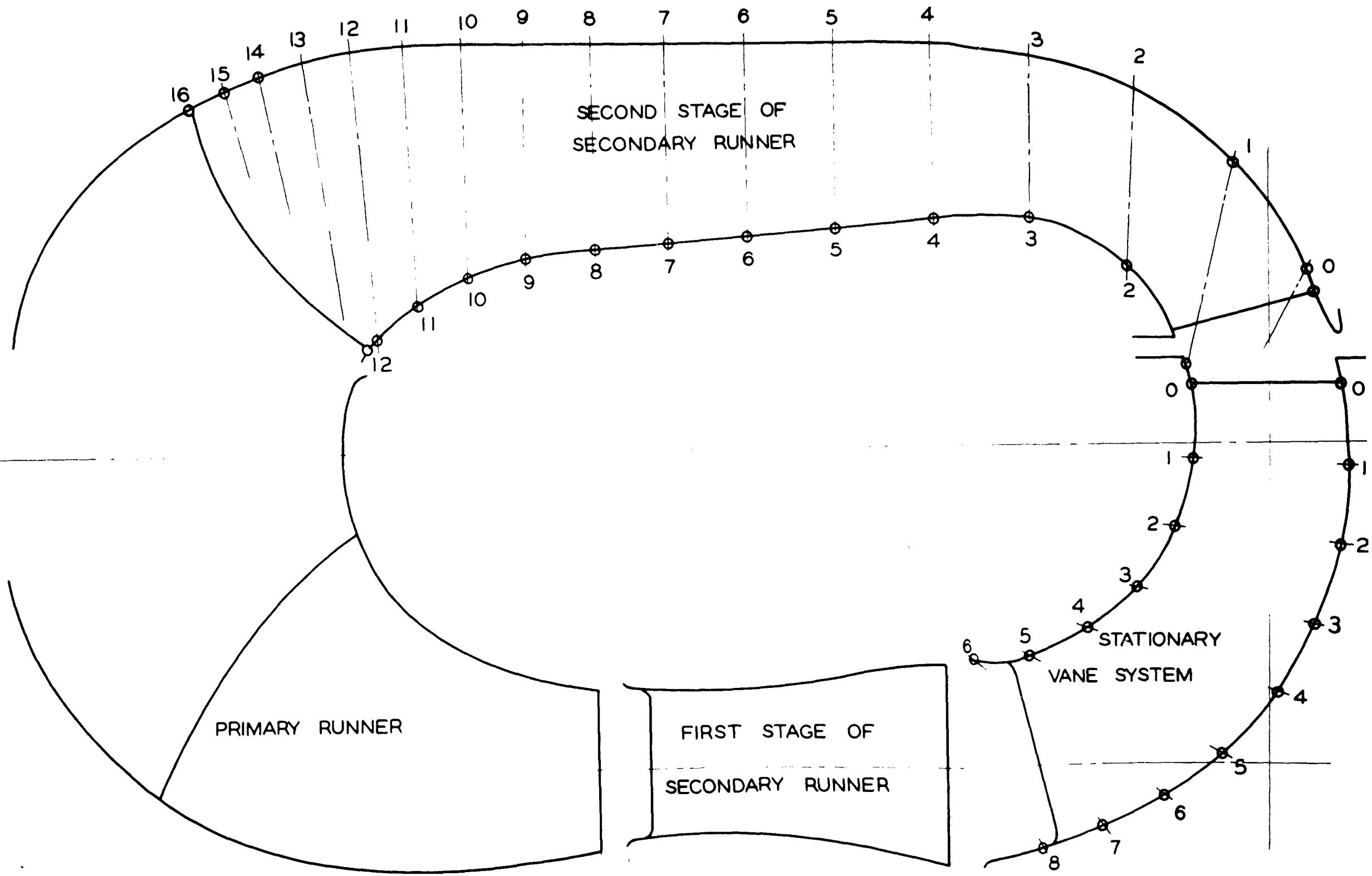

Figure 10

Stationary Vane Systems and Second Stage of Secondary Runner

Vane Layout

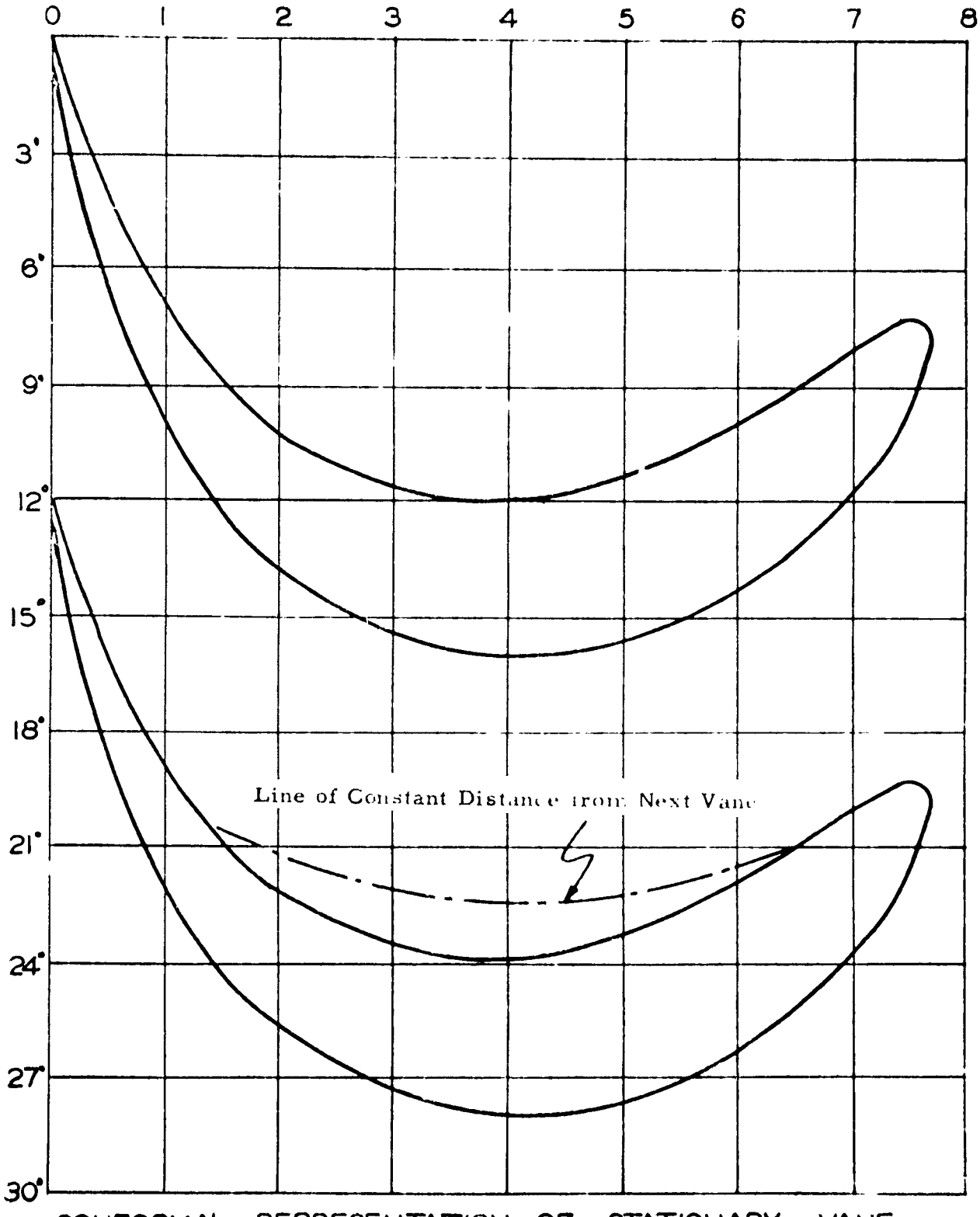

CONFORMAL REPRESENTATION OF STATIONARY VANE SYSTEM — OUTER SHROUD INTERSECTION

FIGURE 11

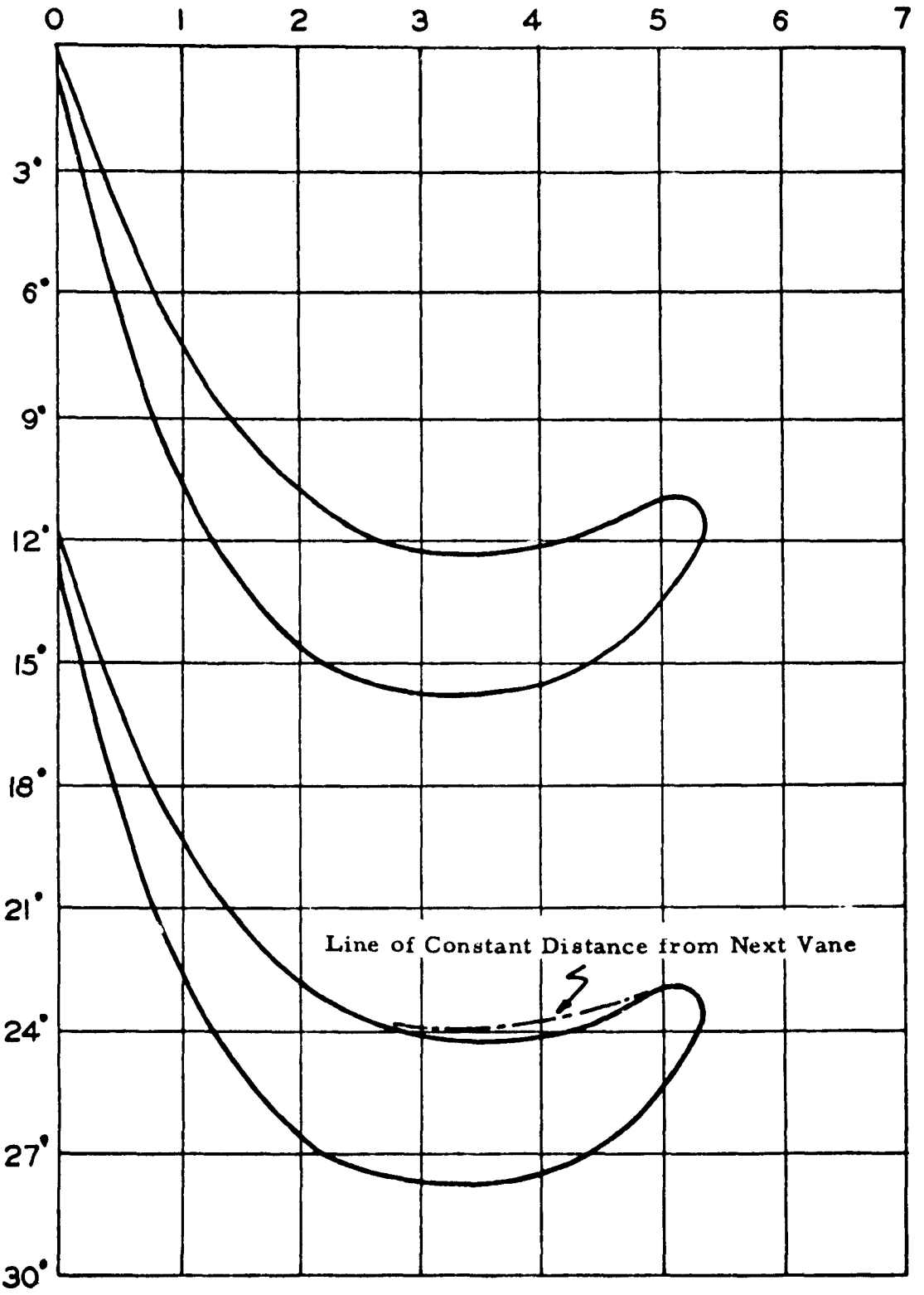

CONFORMAL REPRESENTATION OF STATIONARY VANE SYSTEM — INNER SHROUD INTERSECTION

FIGURE 12

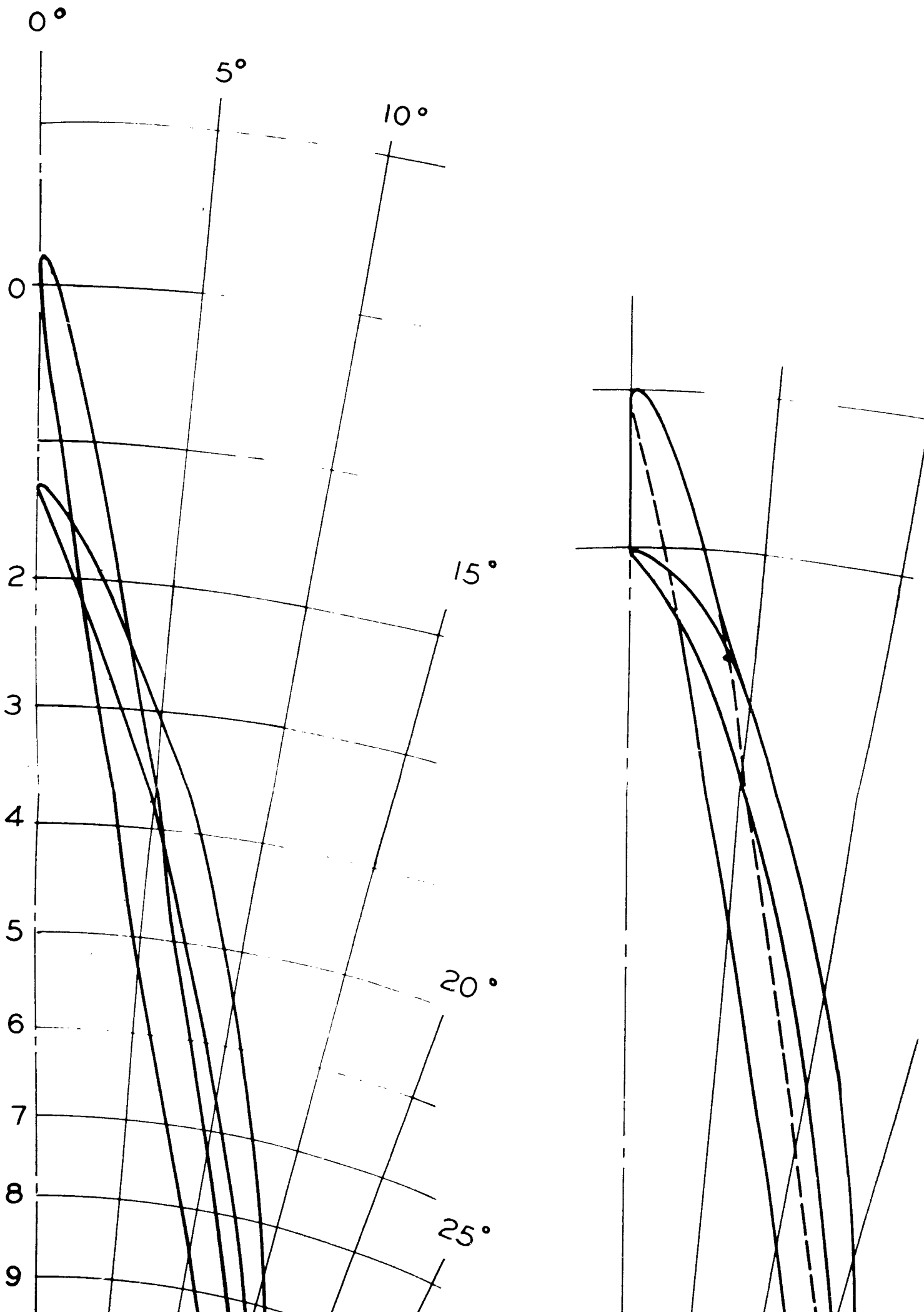
0°
5°
10°
15°
20°
25°
0
2
3
4
5
6
7
8
9

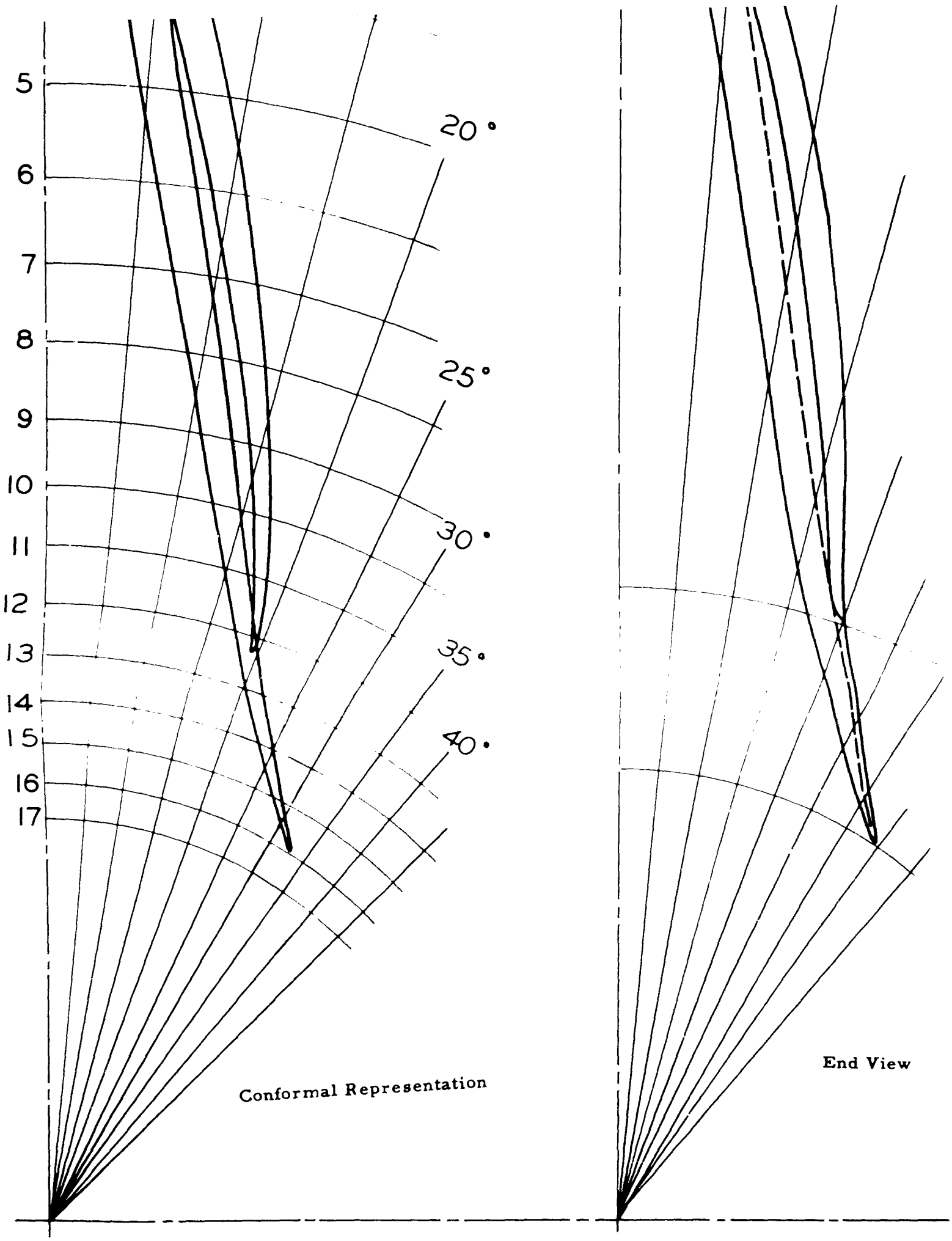

FIGURE 13

Vane Layout of Second Stage of Secondary Runner

CONFIDENTIAL

REVERSE OPERATION CIRCUIT

PRIMARY RUNNER

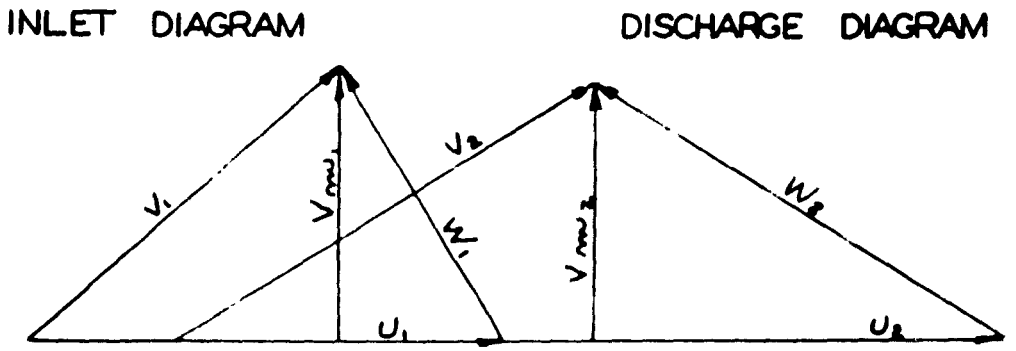

SECONDARY RUNNER

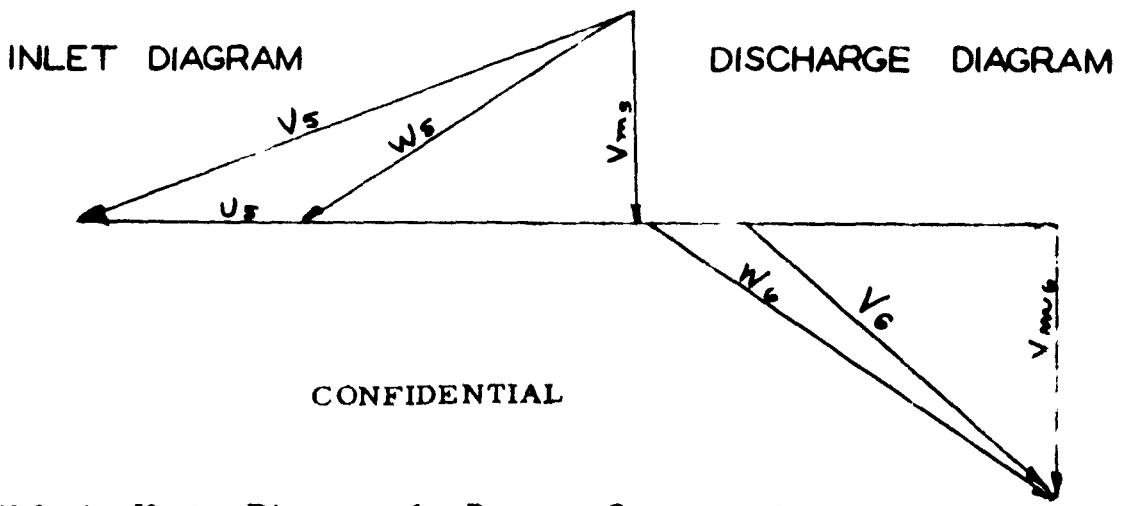

Velocity Vector Diagrams for Reverse Operation Circuit

FIGURE 14

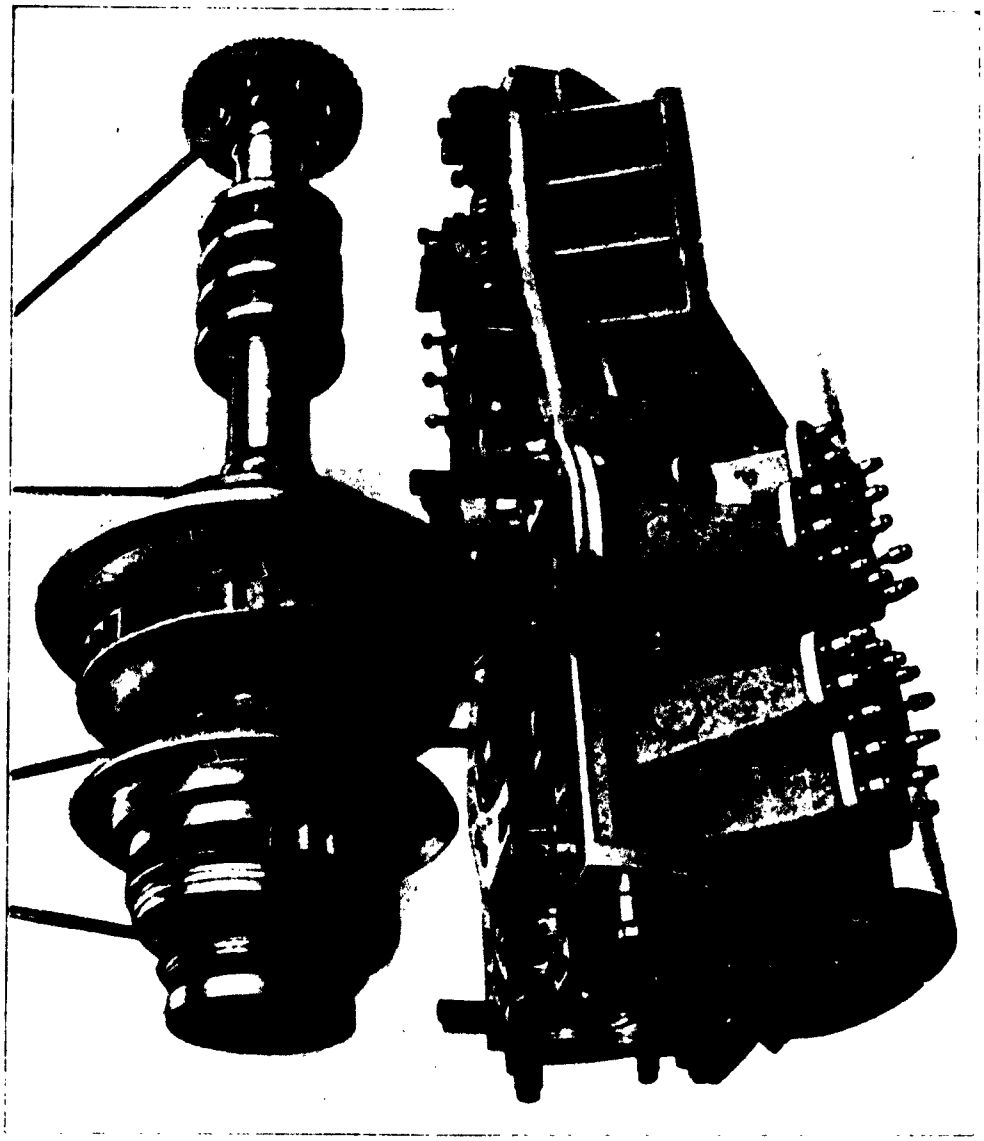

Lower Casing Half and Rotor
of
Foettinger Transformer

Figure 15

CHAPTER IV

General Problems of Increased Transmission Ratios for Foettinger Transformers

It has been mentioned before that the principles of the early Foettinger transformers involved:

a. The direct discharge from the primary into the first stage of the secondary runner;

b. Accelerated fluid motions relative to all vane systems;

c. Approximately constant meridional velocities in the vaneless spaces between successive vane systems.

The success of these early machines makes it desirable to adhere to these principles as far as possible. Thereby one encounters the problem how far the ratio of transmission can be increased without violating one of the principles listed. The first part of this chapter will attempt to answer this question.

In the following analysis the conditions at the inlet to the primary runner shall be designated with subscript 1, those at the discharge of the primary runner with subscript 2, those at the inlet to the first stage of the secondary runner with subscript 3, those at the discharge of the first stage of the secondary runner with subscript 4, and those at the inlet to the stationary vane system following the first stage of the secondary runner with subscript 5.

The locations of flow sections pertaining to these subscripts are so designated in Figure 16 . It should be noted that these designations are, for reasons of simplicity, not the same as those used earlier in connection with Figures 3 and 4.

For the problem stated, obviously the relationship between the flow conditions in the successive sections 2 and 3 (in Figure 16) have to be considered, primarily because it is between these two sections that the flow passes from the primary to the secondary system. Furthermore one has to formalize the condition of accelerated relative flow between sections 3 and 4, and a condition for satisfactory entrance conditions at section 5 safeguarding the adherence to the Foettinger principles and other considerations of good turbine design in the vane systems after section 5.

Designating by V the absolute fluid velocities, W the relative fluid velocities, U the peripheral velocities of the rotating elements, r the distance from the axis of rotation of the section (located by its subscript), λ the ratio of the primary to the secondary speed of rotation, with the subscript u the peripheral components, and with the subscript m the meridional component of any fluid velocity considered, one can derive the following four equations:

$$\frac{V_{u3}}{U_3} = \frac{W_{u3}}{U_3} + 1 = \frac{V_{u2}}{U_2}\,\lambda\left(\frac{r_2}{r_3}\right)^2 \qquad (2)$$

$$\frac{V_{u4}}{U_4} = \frac{V_{u5}}{U_5}\left(\frac{r_5}{r_4}\right)^2 \qquad (3)$$

$$\left|\frac{V_{u4}}{U_4}\right| + 1 = \left|\frac{W_{u4}}{U_4}\right| = \left|\frac{V_{u5}}{U_5}\right|\left(\frac{r_5}{r_4}\right)^2 + 1 \qquad (4)$$

$$V_{m4}^2 + W_{u4}^2 - 1 = 1.69\left[V_{m3}^2 + W_{u3}^2\right] \qquad (5)$$

The last equation (5) obviously expresses the fact that the relative velocity in section 2, i.e. at the discharge of the first stage secondary turbine, is stipulated to be 1.3 times as great as the relative velocity at the inlet section 2 of the same system.

Considering that $V_{m4} = V_{m5}$ and $V_{m3} = V_{m2}$, and by substituting equations 2 and 4 into equation 5 one arrives at the following relationship:

$$\left\{\left(\frac{V_{m5}}{U_5}\right)^2\left(\frac{r_5}{r_4}\right)^2 + \left[\left(\frac{V_{u5}}{U_5}\right)\left(\frac{r_5}{r_4}\right)^2 + 1\right]^2\right\}\left(\frac{r_4}{r_5}\right)^2 =$$

$$1.69\left\{\lambda^2\left(\frac{r_2}{r_3}\right)^2\left[\left(\frac{V_{m2}}{U_2}\right)^2 + \left(\frac{V_{u2}}{U_2}\right)^2\left(\frac{r_2}{r_3}\right)^2\right] - 2\lambda\frac{V_{u2}}{U_2}\left(\frac{r_2}{r_3}\right) + 1\right\} \qquad (6)$$

This equation may obviously be written in the form

$$C\left(\frac{r_4}{r_5}\right)^2 = 1.69\left(\lambda^2 A - 2\lambda B + 1\right) \qquad (7)$$

where C is a function of the flow conditions in section 5 and the ratio r_5 / r_4 only, whereas A and B are functions of the flow conditions in sections 2 and 3 and their respective radii only.

Assuming $r_5 / r_4 = 1.049$, which is in good agreement with the original Foettinger design, and for V_{m5} / U_5 as well as for V_{u5} / U_5 a value of 0.5, which is also in good agreement with the original Foettinger design as well as with axial flow turbine practice, one arrives for C at a value of 2.846.

This reduces eq. (7) to the form:

$$\left(\frac{r_4}{r_3}\right)^2 = \frac{1}{1.684}\left(\lambda^2 A - 2\lambda B + 1\right) \qquad (8)$$

This equation expresses the fact that the ratio of transmission (λ) may be varied as a function of the discharge to inlet radius of the first stage of the secondary runner, assuming certain velocity and geometric relations in sections 2 and 3 that determine the constants A and B.

The first set of assumptions to be made should obviously conform directly with that of the Foettinger transformer described in Chapter III of this report. From Figures 2 and the velocity vector diagram in Figures 3 and 5 one obtains; $r_2/r_3 = 0.94$, $V_{m2} / U_2 = 0.255$, $V_{u2} / U_2 = 0.47$.

Substituting these values into equation (8) one obtains the line A - A in the diagram shown in Figure 17 giving a relationship between the ratio of transmission λ and the radius ratio r_4/r_3.

The reason why the curve A-A does not run through 4.6 at the radius ratio of the original machine lies in the fact that the velocity increase in the first stage of the secondary runner by a factor 1.3 (assumed here) is somewhat less than that of the design described in Chapter III.

* * * *

Two changes in design and flow conditions have been considered in contrast to those presented in Chapter III and represented by curve A-A.

First it was assumed that only the radial distance between the primary runner discharge and the first stage of the secondary runner (section 3) was increased, i.e., the ratio r_2/r_3 was changed from 0.94 to 0.755. The remaining flow characteristics were assumed to be approximately the same as before. The results of this change are indicated by the curve B-B in Figure 17. It is seen that an increase in the radial distance between the primary and the inlet to the first stage of the secondary runner is most effective with respect to increasing the ratio of transmission for otherwise given conditions. However, it should be considered that this change involves also a substantial increase in the diameter of the torque converter.

The second change explored in this general manner involved an alteration in the flow conditions at the primary runner discharge in addition to an increase in the radius ratio r_3/r_2. Specifically, the velocity ratio V_{u2} / U_2 was chosen to be equal to 0.333 combined with a radius ratio r_2/r_3 of 0.755 as in the previous example. The results of substituting these values into equation 8 are represented by curve C-C in Figure 17 . Apparently this latter change has not as much additional effect as the change in the radius ratio represented by the distance between the curves A-A and B-B. However, the change represented by the curve C-C can best be accomplished by a decrease in the primary runner diameter leaving the inlet diameter to the first stage of the secondary runner essentially unchanged. This alteration which will be discussed in greater detail in the following chapter therefore permits the changes suggested without an increase in the overall diameters of the torque converter for given power and secondary speed.

In the wordsof the pump designer the change from the curve B-B to the curve C-C is accomplished by an increase in the "specific speed" of the primary runner which should be expected to lead to minimum overall dimensions for given operating conditions.

* * * *

An inspection of the curves in Figure 17 clearly discloses the limits in ratio of transmission that are likely to be encountered when adhering strictly to the general design principles of the original Foettinger transformer. Specifically, one cannot expect to reach the goal of a transmission ratio of 15 to 1 in this manner. Indeed, transmission ratios in the neighborhood of 10 to 1 can be achieved only by rather large ratios of discharge to inlet radius r_4/r_3 of the first stage secondary runner. This means that for the purpose of reaching such transmission ratios this runner will have to be changed in the direction of increasing the length of its fluid passages or vanes in comparison with the cross section of the passages. In the terminology of modern turbomachinery design, one may describe this change as a decrease in the "aspect ratio" of the first stage vanes of the secondary runner, this ratio being defined as the width or "span" of the vane measured normal to the meridional flow divided by the length of the vane in the direction of the relative flow. A decrease in this ratio below certain values is generally regarded as unfavorable for the efficiency of the machine. This effect should therefore be explored. In the following only the results of a separate investigation of this effect will be presented.

* * * *

It is easy to see that the head loss (measured in ft. lb. /lb., or feet) encountered in the vane passages may be expressed as follows:

$$h_L = C_D \frac{W^2}{2g} l (d + s) \qquad (9)$$

where:

h_L is the head loss in the passage in feet,

C_D the drag coefficient of the blades defined as customary for individual air foils,

W the velocity relative to the blade,

l the length of the blade measured in the direction of the relative flow,

d the distance between the blades measured normal to the relative flow,

s the span of the blades measured normal to the direction of the meridional flow.

In the following the relative velocity (W) and the distance normal to the relative flow (d) shall be understood to be measured at or near to the cross section of maximum relative velocity between the vanes.

Designating by H the total head change that takes place in the complete stage of the machine considered, it is easy to derive the following expression for the head loss in relation to the stage head:

$$\frac{h}{H} = \frac{C_D}{C_L} \frac{V}{U} \frac{t}{l} \left(1 + \frac{s}{l}\right) \qquad (10)$$

In this expression, C_L is the lift coefficient, U an average peripheral velocity of the blades and t the circumferential spacing of the blades.

In order to utilize equation (10) in a general manner, it is necessary to make certain practical assumptions. The most significant is that the stage is assumed to be a "symmetrical" stage. With this assumption, equation (10) may be written in the form:

$$\frac{h_L}{H} = \frac{C_D}{C_L} \left[\frac{1}{4}\left(1 + \frac{\psi}{2}\right)^2 + \phi^2\right] \cdot \left[\frac{1}{\phi} + \frac{1}{\psi} \frac{C_L l}{s}\right] \qquad (11)$$

where :

ϕ is the ratio of the meridional velocity of the section to the peripheral velocity of the runner at that section, and

ψ is the pressure coefficient defined by:

$$\psi = \frac{2gH}{U^2} = 2 \cdot \frac{\Delta V_u}{U}$$

ΔV_u is the change in the peripheral velocity of the absolute flow produced by the vane system, referred to a diameter representative for the change in angular momentum produced by the vane system.

Equation 11 shows that the head loss in relation to the stage head is a function of the lift-drag ratio C_L/C_d, the flow coefficient ϕ, the pressure coefficient ψ, and the expression $C_L 1/s$. The last expression is for a given lift coefficient the ratio of the blade length to the blade span, or in other words the reciprocal of what is usually called the "aspect ratio".

In Figure 18, equation 11 is evaluated under the assumption that $C_L \cdot 1/s$ equals one. The head loss divided by the stage head times the lift drag ratio of the blade is here plotted against the flow coefficient ϕ for various values of the pressure coefficient ψ. In Figure 19 the same plot is repeated for C_L 1/s equals one-half.

Both plots show that the losses for a given lift-drag ratio reach a minimum. For rather high flow coefficients ϕ apparently a high pressure coefficient, i.e., a strong deflection of the flow by the vane system is desirable in order to minimize losses. By comparison between Figure 18 and Figure 19 it is seen that a reduction in the coefficient C_L 1/s is particularly important at high flow coefficients ($\phi \geq 2$) which means that at such high flow coefficients a large aspect ratio is particularly desirable, or, in other words, that (at such high flow coefficients) the detrimental effect of the side walls is particularly pronounced.

In order to show this effect more clearly the head loss in relation to the stage heads times the lift-drag-ratio is plotted in Figure 20 as a function of the coefficient C_L 1/s for two different ϕ values at one value of ψ. This plot shows that particular for high flow coefficients the flow losses increase rapidly with the blade length to span ratio 1/s at a given lift coefficient. It is this result which has to be considered in connection with the curve shown in Figure 17. There it was shown that for increased speed reduction ratios

a large ratio of r_4/r_3 becomes necessary which entails automatically a large ratio of the blade length l to the span s measured normal to the meridional flow. Figure 20 thus indicates that this way of increasing the reduction ratio is likely to lead to an increase of flow losses in the first stage of the secondary runner and is thereby limited in its degree of application. Specifically, ratios r_4/r_3 in excess of (say) 1.5 may not be usable.

It is easy to derive from Figure 3 the flow and pressure coefficients of the vane systems used in the original Foettinger transformer and to compare thereby the values given in Figures 18 through 20 with the characteristics of the original machine. In particular, it will be found that in order to obtain overall efficiencies of 90% the head loss per blade row in the original machine could hardly be greater than 3 to 4% of the stage head, which leads one to the conclusion that the lift-drag ratios of the vane systems employed must have been better than 100 to 1. This appears possible since the drag coefficient as defined here is referred to the maximum velocity relative to the vanes. Nevertheless, it is clear that a rather high quality of the blade finish and blade shape is necessary to obtain results reported.

* * * *

THE GENERAL CONCLUSIONS that may be drawn from the foregoing considerations are the following:

a) That speed reduction ratios close to, or over 10 to 1 cannot be achieved in a single casing without either violating some of the original design principles or encountering appreciable flow losses at least in the first stage of the secondary runner;

b) That as a consequence of this, transformers following closely the original design principles should be limited to transmission ratios in the neighborhood of 7.5 to 1 or less; and

c) That for the achievement of speed reduction ratios of 15 to 1 one has to consider either the use of a separate pump and multi-stage turbine or admit certain departures from the design principles originally used with Foettinger transformers.

* * * *

As a consequence of the foregoing conclusions, the following three chapters will present:

a) A transformer design following closely the original Foettinger principles but advancing the speed reduction ratio to a value in the vicinity of 7.5 to 1;

b) The design principles of a separate pump and multi-stage turbine arrangements and a discussion of its characteristics; and

c) The design of a Foettinger type transformer for a speed reduction of 15 to 1, employing an axial flow type of impeller as primary runner. Obviously, this runner cannot adhere to the Foettinger principle of accelerated relative flow.

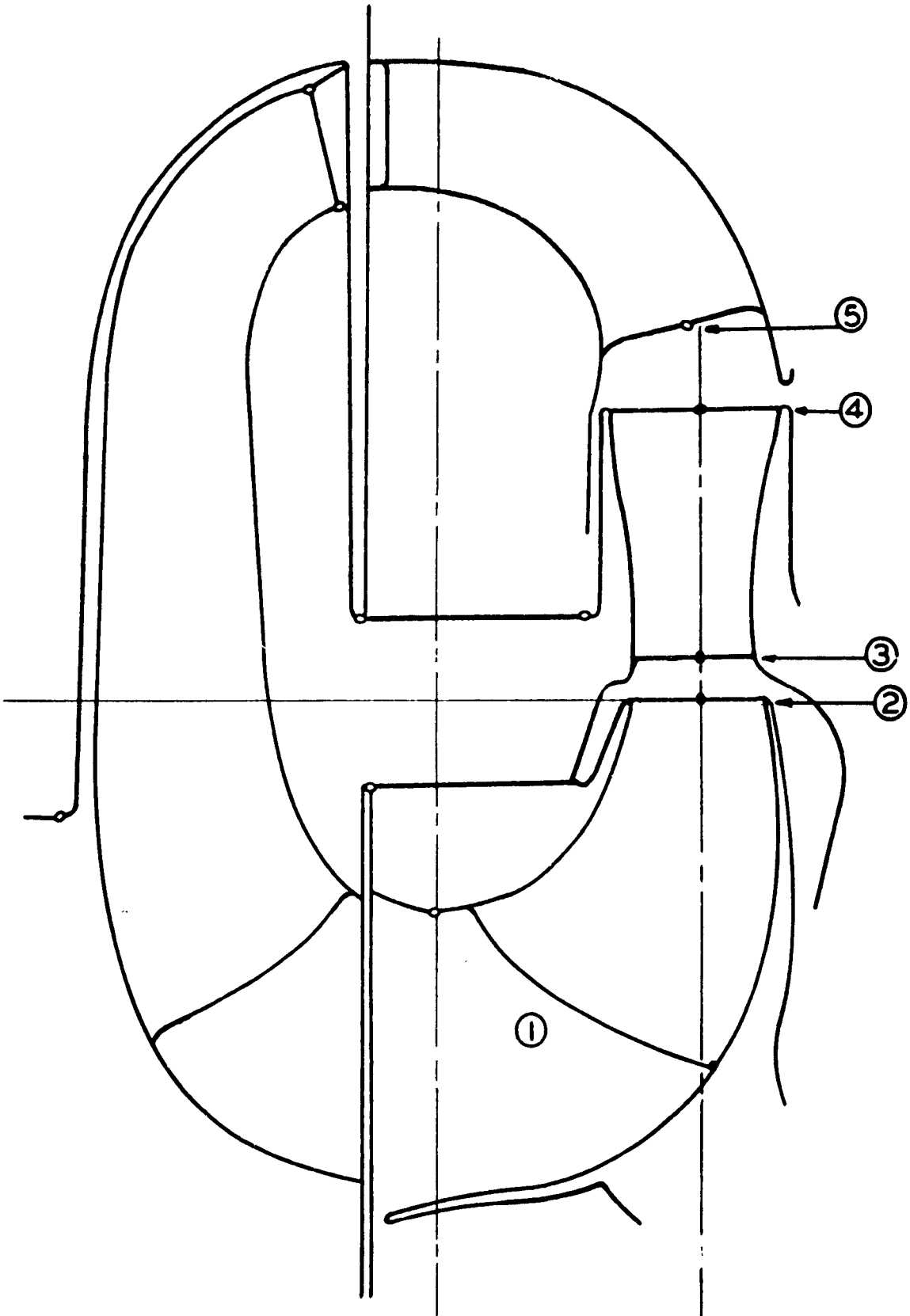

Figure 16 Stations for Analysis of Circuit

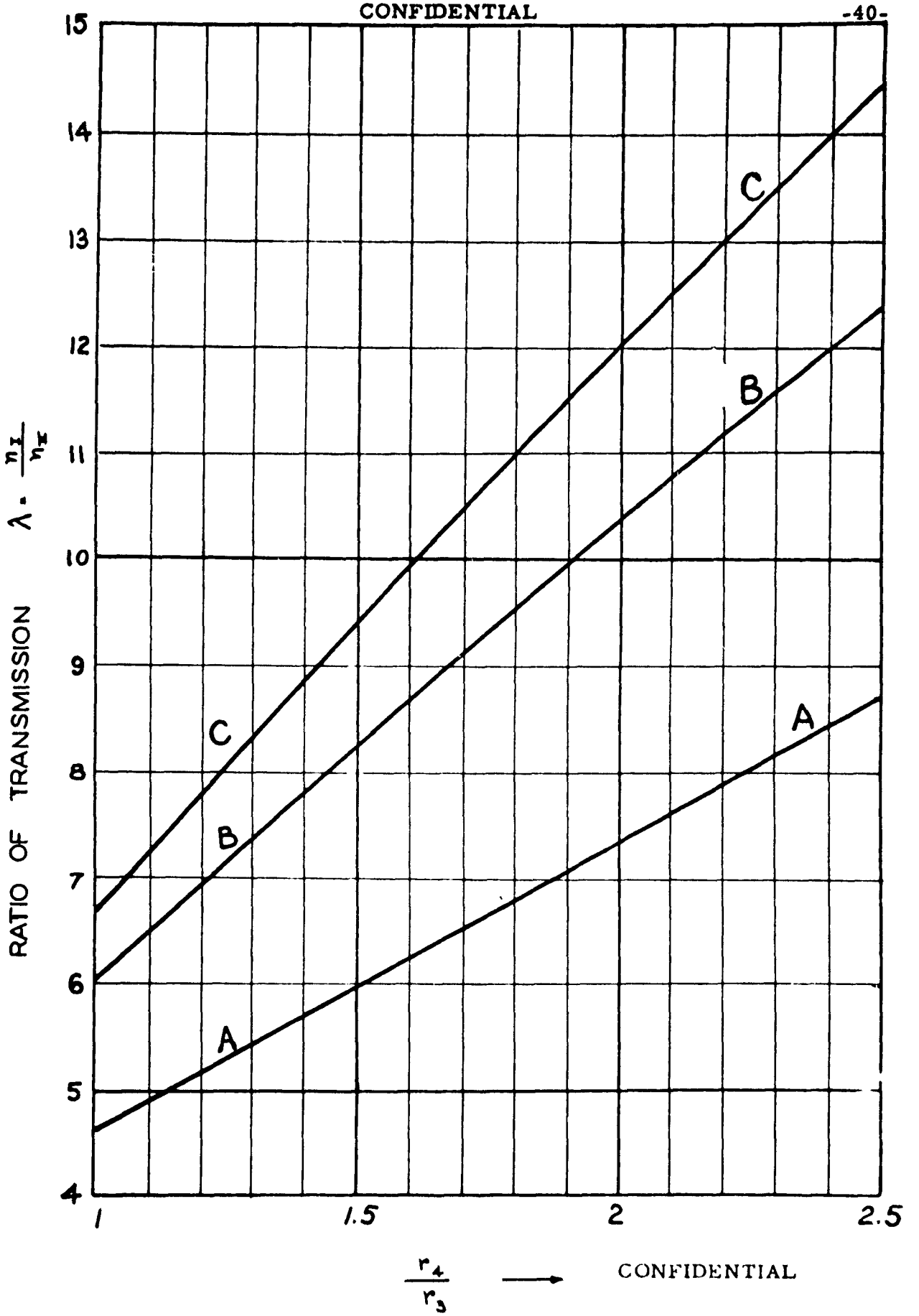

Limits of the Ratio of Transmission of the Original Foettinger Transformers

FIGURE 17

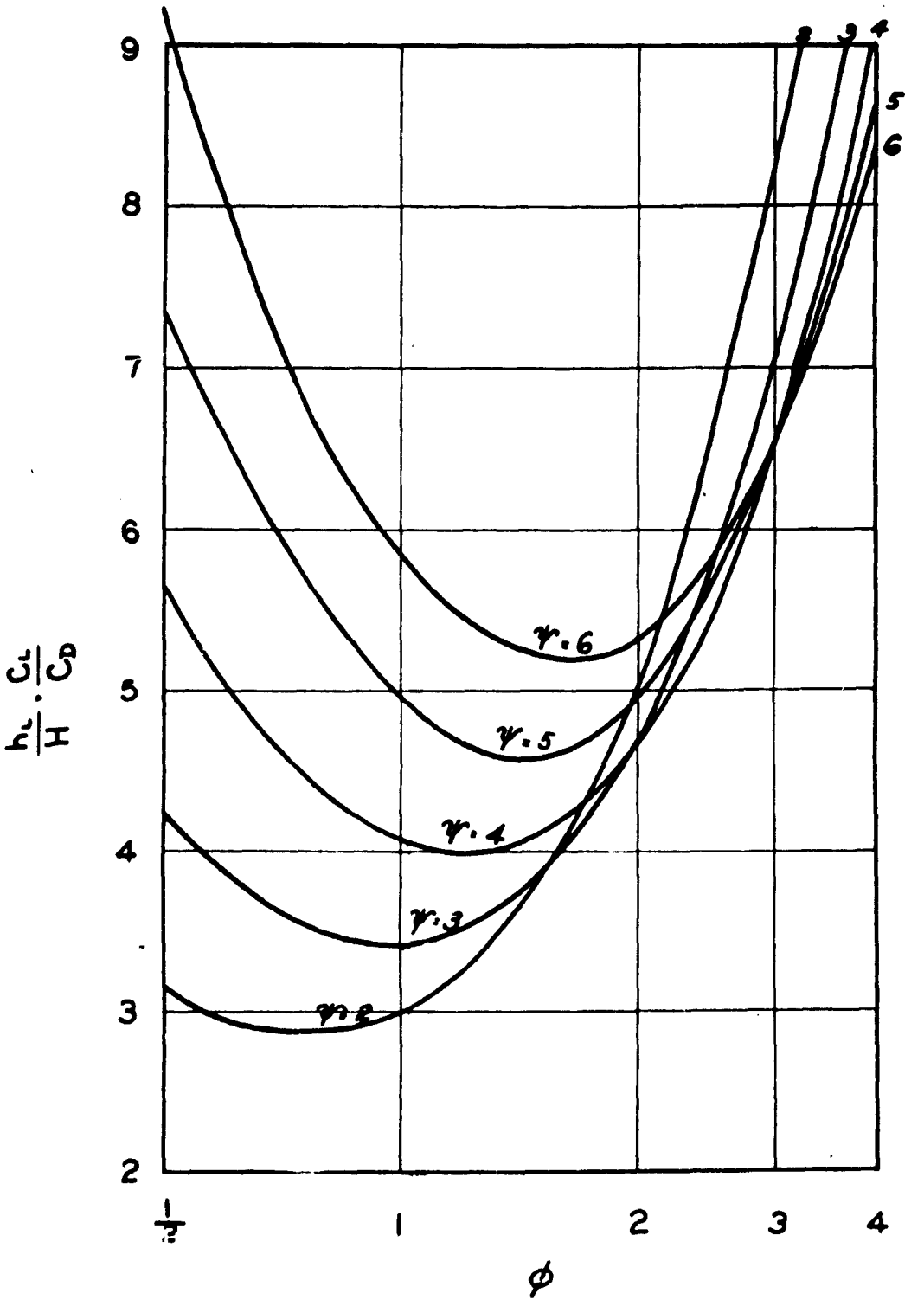

Loss Coefficient for Symetrical Turbine Systems with $\frac{C_L}{S}$ =

CONFIDENTIAL
FIGURE 18

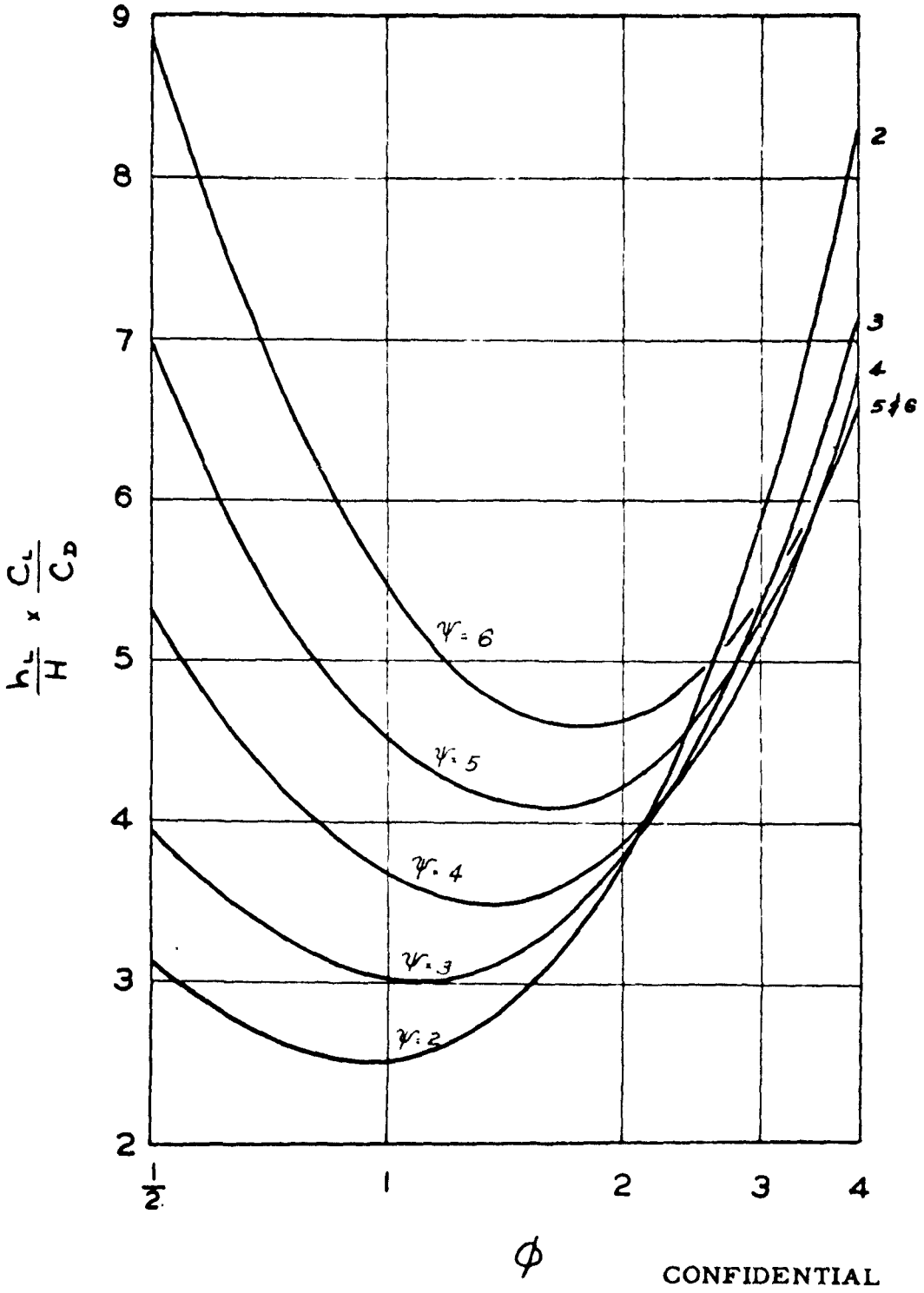

Loss Coefficient for Symetrical Turbine Systems with $\frac{C_L \ell}{S} = \frac{1}{2}$

FIGURE 19

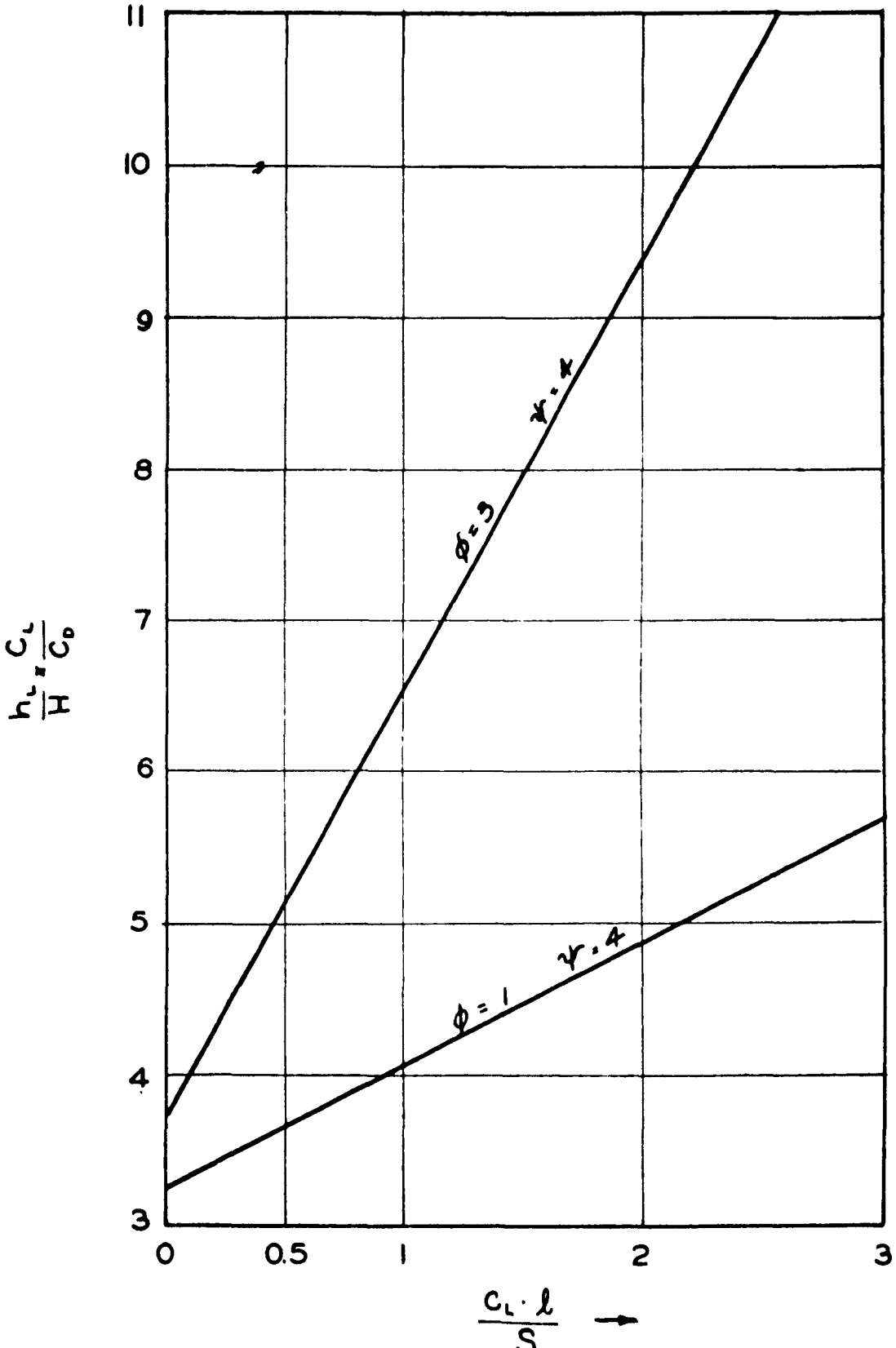

Loss Coefficient for Symmetrical Vane Systems as a Function of $\frac{C_L \cdot l}{S}$

FIGURE 20 CONFIDENTIAL

CHAPTER V

FOETTINGER TRANSFORMER WITH MIXED FLOW PRIMARY RUNNER OF INCREASED SPECIFIC SPEED

This chapter is concerned with a solution of the problem of increasing the speed of rotation of the primary runner within such limits as to permit adherence to the design principles of the original Foettinger transformer. To the pump designer this change clearly appears as an increase in the "specific speed" of the primary impeller. Figure 21 shows the modified primary impeller which has to be compared with that shown in Figs. 2 and 7. It can be regarded in principle as developed by a radial cut-back of the discharge vane edges of the original impeller as shown in Fig. 7, leaving the surroundings of the impeller, in particular the inlet to the first stage of the secondary runner unchanged.

Figure 22 shows the velocity vector diagram assumed for this impeller and should be compared with Fig. 5 for the original impeller.

The change consists primarily in an increase in the angular velocity of the impeller by a factor of 1.6. The angular momentum at the discharge of the impeller is left unchanged, compared with the design discussed in chapter III. Thereby the velocity configuration approaching the first stage of the secondary runner can be exactly the same as in the design previously discussed.

In order to maintain accelerated relative flow through the primary runner it was found necessary to increase the peripheral component of the flow approaching the primary runner. This is also shown in Figure 22. By this increase in the incoming angular momentum the total head of the primary impeller is kept approximately equal to that of the design described in Chapter III, although the angular velocity is 1.6 times greater than that of the primary wheel considered there. Thereby not only the flow approaching the first stage of the secondary runner remains the same, but the entire secondary system can be kept nearly identical with that described in Chapter III. The only exception to this statement is found to exist at the discharge of the second stage of the secondary runner where the flow has to leave with sufficient angular momentum to satisfy the pre-rotation shown by the velocity diagrams in Figure 22. It is probable that this change can be accomplished most efficiently by ending the vanes of the second stage of the secondary runner at a slightly larger diameter than in the original design.

To satisfy the velocity diagram shown in Figure 22 the impeller vanes have to have a shape represented conformally by the diagram shown in Figure 23. The principal of this type of representation has been discussed in Chapter III and is further explained in reference 3. The lines given in Figure 23 represent the lower vane surface, i.e. the surface nearest to the center of the impeller. From this conformal representation the vane shape is determined by radial section shown in Figure 21. An axial view of the lower side of the vane is given in Figure 24.

* * * *

For the design change discussed here the NUMBER OF IMPELLER VANES is of considerable importance. If the vane surface were approximately the same as in the design described in Chapter III it would be justified to assume that the flow losses in the primary impeller increase according to the second power of the relative velocities. Under this assumption one arrives at an efficiency reduction of approximately three percent as shown by point No. 2 in Figure 1 of this report. However, the increase in relative velocity permits a substantial reduction in the vane surface without a foreseeable danger of reaching the stalling limits of the impeller vanes. To permit an estimate of the number of vanes suitable for the new configuration one may assume that the lift coefficient of the runner vanes shall be not greater than of the impeller of the original Foettinger transformer described in Chapter III. With 12 vanes as assumed there the lift coefficient would be in the neighborhood of unity, a very reasonable value. With the same lift coefficient the new impeller described here would seem to require perhaps only half as many vanes which, of course, would be very widely spaced. From practical experience it seems more reasonable to assume 8 vanes for this runner, but the best value of this important figure can be ascertained only by experiment.

It may be assumed that by careful selection of the design and number of impeller vanes the increase in flow losses in the primary runner can be kept well below the value resulting from assuming these losses to be simply proportional to the square of the relative velocities. Point 3 in Figure 1 assumes that by such design measures the losses can be reduced to 1.5 points on the efficiency scale, giving a transformer of the design described in this Chapter an overall efficiency of about 88.5%, assuming that the design described in Chapter III has 90% overall efficiency. Since the speed of rotation of the primary runner has been increased by a factor of 1.6 as compared with the original design described in Chapter III, the transformer using the impeller of increased specific speed(shown in Figures 21 through 24) will give this transformer a ratio of transmission of 7.4 to 1. It is believed that this value

is not very far from the limit to which the principles of the original Foettinger transformers can be employed without changes demanding new and major developments.

* * * *

In closing it may be mentioned that for the same power and the same secondary speed the transformer so revised will have the same overall dimensions as the transformer described in Chapter III. Its power, overall diameter, and secondary speed are therefore given by equation (1) as that of the original machine described before.

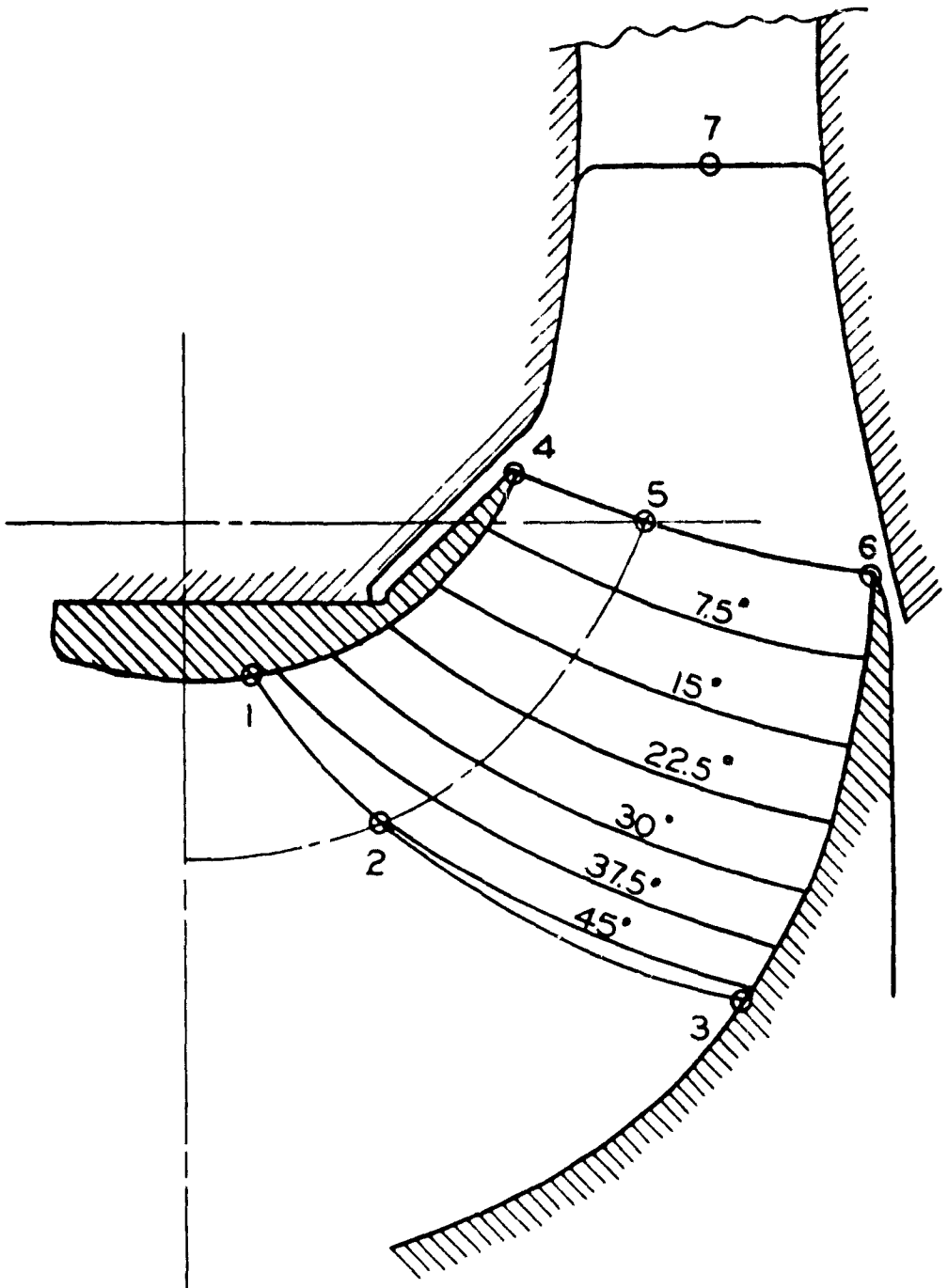

Meridional Section of Primary Runner for a Transmission Ratio of 7.4 to 1.

FIGURE 21

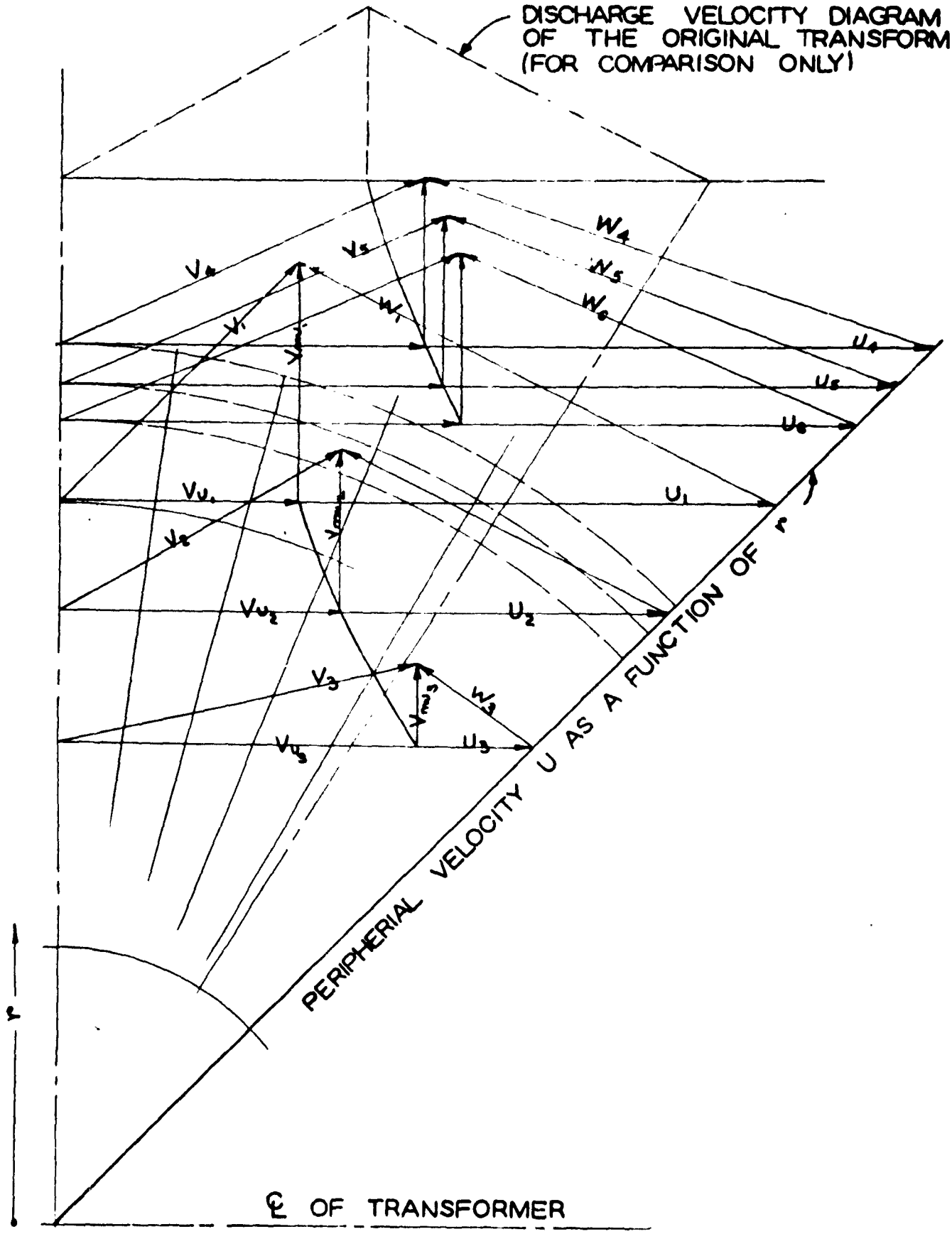

Velocity Diagrams of Primary Runner for a Transmission Ratio of 7.4 to 1

FIGURE 22

CONFORMAL REPRESENTATION OF PRIMARY RUNNER VANE "LOWER" SIDE

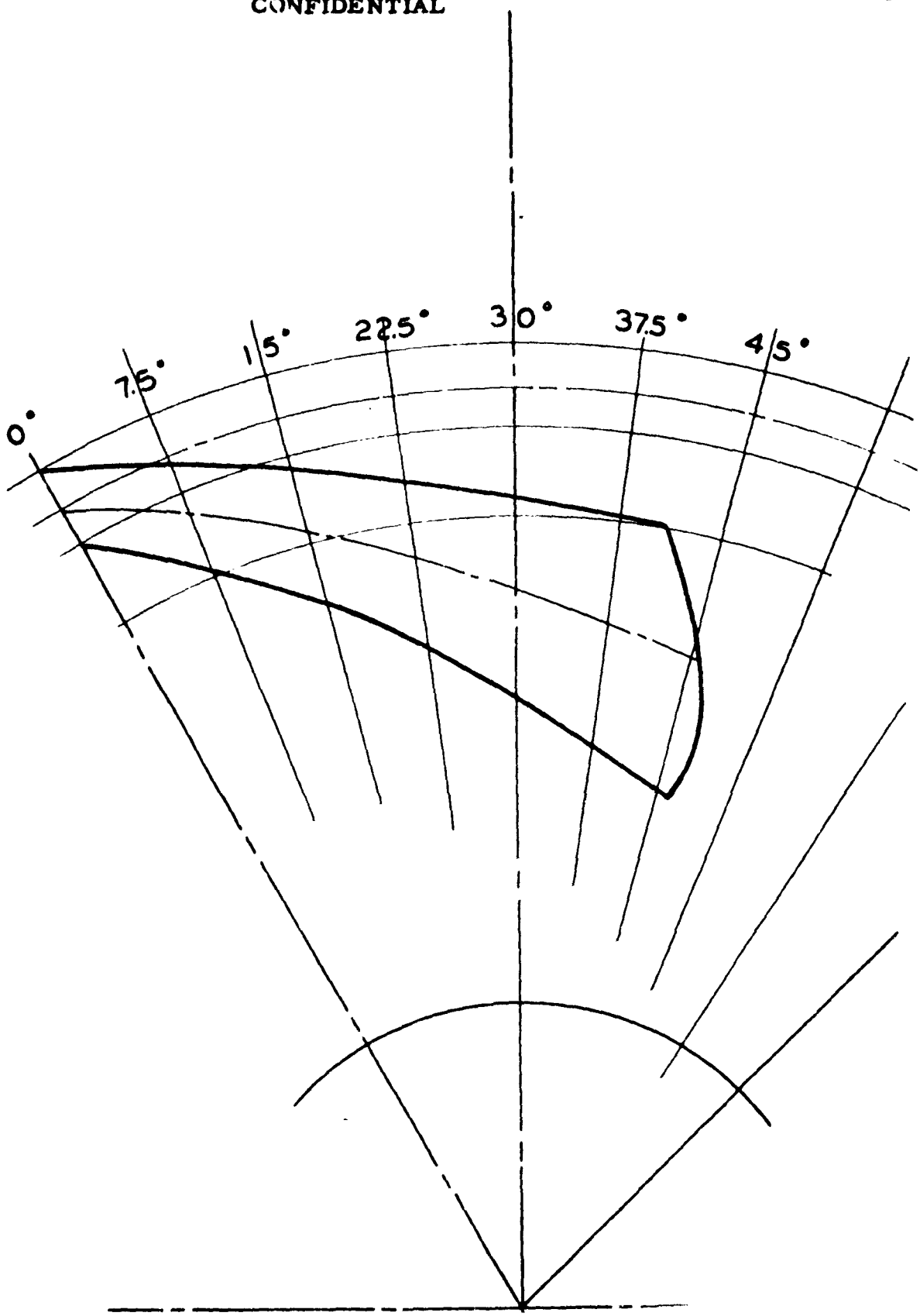

Lower Vane Surface of Primary Runner for a Transmission Ratio of 7.4 to 1

FIGURE 24 CONFIDENTIAL

CHAPTER VI

HYDRODYNAMIC POWER TRANSMISSION BY SEPARATE PUMPS AND MULTISTAGE TURBINE(S).

It has been shown in Chapter IV that it is unreasonable to expect the application of the original Foettinger design principles to hydrodynamic speed reducers for speed reduction ratios of 15 to 1. In this chapter the use of a separate multistage axial flow turbine and separate pumps of the most favorable specific speed (for achieving high efficiency) will be discussed briefly.

Experience has shown that radial flow centrifugal pumps with specific speeds in the neighborhood of 100 (the capacity measured in cubic ft. per second) can be built reliably to achieve overall efficiencies between 91% and 92%. Obviously a very high quality of surface finish is required for obtaining such results.

A design of this type is for example in the hands of the Worthington Machinery Corporation in Harrison, New Jersey, as one of the twin volute model pumps which that Company delivered to the laboratory of the California Institute of Technology in 1939 for investigation of the Grand Coulee pumps.

The turbine that is to be supplied by this pump and is to drive the propeller shaft must necessarily be of the multi-stage type, since a single stage turbine with a specific speed of only 1/15th of that of thepump just described would be certain to have a very low efficiency and necessarily a very large diameter. It is for that reason that this chapter will consider for the turbine a multistage axial flow arrangement only.

For a ratio of speed reduction of 15 to 1 it is reasonable to assume 13 turbine stages with a constant hub to tip diameter ratio of 0.85. The ratio of the meridional to the peripheral runner velocity at the mean diameter of this blade space shall be 0.55, and the pressure coefficient referred to the same diameter shall be 4. This specification can be satisfied by a symmetrical arrangement with a velocity configuration and blade shape as shown in Figure 25.

With the transmission ratio chosen, a single primary pump supplying such a multistage turbine would have a specific speed of 115 (with the capacity measured in cubic ft. per second). This value may be regarded as near an optimum with respect to efficiency.

For the turbine blades we may assume a ratio of radial blade span to axial extent of each blade row of 2 to 1, and a span to gap ratio of ten. Under this assumption one finds that the total length of the vane system is equal to approximately 1.5 times its outer diameter.

Furthermore, under the assumptions made one finds that the relation between the power transmitted, the outside diameter of the casing (D_o) and of the speed of the shaft driven by the secondary turbine is

$$HP = 78.5 \times 10^{-8} \times D_o^{5} \times n_{(II)}^{3} \qquad (12)$$

where the outside diameter D_o is measured in ft. and is assumed to be 10% larger than the maximum diameter of the blade space. This assumption conforms with that made in Chapter III on basis of the drawings of the original Foettinger transformer.

Equation 12 indicates that the power which the multistage turbine described here can transmit for a given diameter and speed of rotation is somewhat over 28 times as great as that transmitted by the transformer design described in Chapter III (note that the coefficient of the same relation given for that transformer in equation (1) was 2.75). However, it should be considered that the turbine described here has a length of 1.5 times its outside diameter whereas the foreward circuit of the original Foettinger transformer has a length to diameter ratio of considerably less than one half. In order to evaluate this effect it is indicated to compare the two designs on basis of their outside diameters for the same power and speed, rather than on basis of their power for the same diameter (and speed) as was done before. It then appears that the diameter of the Foettinger transformer described in Chapter III is for the same power and speed about 1.95 times as great as the diameter of the 13-stage turbine described here. In spite of its smaller length the volume and weight of the foreward circuit of the original design is at least twice as great as that of the multistage turbine. This advantage of the latter results of course from its more compact arrangement of a large number of stages, made possible primarily by the use of a much greater "aspect ratio" of its blades. The price to be paid for this advantage lies in the higher blade stresses, demanding far more exacting mechanical design and more precise manufacturing methods than the original construction. Whereas the latter was made from standard bronze castings, the turbine described here would require machined or precision-cast blades and blade fastening similar in quality to those used in gas turbines.

To be added is of course the size and weight of the separate primary pump(s) and connecting pipes to the size of the secondary turbine. This may cancel a fair part of the size and weight advantage of a separate multistage turbine unless the resulting freedom of arrangement can be used to a decisive advantage. Chapter IV and Figure IV-11 of reference 5 describe such a special arrangement.

It should be considered here that for multistage axial flow turbines the ratio of length to diameter can be changed over rather wide limits. An approximate analysis of such changes reveals that the total volume of the machine remains essentially the same, i. e. that an increase in diameter permits a reduction in length approximately according to the square of the ratio of diameter increase or decrease.

REVERSING of the secondary can, of course, be accomplished by the use of a separate reversing turbine to be filled only for reverse operation. There appears to be a good possibility of avoiding this increase in size and weight by interchanging the part played by the rotor and the stator of the turbine. The mechanical problems of coupling alternatingly one or the other of the two vane systems to the propeller shaft is of course a difficult one, which, however, falls definitely outside of the scope of the present investigation.

* * * * *

The product of the efficiencies of the best pumps available for separate pump and turbine operation and of multistage turbines as described lies in the general neighborhood of 85%. It is of course difficult to estimate the hydrodynamic losses connected with piping the power transmitting fluid from the primary pump (or pumps) to the secondary turbine (s). There is however no reason why these transmission losses should lower the overall efficiency of such an arrangement necessarily by more than 1 to 3 points on the efficiency scale. It is therefore safe to assume that separate pumps and turbines are capable of efficiencies of not less than 82% with ratios of transmission which, obviously, can be increased well beyond the value of 15 to 1 assumed here. For larger ratios it becomes necessary to equip the turbine with a larger number of stages than previously assumed which makes the secondary turbine somewhat longer than described before.

* * * * *

It is of interest to consider in this connection the possibility of supplying each turbine by more than one primary pump.

In the first place several primary pumps in parallel would have, for the same power transmitted, at increased speeds of rotation. Indeed the stream could be divided into two unequal parts with two pumps of different capacities and therefore different speeds of rotation but the same head. The smaller and faster running unit could be driven by the high pressure steam turbine and the larger and slower running pump by the low pressure steam turbine.

Furthermore one can envisage rather favorable arrangement for part load operation at cruising speeds. For example if at full speed operation one would use for each turbine three primary pumps in parallel and two in series, i.e. six primary pumps in all, one could operate two pumps in parallel at practically full primary speed in order to obtain a propeller speed of approximately $1/\sqrt{2}$ of the full load speed. It is seen that separate pump and multistage turbine arrangements can have in this respect characteristics that are comparable to those of electrical transmissions. However the weight and size of the hydrodynamic transmitting mechanism would probably be considerably less than that of electrical transmission machinery, although no final statement on this comparison is within the scope of this report.

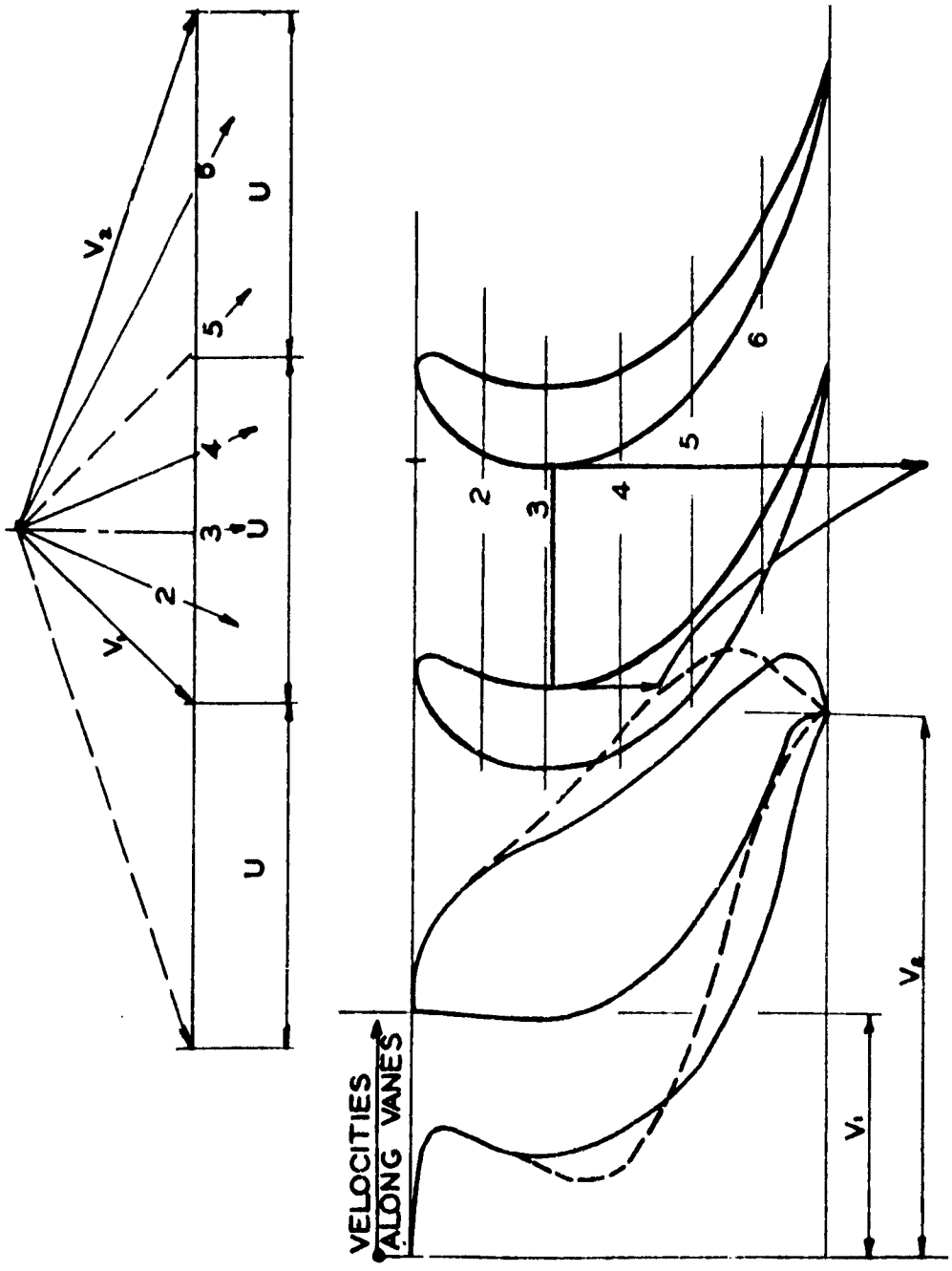

Vane Layout for "Symmetric" Axial-Flow Turbine Stage

Figure 25

CHAPTER VII

TRANSFORMER WITH AXIAL FLOW PRIMARY RUNNER

In the preceding Chapter V it was demonstrated that an increase in the ratio of speed reduction can be obtained by increasing the specific speed of the primary runner of the transformer. Within the limits set by the design principles of the original Foettinger transformer it was found that the speed increases obtainable in this manner are limited to ratios of approximately 7.5 to 1. However, without insisting on the principle of accelerated relative flow in the primary runner it is clear that the specific speed of the latter can be increased well beyond that of the mixed flow runner described in Chapter V. The ultimate limit of this development is obviously the use of an axial flow primary runner for hydraulic speed reducers. For this reason the Mechanical Engineering Department of The Johns Hopkins University suggested over two years ago the investigation of this limit of hydraulic speed reducers. The contract under which the present report is made was awarded originally in response to this suggestion.

Besides affording the possibility of larger ratios of transmission, the use of an axial flow runner as primary element of a hydrodynamic speed reducer involves the advantage of using the far reaching developments in axial flow compressor and turbine designs that have been accomplished during the last decade. On the other hand the use of an axial flow primary runner involves some basic problems of the flow in turbomachinery that had to be answered before the feasibility of this suggestion could be decided.

* * * *

In order to permit large ratios of speed reduction it appears necessary to place the inlet to the secondary runner systems at a larger diameter than the discharge from the axial flow primary runner. For this reason the flow leaving the axial flow runner has to pass from its predominantly axial into a radial direction within a space of revolution not unlike that formed by the shrouds of the primary runners of the original Foettinger transformers. Whether or not the flow in such a space of revolution would involve major hydrodynamic losses was unknown and was the principal objective of the experimental investigations carried out at this University for this purpose.

Part B of this report presents the apparatus, the techniques of investigation, and the results of the tests performed, together with their theoretical analysis. In the present chapter only the results pertaining directly to the design of a transformer of this type will be stated and used for the purpose of deciding the feasibility of a hydraulic speed reducer with axial flow primary runner.

The most essential results of these investigations were the following:

1. The hydrodynamic losses in the "quadrant" between the axial flow primary and the first stage secondary runner where approximately 1 1/2% of the primary runner head. This result establishes in principle the feasibility of a speed reducer with an axial-flow primary runner.

2. In the "quadrant" leading from the discharge of the primary to the inlet of the secondary runner satisfactory flow was maintained only if the meridional flow was kept at approximately constant mean velocity. In other words the annular cross-sections of this vaneless "quadrant" had to be kept approximately constant from the primary to the secondary runner, which conforms with the design principles employed in the original Foettinger transformers for the vaneless regions between successive vane systems.

3. The efficiency of the primary runner used for this investigation was between 85% and 86%. This leads to an overall efficiency of less than 85% for the primary stage as investigated, which indicates that the primary runner used for this investigation is not suitable for the application intended.

* * * *

In the foregoing results the efficiency of the primary runner tested should not be regarded as a significant result for this application since axial-flow runners have regularly been found to achieve by themselves efficiencies in the vicinity of 95%. For example, another axial-flow runner tested recently at the laboratory for Internal Fluid Mechanics at The Johns Hopkins University has shown an efficiency of over 95%. It should be noted, however, that this runner had a ratio of its average meridional velocity to its peripheral (tip) velocity of somewhat over 0.5 whereas the runner used for the tests pertaining to hydraulic speed reducers had a flow ration of 0.29. Without retardation of the meridional flow between the primary and secondary runner, meridional velocities which appear standard for the primary wheel must necessarily be very large compared with the peripheral velocities of the secondary runner rotating at only 1/15 of the primary speed. Therefore it is natural that for this application a relatively low flow ratio (ϕ) was chosen for the primary runner.

However, on basis of the present test results as well as other information it must be concluded that this low flow ratio (0.29) may well be too low for reaching optimum efficiency. It follows that it is necessary to investigate the feasibility of higher flow ratios than 0.29 for the primary runner in connection with its use in a hydrodynamic speed reducer. Under the condition of constant average meridional velocity between the primary and the secondary runner, this means that at least the first stage of the secondary has an extraordinarily high flow ratio. The compatibility of such high flow ratios with good efficiency of the first turbine stage and with acceptable design characteristics for the following stages therefore appears to be decisive for the use of axial-flow primary runners in hydrodynamic speed reducers. The present Chapter therefore aims primarily at deriving a practically useful answer to this question.

* * * *

The general hydrodynamic problem underlying this question has already been treated in Chapter IV. The most significant results of this investigation were expressed there by equation (11), and were numerically evaluated in form of the diagrams presented in Figures 18, 19, and 20. With these general results on hand it was decided to examine the before-mentioned problem on the basis of an actual design example of a speed reducer with an axial-flow primary runner. The design characteristics of this runner were to be chosen primarily for obtaining a high efficiency without concession with respect to its intended use in a speed reducer such as made in the case of the test unit.

The assumed design characteristics for the axial-flow primary runner are the following:

The average through flow ratio $\phi = 0.40$, assuming V_m = constant.

The pressure coefficient referred to the tip velocity of the runner $\psi = 0.36$.

The hub to tip ratio of the primary runner is equal to 1/2.

The ratio of the inlet radius to the first stage secondary runner to the outside radius of the primary runner is $r_3/r_o = 1.6$.

The meridional velocity between the primary and the inlet to the secondary runner is constant and, therefore, $V_{m_3} = V_{m_2}$.

The assumptions made determine to some extent the proportions of the "quadrant" between the primary and the inlet to the secondary runner, as well as the inlet flow conditions to the first secondary runner. Particularly, it is found that the inlet flow ratio of the secondary runner at the radius r_3 is $\phi_3 = 3.75$.

As may be expected, Figure 18 and 19 of Chapter IV show that this high flow ratio does involve some increase in the flow losses. With further reference to equation (11) and Figure 20 of Chapter IV, it is seen that this increase in losses at high flow ratios is particularly severe if the value of C_L l/s is large. This means that for a given lift coefficient one should choose the aspect ratio s/l of this stage as high as possible. This naturally leads to the question what aspect ratio appears feasible for hydrodynamic speed reducers. Since the Reynolds' number for this application is always very high, the question of the highest feasible aspect ratio becomes in this case one of mechanical stresses.

Whereas no precise answer to this question is possible without considering a specific design form, it is possible to estimate the order of magnitude of the bending stresses in the turbine blades in relation to the hydrodynamic forces acting on the blades. This relationship may be expressed in the form:

$$\sigma = 100\ C_L \frac{\rho W^2}{2} \frac{s}{l} \qquad (13)$$

where s is the span, and therefore s/l the aspect ratio of the blades. In this equation the bending stress σ appears in the same units as the velocity pressure $\rho W^2/2$. Naval applications of a speed reducer of this type will probably lead for $\rho W^2/2$ to values in the vicinity of 200 lbs per square inch, leading to stresses in the neighborhood of 20,000 lbs per square inch for an aspect ratio of unity. Therefore, aspect ratios slightly in excess of unity are probably admissible assuming a high-grade stainless steel for the transformer blades. It should be mentioned here that the foregoing equation (13) is based on the assumption that the vane system is shrouded on both sides. If the runner blades are over-hanging, the bending stress would be about twice as high as indicated by equation (13).

* * * *

After the foregoing considerations, several complete transformer arrangements were subjected to approximate analyses of their flow conditions. On this basis the design shown in Figure 26 was chosen and its flow conditions along a mean flow surface through the secondary runner analyzed. Overall results of this analysis are given in the following tabulation, describing the conditions at the mean inlet and discharge radius of each runner vane system.

Table
of
Design and Flow Characteristics
of the Secondary Part of the Transformer
Shown in Figure 26.

The Outside Radius of the Primary Runner is Used as Unit of Dimensions

Stage	Radius Runner Inlet	Radius Runner Discharge	Span of Flow Passage	Flow Coefficient ϕ	Pressure Coefficient $\psi = \frac{2gH}{U_1^2}$	Stage Head ref. to U_3 $\frac{2gH}{U_3^2}$	Estimated Head Loss Coefficient $\frac{h_L}{H} \cdot \frac{C_L}{C_D}$
1st	1.6		0.255	3.75	4.3	4.3	7
		1.79	0.24	2.95			
2nd	2.0		0.25	2.265	2.89	4.51	4.5
		2.17	0.255	1.98			
3rd	2.35		0.30	1.36	2	4.30	3.0
		2.34	0.31	1.33			
4th	2.33		0.33	1.26	2	4.22	3.0
		2.32	0.34	1.235			
5th	2.31		0.35	1.215	2	4.17	3.0
		2.29	0.35	1.20			
6th	2.01		0.37	1.52	2	3.15	3.4
		1.83	0.38	1.78			
7th	1.50		0.44	2.28	2	1.75	(4.5)
			Total Head =			26.40	

The foregoing table and Figure 26 show that the suggested transformer design requires seven turbine stages of which only the last one is a radial flow stage of rather small diameter while all others are similar in design to steam turbines of the reaction type, or to the design of an axial-flow multistage turbine described in the preceding chapter and shown in Figure 25. The difference between these rather classical designs and that proposed for the speed reducer shown in Figure 26 lies primary in the flow coefficients which start with very high values, as mentioned before, and reach somewhat more convential values in the stages of large diameter. In all cases, however, the flow coefficients of this speed reducer remain on the high side.

The flow and pressure coefficients of the foregoing tabulation may now be examined with respect to the relative head loss per stage as expressed by equation (11) in Chapter IV by the curves in Figures 18 and 19. It will be seen that the values of $h_{/H}\, C_{/C_p}$ for this transformer, listed in the foregoing table, are not too far from the optimum values suggested by these curves excepting, of course, the first stage because of its extraordinarily high ϕ value. Specifically, it will be found that the head loss in terms of $h_{/H}\, C_{/C_p}$ is, according to the tabulated values of ϕ and ψ, for most stages lower than the corresponding values for the original Foettinger transformer. Therefore the design shown in Figure 26 and characterized by the foregoing tabulation may well be expected to have rather a favorable efficiency.

THE VELOCITY VECTOR DIAGRAMS of the Axial-Flow Primary Runner of this transformer are shown in Figure 27. The velocities at the runner Tip are designated with subscripts "0", and those at the blade roots (hub) with subscripts "h". Subscripts "1" pertain to the inlet, subscripts "2" to the discharge of this runner. As previously, U denotes the circumpherential velocity of the blades, V the absolute, and W the relative fluid velocities.

The diagrams in Figure 27 are drawn for zero rotation of the flow at the inlet to the runner. The difference between the axial velocities at root and tip is estimated from the curvature of the meridional flow through the runner and the effect of the inclination of the vanes (shown in Figure 26) which tends to reduce the effect of this curvature. The velocity diagram at the hub comes close to the stalling limit for axial flow vane systems, and requires a ratio of blade chord to blade spacing of about 1.75.

Figure 28 shows the velocity diagrams of the first and second blade rows of the secondary runner, taken at the points 3, 4, 7, and 8 marked in Figure 26 in the middle of the respective blade edges. The subscripts of the velocity vectors in Figure 28 correspond to the number designations of these points. An estimate of the blade profiles corresponding to these flow conditions is given in Fig. 29. The blade spacing corresponds to lift coefficients in the neighborhood of 1.1. Obviously neither the blade shapes nor spacings can be regarded as final, since for the efficiencies required, these characteristics can be determined only by careful cascade tests similar to those reported in reference 4. Probably a radial flow rig will be necessary for these tests.

* * * *

THE CAVITATION PROBLEM of the transformer described here requires particular attention.

The critical section with respect to cavitation is in all transformers discussed in this report the inlet to the Primary Runner, which contains the point of lowest mean static pressure in the circuit. In the case of radial flow primary runners the total inlet head above the vapor pressure needs to be only about one half or less of the primary runner head in order to prevent cavitation (for more detailed information see, for example, reference 3). However for an axial flow runner of the specific speed considered here the inlet head has to be between one and two times as great as the primary runner head. In other words the minimum pressure in the transformer has to be rather high compared with pressure differences within the circuit, thereby giving the general pressure level in the machine correspondingly high values. It will be found that for modern naval applications the average pressure in the transformer casing may easily reach values in the vicinity of 1000 lbs. per sq. inch.

The calculation of the pressure required to prevent cavitation should be based on the design and flow characteristics of the primary runner. It is easy to determine first on basis of its assumed flow characteristics (here, ϕ x 0.40 and ψ = 0.36) the dimensions and absolute velocities of the primary runner for a given power and speed of rotation, which gives also its rate of flow (Q) and head (H). To determine from this data the required total inlet head above the vapor pressure ' H_{sv} it is most convenient to assume a value for the so-called "Suction Specific Speed"

$$S = \frac{n_r \sqrt{Q}}{H_{sv}^{3/4}}$$

It is felt that S should be not greater than 300 (where Q is measured in ft^3/sec), which is a conservative value except in cases where LOCAL cavitation has to be avoided. This condition probably pertains here.

A more dependable but also more difficult way of determining the required inlet pressure or head (H_{sv}) is based on the pressure reduction on the runner vanes. This pressure reduction can be derived from available NACA airfoil data and the velocity relative to the blades (see also references 3 and 4, considering that speed limitations due to compressibility effects can readily be translated into cavitation limits). A detailed description of these calculations is unnecessary as they are well-known in the fields of hydrodynamic machinery and marine propellers.

* * * *

THE SIZE OF THE TRANSFORMER will be expressed as before in form of the familiar relation between the power, the diameter, and the speed (rpm) of a hydrodynamic machine. For the transformer with axial-flow primary runner described in this chapter, this relation is:

$$HP = 32.7 \times 10^{-8} D_o \quad n_{II}^3 \qquad (14)$$

where D_o is again the outside diameter of the casing in feet, and n_{II} the secondary number of rpm.

This relationship is to be compared primarily with equation (12) which applies to an axial flow, 13-stage turbine as (separate) secondary element: It is seen that the transformer with axial flow primary runner requires a 19% larger outside diameter than the 13-stage turbine to transmit the same power at the same secondary speed. (Note that the 5th root of the ratio of the power coefficients, $\sqrt[5]{78.5 / 32.7} = 1.19$). However the transformer with axial flow primary runner has a length of approximately $D_o/2$ in contrast to 1.5 D_o for the 13-stage turbine. The volume and weight of the 13-stage turbine is thereby found to be about 1.75 times as great as that of the transformer described in this chapter, considering only one circuit (foreward circuit) as shown in Figure 26.

With a reverse-operation circuit this transformer would have about the same size and weight as the 13-stage turbine without any means of reversing. The transformer considered here would be, of course, substantially smaller than a Foettinger transformer of the type described in Chapter III.

In order to obtain a picture of the actual dimensions, consider for example a transformer for 35,000 HP primary power input at a primary speed of 4000 rpm and a secondary speed of 267 rpm. Equation (14) shows that with these assumptions the outside diameter would be about 5.7 ft, the length of its forward circuit casing (without bearings) about 3.5 ft, and the casing length for forward and reverse operation circuits about 6 ft.

THE MECHANICAL CHARACTERISTICS of the transformer described in this chapter warrant special consideration.

It has already been mentioned that rather high absolute pressures will be necessary to prevent cavitation. The casing design indicated in Figure 26 is likely to be sufficient for forseeable naval application, assuming rather high grade materials for casing and bolting. The bolts are studded alternatingly into the upper and lower casing halves in order to make room for their nuts. It has also been mentioned that the transformer blades are highly stressed, requiring high grade stainless steels and first class mechanical design for blade fastenings and shrouds. Special attention should be given to the blade design of the primary runner. It is expected that these blades have to be inclined as indicated in Figure 26, in order to balance a major part of the hydrodynamic bending load by the centrifugal forces of the rotating blades.

In the case that a reverse-operation circuit is used in the manner established by the original Foettinger transformers, the blades of the first stage of the secondary runner (marked "R1" in Figure 26) will probably be the most highly stressed parts of the machine during reverse operation. Under this condition the Entire secondary torque of the reversing circuit has to be transmitted mechanically through this vane system. It is believed that these blades will then have to be inclined against the axial direction in alternatingly opposite directions (resembling a bridge structure). The blade spacing will thereby vary alternatingly at the two ends of the blades. (The blade spacing indicated for this system in Figure 29 may well be regarded as the maximum, with alternate blades spaces being substantially reduced at the blade ends.)

* * * *

THE CONCLUSIONS that may be drawn from the foregoing design study of a transformer with axial-flow primary runner are the following:

1. It is feasible to use an Axial-Flow Primary Runner as a means of increasing the transmission ratio of hydrodynamic speed reducers for ships.

2. The design described applies directly to a transmission ratio of 15 to 1. Ratios from 12 to 1, to about 18 to 1 are believed to be obtainable, primarily by changes in the number of secondary stages.

3. The losses in the transition "quadrant" from the primary to the first stage of the secondary runner were found to lie between one and two percent of the primary runner head provided the average meridional velocity is held constant in this passage.

4. As a consequence of item 3 and on basis of available results obtained with axial-flow runners it is expected that a transformer as described here can have an overall efficiency of 85% $\approx (0.93^2)$. To achieve this it is necessary to choose a favorable flow ratio (V_m/U_o) for the primary runner. The primary runner blades can be designed according to reference 4, whereas the secondary runner blades must be developed by cascade tests directed at the somewhat unusual flow characteristics of these blades. The required quality of blade shapes and surface finish is expected to call for precision castings or machining for these blades.

5. The size of a speed reducer with axial-flow primary runner appears to be quite attractive for naval application.

6. The development of a speed reducer of the type described in this chapter should be regarded as a task of the same magnitude as the development of a gas turbine for ship drive.

* * * *

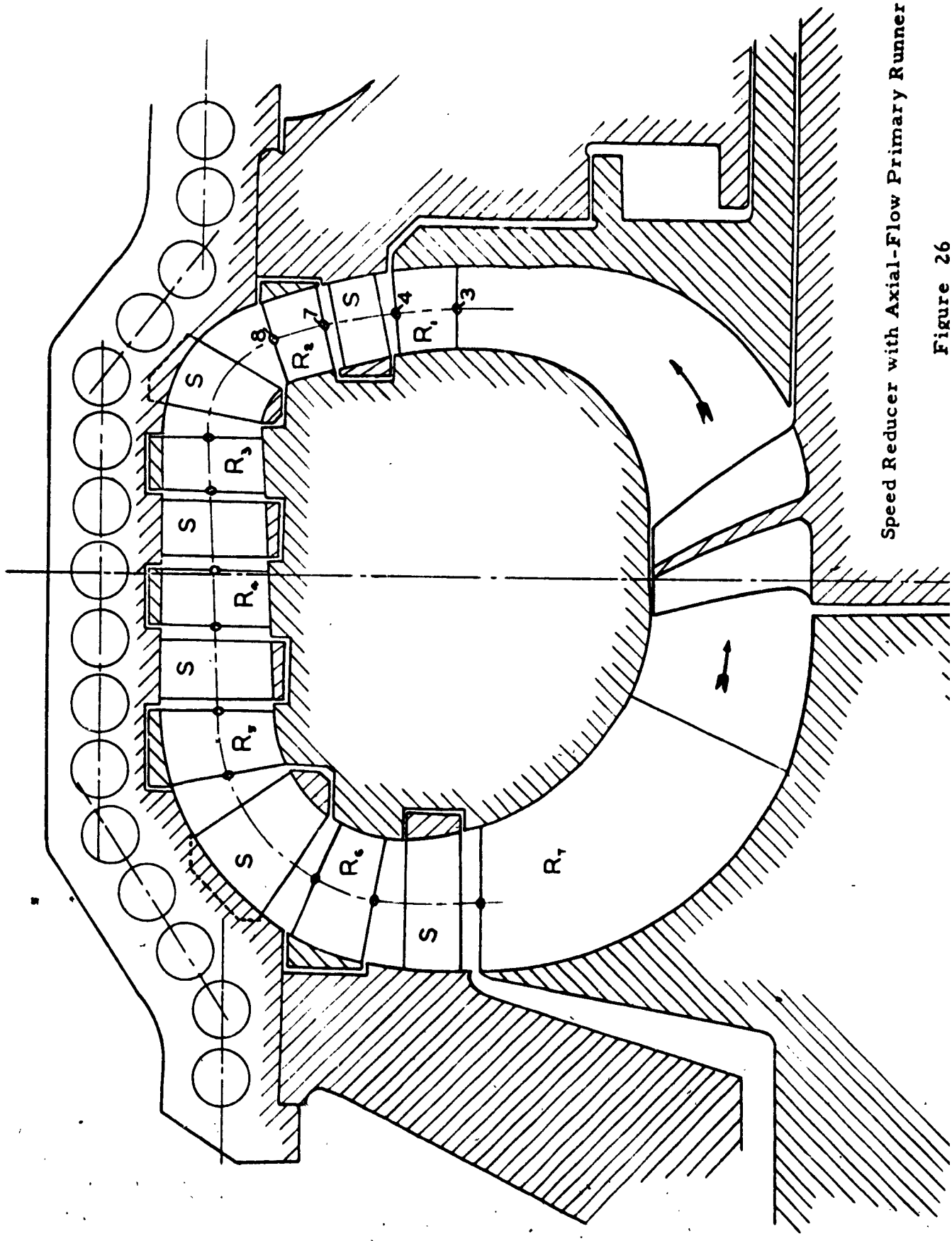

Figure 26 Speed Reducer with Axial-Flow Primary Runner

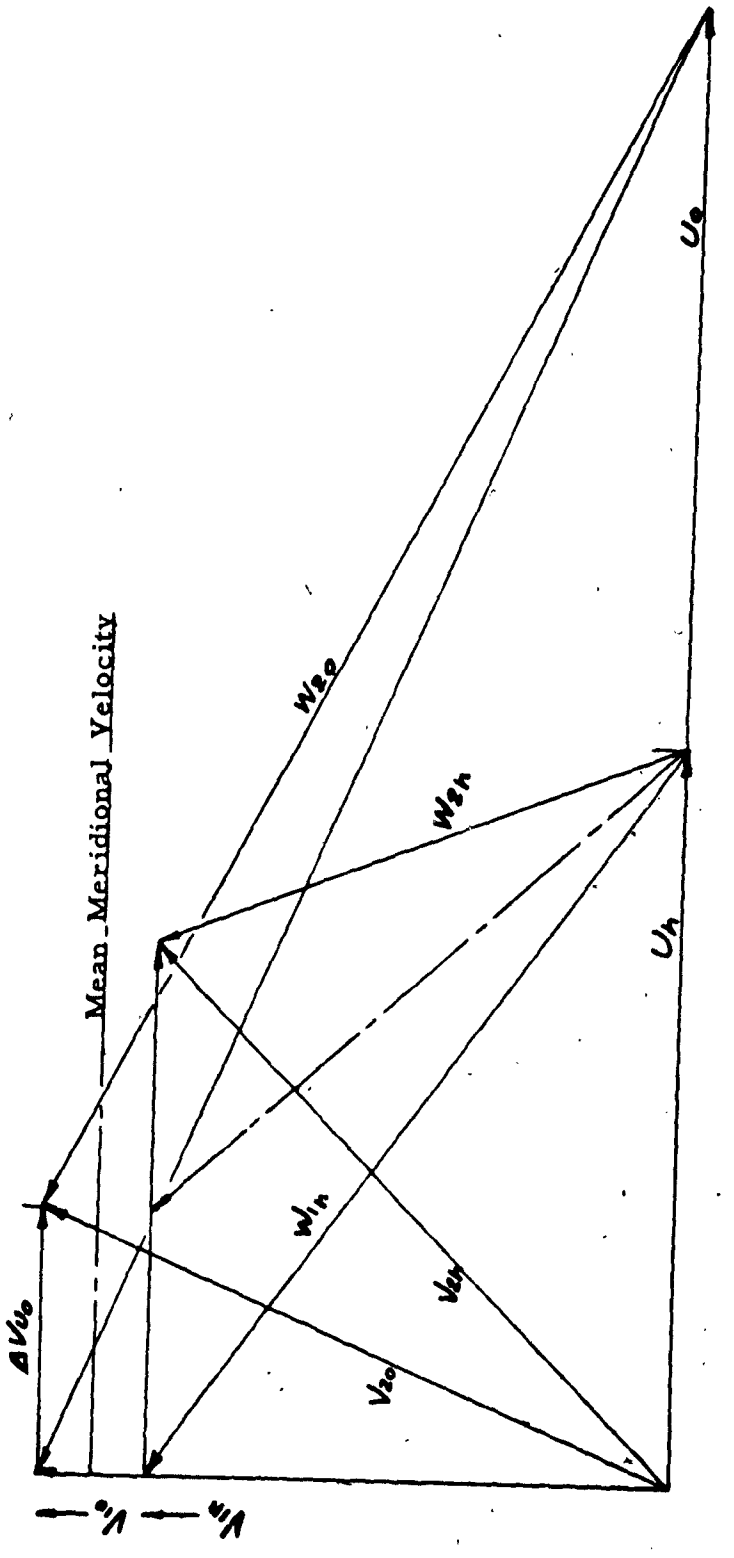

Figure 27 Velocity Diagrams of Axial-Flow Primary Runner

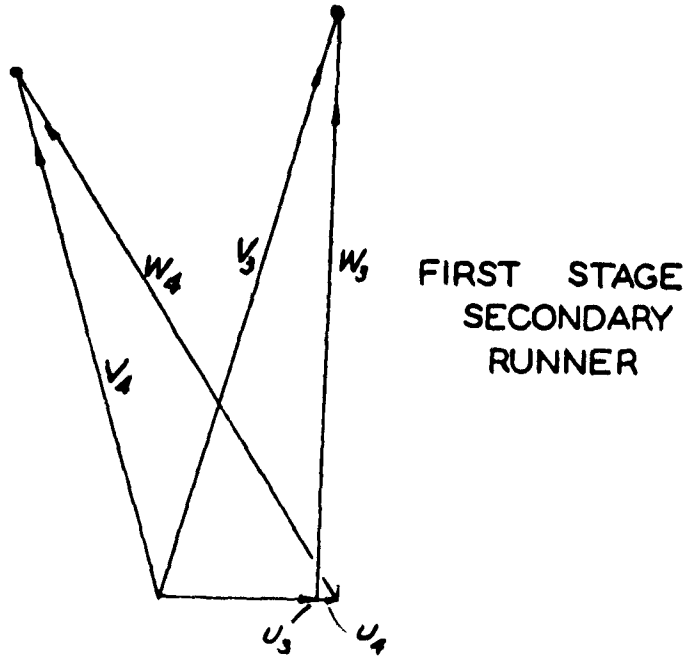

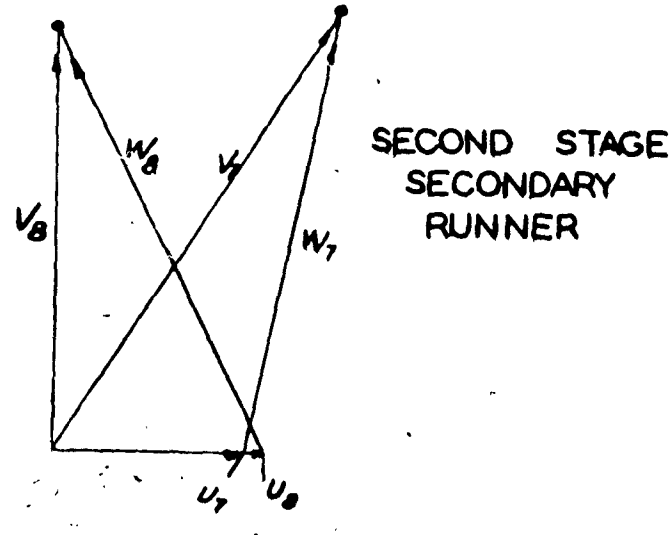

Figure 28 Velocity Diagrams of Secondary Runner First and Second Stages

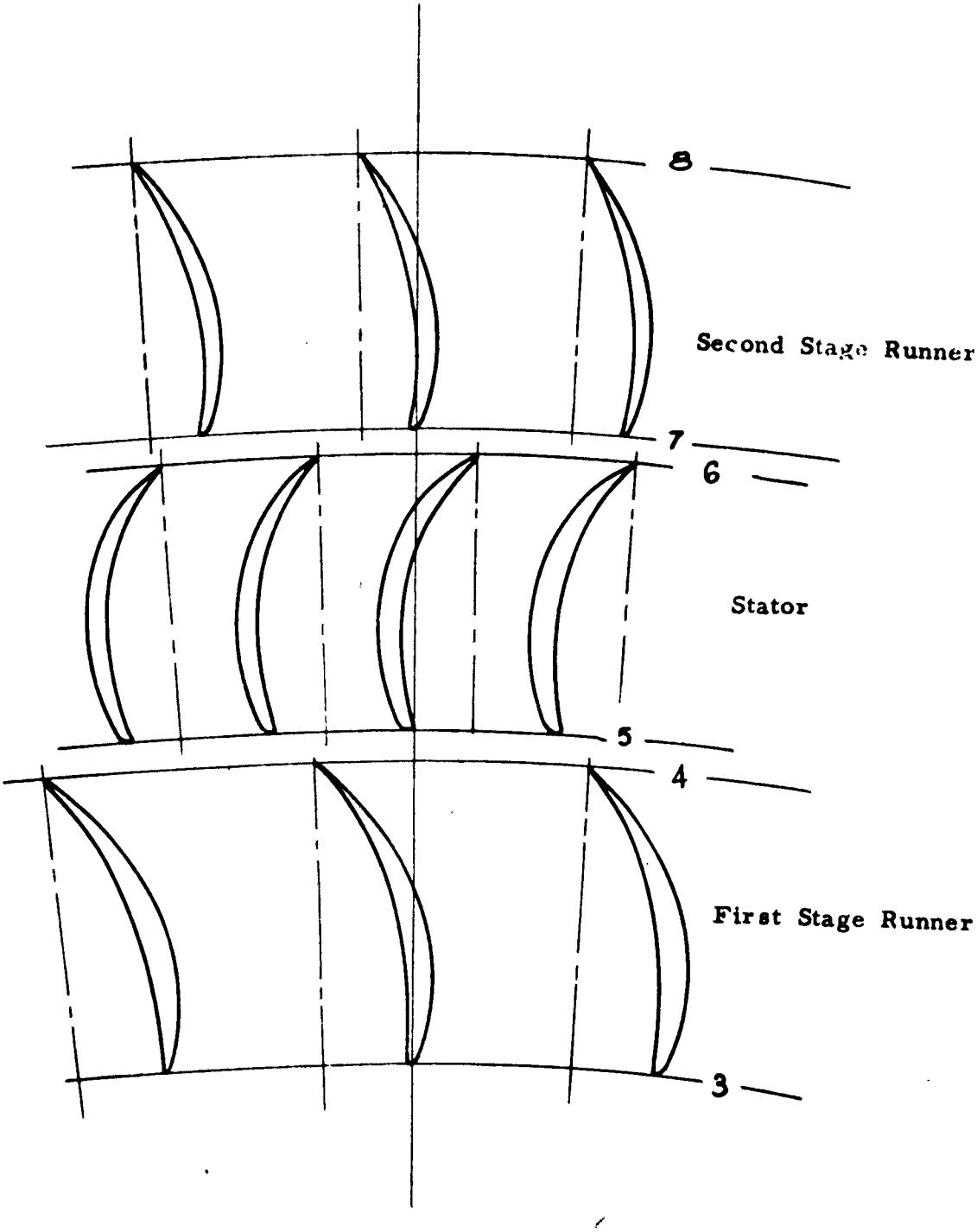

Approximate Vane Layouts
First and Second Stage
of Secondary System

Figure 29

CHAPTER VIII

TRANSFORMER WITH COUNTER-ROTATING SECONDARY ELEMENTS AND ITS APPLICATION

In this chapter the advantages of using counter-rotating secondary elements will be briefly outlined. Any detailed description of machines and arrangements using this principle cannot be given in this report as the establishment of such details would constitute in itself an investigation of considerable magnitude.

In reading the preceding chapters it will have become clear that hydrodynamic speed reducers, with the possible exception of the separate pump and turbine (Chapter VI), will not achieve in the forms presented so far the Increased Speed Reductions that are needed to improve basically the Cavitation Characteristics of the external propelling mechanism. To be specific, a speed reduction of 15 to 1 will give for 5000 rpm primary speed a secondary speed of 333 rpm which is not substantially lower than the propeller speed commonly used on destroyers. To make as substantial contribution to the pressing problem of greater speed reduction, secondary speeds of less than 200 rpm should be made possible without demanding unduely low speeds of the primary steam or gas turbine, nor unduly large dimensions of the power transmitting machinery.

This problem can be solved to a very satisfactory degree if it is possible to use two coaxial secondary shafts with two counter-rotating propellers or jet-pump runners. By coupling the outer shaft, carrying the forward propeller or pump runner, to the transformer element that was previously described as stationary (casing), it is obviously possible to have the forward propeller or pump runner rotate as slowly as desired since the limit of zero speed of this element is represented by the transformers as described so far.

It will be shown presently that this arrangement is advantageous primarily in connection with an axial-flow pump-jet. For this reason Figure 30 illustrates the described arrangement in this connection.

If used with a transformer combining the primary and secondary elements in one casing (as shown) it should be clear from the preceding chapters that the inner shaft, connected with the rearward pump runner and with the First Secondary blade row (and others) of the transformer, cannot rotate at a lower speed than previously described on basis of the hydrodynamic relationship between the first secondary blade row and the primary runner. However in a pump-jet the slower running forward runner (connected to the slowly counter-rotating casing of the transformer) will increase the pressure at the inlet to the rearward jet pump runner. This increase in inlet pressure obviously tends to suppress cavitation at this runner which may render its higher speed quite acceptable, whereas a propeller in the open stream has at best a minor effect on the cavitation limits of a second propeller on the same axis. The problem is complicated by the fact that the counter-rotating forward runner increases the velocities relative to the rearward runner blades. Further investigation of this detail, however, clearly lies outside of the scope of the present report.

Both Secondary Elements can have very nearly the same torque. Specifically, the torque of the counter-rotating element will be lower than that of the other element just by the torque of the primary runner of the transformer. Therefore a counter-rotating pump-jet so driven does not require any stationary element since the changes in angular momentum produced by its two counter-rotating runners very nearly cancel each other The absence of a stationary system obviously invites the use of rotating shrouds for the jet-pump runners and no stationary casing. This brings the mechanical arrangement of the counter-rotating pump-jet much closer to that of conventional propellers than that of a pump-jet in a stationary housing. Figure 30 indicates that the resulting overall arrangement is, in principle, quite simple.

* * * *

In connection with open propellers the advantage of counter-rotation is probably limited to hydrodynamic speed reducers with separate pumps and turbines, as described in Chapter VI. In this case the hydrodynamically effective speed of the secondary element is the DIFFERENCE in speed between the two counter-rotating parts. Therefore the absolute speed of each element can be reduced to half of that of a corresponding singly rotating machine. Externally this means that one propeller is replaced by two propellers counter-rotating at half the speed of the single propeller, without changing the driving machinery appreciably in size or weight (assuming that the casing of the secondary turbine is permitted to rotate with the outer one of the two coaxial propeller shafts).

* * * *

THE PROBLEM OF REVERSING Counter-rotating Propelling Machinery can be solved in Principle by the classical method of using two transformers, one for Ahead, and one for Astern operation. Although the supply and withdrawal of the working fluid to and from the rotating casing is an obvious complication, there is no foreseeable reason why this and other problems of arrangement and design cannot be met by a competent and determined engineering effort.

Of course, other accepted methods of reversing can be considered, particularly the use of reversible pitch propellers or jet-pumps. It appears, however, that the mechanical problems encountered are greater with counter-rotating shafts than with the normal arrangement.

* * * *

THE SIZE OF A TRANSFORMER with Counter-rotating Secondary Elements will in general be somewhat less than with one Singly Rotating Output Shaft, because the head per stage (two rows) may in many cases be increased over that with stationary vane systems. This statement remains true under the (least favorable) assumption that the **HIGHER** of the two secondary speeds is used in the power-size-speed relations presented before (see equations (1), (12), and (14)). The number of stages shown in Figure 30 was chosen for reasons of representation and should therefore not be regarded in any sense as final.

When using a separate pump and multistage turbine the simplest comparison results from assuming counter-rotation of both elements at half speed although two different secondary speeds are equally possible. This decrease in speed is obtained without any increase in size of the secondary turbine, or, in other words, equation (12) applies when inserting for n_{II} the algebraic **DIFFERENCE** in speed between the two secondary shafts, e. g. twice the absolute speed of either shaft.

It should be clear that with reference to the **LOWER** of the two secondary speeds of a counter-rotating transformer, as well as with reference to the absolute speed of either of the two secondary shafts of a counter-rotating turbine, the size of the transformer or turbine is very substantially smaller than with any other type of hydrodynamic transmission, probably smaller than with any type of mechanical or electrical transmission as well.

* * * *

THE CONCLUSION from this consideration of counter-rotating hydrodynamic transmissions is that (1) by this principal it is possible to achieve very much lower effective speeds of the external propelling mechanism than with other types of hydrodynamic transmissions, that (2) in this respect the counter-rotating hydrodynamic transmission may be superior to other types of transmissions of any type, and that (3) the speeds of the external propulsion device (propellers or pump) can thereby be lowered sufficiently to meet the foreseeable requirements of their cavitation-free operation.

* * * *

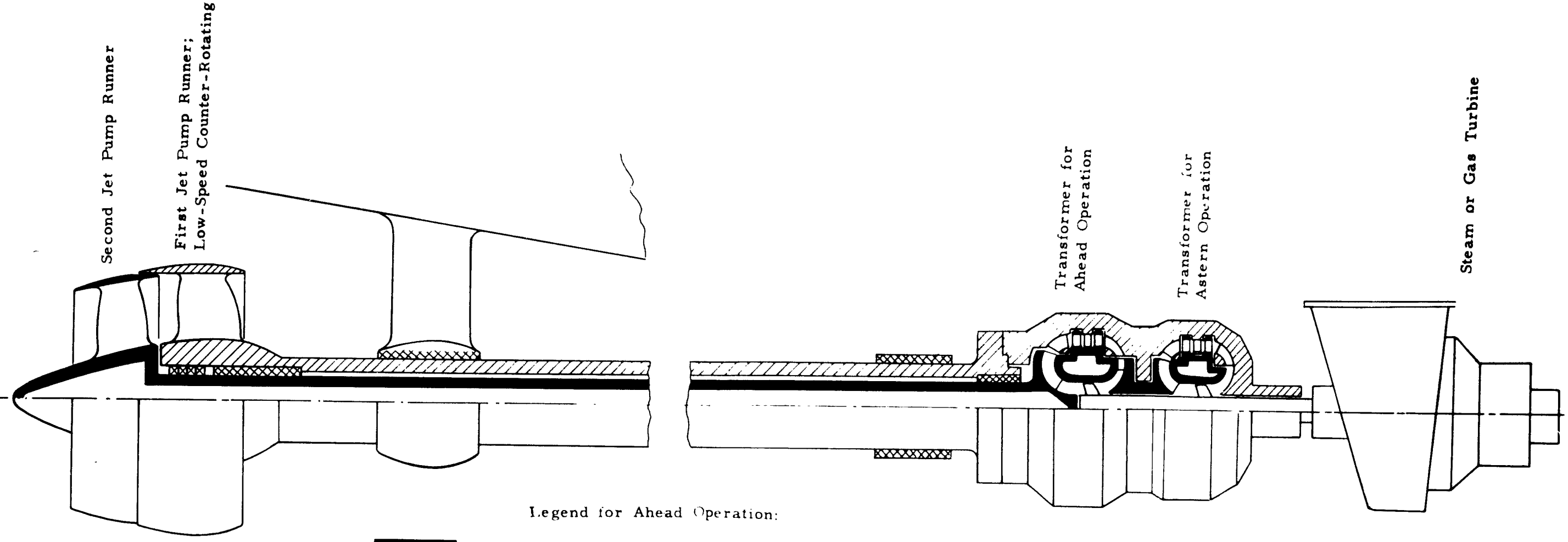

Legend for Ahead Operation:

Forward Rotating Parts (example: 300 rpm)

Counter-Rotating **P**arts (example: 120 rpm)

Main Bearing, Stationary and Counterrotating

Diagrammatic Layout of Counter- Rotating Transformer and Pump Jet Combination

Figure 30

References:

1. "Die neueste Ausfuehrung des Foettinger-Transformators" by Dipl. Ing. Wjlhelm Spannhake. Zeitschrift des Vereines Deutscher Ingenieure, 1913, page 721.

2. "Die Transformatorenanlage des Seebäderdampfers ' Koenigin Luise' der Hamburg-Amerika-Linie." Zeitschrift des Vereines Deutscher Ingenieure, 1914, page 481.

3. "Fluid Mechanics of Turbomachinery" by George F. Wislicenus. McGraw-Hill Book Co., 1947.

4. "Systematic Two-Dimensional Cascade Tests of NACA 65-Series Compressor Blades at Low Speeds." NACA RM L51 G31 - CONFIDENTIAL.

5. "Hydraulic Jet Propulsion and Incipient Cavitation" Report I-6, Part A. Mechanical Engineering Department, The Johns Hopkins University, March 1952 - CONFIDENTIAL.

HYDRODYNAMIC SPEED REDUCERS FOR SHIP DRIVE

Part B

EXPERIMENTAL INVESTIGATION AND THEORETICAL ANALYSIS OF AN AXIAL FLOW PRIMARY STAGE.

By

W. G. Rose

Chapter I.
The Experimental Investigation

1. The Immediate Objectives of the Experimental Investigation.

Employment of an axial-flow vane system as the pump (primary runner) of a hydraulic speed reducer introduces many new problems, some of which can be anticipated and some which cannot. The investigation to be presently reported strives toward two ends; the first, to identify any unpredicted phenomenon and enable evaluation of its effects; the second, to provide information that will allow quantitative attack on those problems that are foreseen.

It was expected that the most critical portion of the flow passage, Figures 1 and 2, would be the 90-degree bend (henceforth called the quadrant) beginning immediately downstream of the primary runner and extending to the inlet of the proposed first turbine stage. The working fluid in travelling through this section is subjected to turning and, if possible, diffusion. The limit to which diffusion is possible without the flow separating from the bounding walls must be determined. Flow in an actual torque converter experiences an additional effect in passage through this same section; namely, that due to the rotation of the bounding walls at the speed of the secondary. It is expected that this rotation would tend to forestall separation; whatever the effect, its magnitude must be determined.

An additional objective is realized by the investigation. It provides information on the real flow, which can be compared with theoretically predictable characteristics of this flow field.

2. Test Facilities

The experimental set-up employed in attaining the aforementioned objectives is shown in Figures 1, 2, 3 and 4. The unit intakes from and discharges to the atmosphere; and the working fluid is air.

The major elements comprising the unit are casing walls constructed of mahogony, cylindrical inlet guide-vanes, a ten-blade axial-flow pump runner, Figure 5, and an adjustable discharge throttle for regulating the operating conditions. Those sections of the casing walls adjacent to the pump runner are one-half inch plastic inserts which can be removed to vary the width of the quadrant discharge, Figures 1 and 5. In addition, the casings bounding the quadrant can be rotated at a speed dictated by the amount of speed reduction required. Downstream of the quadrant, the walls are fixed aluminum plates. Power for the primary of the pump drive is supplied by a 40 H. P. motor running at 3580 RPM. Drive for the quadrant walls is drawn from a D. C. variable speed source.

3. Instrumentation

Measurement of the quantities necessary to define the three-dimensional flow field, wherein large gradients of these quantities exist, was accomplished by the design of a special traversing mechanism. The distinguishing feature of this traversing mechanism (See Figures 6, 7, 8, and 9) is that with it the probe can be given any orientation, while the impact end of the probe head is maintained on a point of the traversing path, Figure 9. Freedom to adjust the probe in the following manner was found necessary:

1. motion across the flow passage with the impact end remaining on a line (the path of traverse)

2. rotation of the probe stem about the impact end as center in any plane containing the path of traverse

3. rotation of the probe head in a plane normal to the path of traverse with the impact end as center.

In order to obtain the motions of 2 and 3, the distance from the impact end to the point at which the stem is fixed to the carriage of the traversing mechanism, Figure 7, is maintained constant; while the point at which the stem is fixed moves on an arc whose radius equals this distance. This accounts for motion in one plane containing the traversing path. To orient the probe head into any such plane, the traversing arm and carriage rotates as a unit about the impact end as center. All directional measurements were accurate to within one degree.

The following probe-types were used; a kiel probe for measuring total pressure, a yaw-probe and a pitch-probe for recording the direction of the absolute flow, and a static pressure-probe, Figure 10. Calibration of the probes was conducted in a low turbulence tunnel, Figure 11, where the flow direction was known. The kiel probe and the static probe response to flow incidence was determined. The directional probes were calibrated to obtain their null reading position relative to the known flow direction. All directional measurements were obtained by nulled readings.

Static pressure distributions along the inner and outer casings of the quadrant were taken from wall taps whose locations are shown in Figure 4.

All pressures were read on calibrated inclined manometers, excepting low pressures requiring the use of a micro-manometer capable of reading to within 0.001" of water. The accuracy required of these pressure measurements has been ± 1% of the local average dynamic pressure for the section.

Further measurements necessary are concerned with the determination of energy input to the system. The primary drive shaft speed and torque output, taking into account the bearing drag, complete the variables to be determined. In detail, the torque was metered by strain gages attached to a torque tube of 3/4" cold-rolled steel from which the driving motor was suspended. The strain gages were positioned on this tube with three purposes in mind: the first being elimination of any variation in strain indication with temperature change; the second freedom from variations due to changes in axial-loading of the primary drive shaft, and the third maximum sensitivity of the measuring system. To realize these desires two active gages were employed, each placed in opposing legs of the indicator bridge circuit. The gages were glued on opposite sides of the tube at 45-degrees to its axis with their major axes in a common plane. With this arrangement of the gages a torsional load places one gage in tension and the other in compression, thereby giving the bridge circuit double the unbalance it would have if one active gage were used. Changes in temperature or axial-loading effect the same increment of resistance in the bridge legs with no net effect on the balance of the bridge circuit. All such measurements were taken with a Baldwin portable strain gage indicator.

The torque metering system was calibrated so that the indicator readings were translated directly into horsepower by statically applying a known torque to the system and recording the indicator reading. Under actual running conditions a check of the calibration was found by adding and subtracting known torques. This served also as a check on the insensitivity of the metering system to changes in axial loading. The calibration was very stable and was checked before and after each run with no detectable change. The accuracy of the torque readings is ± 1% of the total torque input.

4. Preliminary Tests

The operating point of the unit selected for testing was determined by variation of the through-flow (controlled by the discharge throttle) until a maximum total-head rise for the system was obtained with no apparent stall of the primary runner. This operating condition was further investigated to ascertain if non-uniformities of the flow were present at the intake of the unit. Suspicion which arose in regard to the existence of non-uniformities was confirmed. It was found to occur because of the unit's position with respect to a room wall. Air from the discharge was reflected back to the intake over a small portion of the intake periphery.

A remedy was effected by placing baffles between the intake, discharge and offending wall. It was also determined by flag surveys that separation occurred in the discharge of the quadrant. Removal of two plastic inserts, immediately after the pump discharge eliminated this separation. The ratio of the quadrant inlet area to its discharge area was thereby reduced to unity and no static pressure recovery from the through-flow velocity at this section was attempted. Specifically, the separation had occurred on the outer casing wall (Ψ_o)[1] ; later on in the investigation, a very rapid pressure-rise was found to exist at this point.

To ascertain the effect of the rotation of the quadrant casing on the stream properties at the entrance of the proposed initial turbine stage, measurements of total pressure, static pressure and flow direction were taken in this section. To eliminate the effects of extraneous variables, the readings were taken at each point with the casing rotating and with no rotation, the probe remaining fixed. The rotational speed of the casing was approximately 300 RPM; which corresponds to an overall speed reduction for the unit of nearly 1/12. This test yielded no detectable change in flow direction, and an increase in total pressure in the neighborhood of the wall of 2%, decreasing to zero at 1/2 inch from the wall. The static pressure at the section was not changed. Therefore it was concluded that rotation of the quadrant casing had no significant effect on the flow.

5. Test Procedure

Detailed measurements were taken at the primary runner inlet and discharge and at the entrance to the proposed first stage turbine inlet. They were so selected as to allow evaluation of the following quantities at the designated sections: total energy, volume-rate-of-flow, and angular momentum. The variables measured were total pressure, flow direction, and static pressure. In order to translate these variables into the desired quantities, the absolute velocity was broken down into three components, utilizing the measured flow direction. The three components selected were the axial velocity, the radial velocity, and the peripheral velocity. A schematic diagram, Figure 9, shows the absolute velocity and its components in relation to the measured angles determining the flow direction.

---

[1] Ψ is to be distinguished from ψ (small psi) which refers to the pressure rise.

In order to be certain the non-uniformities which had previously been detected at the proposed turbine inlet were truly reduced to a negligible effect, four sample surveys about the periphery not symmetrically spaced were taken. The non-uniformities remaining were small and found to be due mainly to leakage through the connection of the stationary and non-stationary parts of the casing. The four surveys were averaged and the result used to define the properties of the stream at this section. The volume rate of flow computed from the average was within $\pm$ 1% of the values calculated from each separate survey. The average variation in total pressure for the four surveys was within 2% of its mean value.

The energy input was measured, as previously described. All variables were adjusted to a similar operating condition by a common base density of the fluid medium. Simultaneously with all readings note was made of the shaft speed and the variation in the reference pressure located downstream of the intake guide vanes.

6. RESULTS OF THE INVESTIGATION

The direct results of the measurements are presented in a dimensionless form. All pressures are represented by their ratio to the dynamic pressure $\rho U_o^2/2$ where (ρ) is the reference mass density. The velocities are given by their ratio to the tip speed U_o.

All linear dimensions are reduced by their ratio to the tip radius (r_o), or where more pertinent to the width of the passage n_o.

For each section traversed, the stream properties are plotted as a function of position with respect to the bounding walls, Figures 12, 13 and 14. Separate graphs compare similar quantities at the different sections, Figures 15, 16, 17 and 18, the independent variable being the stream function Ψ . These properties are total pressure, static pressure, meridional velocity, peripheral velocity and the angles measured to determine the orientation of the absolute velocity. In addition, the static pressure distributions along the inner and outer casing walls are plotted respectively as a function of the ratio σ_i / S_i and σ_o / S_o (see Figure 19). S_i and So are the total distances, measured along the runner and outer casing walls, extending from the blade center line to the proposed turbine inlet. The variables σ_i and σ_o specify the location of any point along this distance, relative to the blade center line.

Quantities derived from the preceding measurements are now presented along with the methods by which they were evaluated. The form of presentation is a heading denoting the quantity to be presented and its representative symbol. Listed under each heading are the definition of the quantity, or the method by which it is evaluated, and the results of the evaluation.

1. THE VOLUME RATE OF FLOW (Q)AS RECORDED AT THE THREE SECTIONS SURVEYED

$$Q = 2\pi \int_{r_i}^{r_o} r V_A \, dr \qquad \left[\frac{FT^3}{SEC}\right]$$

at the pump inlet and discharge.

$$Q = 2\pi r \int_{o}^{n_o} V_r \, dn \qquad \left[\frac{FT^3}{SEC}\right]$$

at the turbine inlet.

RESULTS

Location	$Q_{SECTION}\ \left[\frac{FT^3}{SEC}\right]$	The Through Flow Coefficient $\phi_0 = \frac{Q_{SECTION}}{A_{SECTION} \times U_0}$
Pump Inlet	148	O. 29
Pump Discharge	152	O. 29
Turbine Inlet	149	O. 25

Where A section refers to the cross-sectional area of the channel at the particular section considered.

2. **THE MEAN VALUE OF THE TOTAL PRESSURE (P_T)**

$$\overline{P}_T = \frac{2\pi}{Q_{SECTION}} \int_{r_i}^{r_0} V_A P_T \, dr \quad \left[\frac{lb}{FT^2}\right]$$ at the pump inlet and discharge

$$\overline{P}_T = \frac{2\pi r}{Q_{SECTION}} \int_{0}^{r_0} V_r P_T \, dn \quad \left[\frac{lb}{FT^2}\right]$$ at the turbine inlet

RESULTS

Location	$\overline{P}_T\ \left[\frac{lb}{FT^2}\right]$	Mean Pressure Rise Coefficient $\overline{\psi}_0 = \frac{\overline{P}_T}{\rho U_0^2/2}$	Power Measured at each section $H.P. = \frac{\overline{P}_T \times Q_{SECTION}}{550}$
Pump Inlet	-0.162	-1.48×10^{-3}	-0.044
Pump Discharge	34. 8	0. 317	9. 62
Turbine Inlet	34. 4	0. 313	9. 30

3. THE POWER ATTRIBUTABLE TO THE KINETIC ENERGY OF THE PERIPHERAL MOTION $(K.E.)_\theta$

$$(K.E.)_\theta = \rho\pi\int_{r_i}^{r_o} r V_A V_\theta^2 \, dr \quad \left[\frac{FT\text{-}lb}{SEC}\right]$$ at the pump discharge.

$$(K.E)_\theta = \rho\pi r\int_{o}^{n_o} V_r V_\theta^2 \, dn \quad \left[\frac{FT\text{-}lb}{SEC}\right]$$ at the turbine inlet

RESULTS

Location	$(K.E.)_\theta \left[\frac{FT\text{-}lb}{SEC}\right]$	$H.P = \frac{(K.E.)_\theta}{550}$
Pump Discharge	888	1.61
Turbine Inlet	125	O. 227

4. THE POWER ATTRIBUTABLE TO THE KINETIC ENERGY OF THE MERIDIONAL MOTION $(K.E.)_M$

$$(K.E.)_M = \pi\rho\int_{r_i}^{r_o} r V_A V_M^2 \, dr \quad \left[\frac{FT\text{-}lb}{SEC}\right]$$ at the pump discharge.

$$(K.E.)_M = \pi\rho r\int_{o}^{n_o} V_r^3 \, dn \quad \left[\frac{FT\text{-}lb}{SEC}\right]$$ at the turbine inlet.

RESULTS

Location	$(K.E.)_M \left[\frac{FT\text{-}lb}{SEC}\right]$	$H.P. = \frac{(K.E.)_M}{550}$
Pump Discharge	1.62×10^3	2.95
Turbine Inlet	1.16×10^3	2.11

5. THE POWER AVAILABLE AS STATIC PRESSURE $(\bar{P}_s \times Q_{SECTION})$

$$\bar{P}_s \times Q_{SECTION} = 2\pi\int_{r_i}^{r_o} r V_A P_s \, dr \quad \left[\frac{FT\text{-}lb}{SEC}\right]$$ at the pump discharge.

$$\bar{P}_s \times Q_{SECTION} = 2\pi r P_s\int_{}^{n_o} V_r \, dn \left[\frac{FT\text{-}lb}{SEC}\right]$$ at the turbine inlet.

RESULTS

Location	$\bar{P}_s \times Q_{SECTION}$ $\left[\frac{FT\text{-}lb}{SEC}\right]$	$H.P. = \frac{\bar{P}_s \times Q_{SECTION}}{550}$
Pump Discharge	2740	4.98
Turbine Inlet	3840	6.98

A summation of the preceding gives the following energy balance:

	Pump Discharge	Turbine Inlet
$(K.E.)_\theta$	1.61	0.227
$(K.E.)_M$	2.95	2.11
$\bar{P}_s \times Q$ section	4.98	6.98
Total	9.54 H. P.	9.32 H. P.
Measured Power	9.62 H. P.	9.30 H. P.
Un-balance	0.83% low	0.21% high

6. THE RATE OF FLOW OF ANGULAR MOMENTUM (M)

$$M = 2\pi\rho\int_{r_i}^{r_o} r V_A (r V_\theta)\, dr \quad \left[FT\text{-}lb\right]$$ at the pump discharge.

$$M = 2\pi\rho r^2 \int_0^{n_o} V r V_\theta \, dn \quad \left[FT\text{-}lb\right]$$ at the turbine inlet

RESULTS

Location	M [FT-lb]	
Pump Discharge	16.1	)
		) or an 11.8% reduction (see Figure 20)
Turbine Inlet	14.2	)

7. POWER INPUT TO THE SYSTEM

	H. P.
Measured by strain gages	11.2
Bearing drag determined experimentally	0.2
Net Input To the System	11.0 H. P.

8. EFFICIENCIES

It is expedient at this point to define a pressure-rise coefficient based on the net input to the system; which is 11.0 H. P. This pressure-rise coefficient will be denoted by the symbol ψ_I, and defined by the relationship

$$\psi_I = \frac{\text{(Net input to the system)x550}}{\overline{Q} \times \rho U_o^2/2}$$

Where $\overline{Q}$ is the mean value of the volume. Flow rates measured at the three sections surveyed. Therefore,

$$\overline{Q} = 149.7 \left[\frac{FT^3}{SEC}\right]$$

Then

$$\psi_I = \frac{11.0 \times 550}{149.7 \times 109.5} = 0.369$$

The various efficiencies will now be defined and their values recorded.

a. Overall Efficiency

$$\eta_o = \frac{\text{The Pressure-Rise Coefficient at Turbine Inlet}}{\psi_I}$$

$$\eta_o = \frac{0.313}{0.369} = 84.8\%$$

b. Pump Efficiency

$$\eta_P = \frac{\text{The Pressure-Rise Coefficient at Pump Discharge}}{\Psi_I}$$

$$\eta_P = \frac{0.317}{0.369} = 85.8\%$$

c. Efficiency of the flow through the quadrant (η_Q) Based on the net power input to the system

$$\eta_Q = \frac{\eta_o}{\eta_P} = 98.8\%$$

d. Efficiency of the flow through the quadrant based on the power attributable to the total kinetic energy of the fluid at the pump discharge.

The total kinetic energy at the pump discharge (Power)

$$(K.E.)\ \text{Total} = (K.E.)_M + (K.E.)_\theta$$

$$= 1620 + 888 = 2508 \left[\frac{FT\text{-}lb}{SEC}\right]$$

Then $\dfrac{(K.E.)\ \text{total}}{Q_{SECTION} \times \rho U_o^2/2} = \dfrac{2508}{152 \times 109.5} = 0.151$

$$\text{The efficiency} = 1 - \frac{\Psi_o(\text{Pump Discharge}) - \Psi_o(\text{Turbine Inlet})}{(K.E.)\ \text{Total} / Q_{SECTION} \times \rho U_o^2/2}$$

$$= 1 - \frac{0.317 - 0.313}{0.151}$$

$$= 1 - \frac{0.004}{0.151} = 1 - 0.027$$

$$= 97.3\%$$

DISCUSSION OF THE RESULTS

Items evaluated in the previous section can now be utilized to check the validity and consistency of the data as recorded by measurements.

The major point of uncertainty in this experimental investigation is the accuracy of pressure and directional measurements in a fluctuating field, such as exists in the discharge of the rotating vane system. However, a possibility exists that allows substantiation of the values obtained in this region. The volume rate of flow is evaluated at three different locations along the stream path.

The three values of this flow rate agreed to within 1.33% of their mean value. The flow rates determined at the pump inlet and at the quadrant discharge agreed to within 0.33% of their average value.

The quality of the measurements taken at the pump inlet is limited only by the measuring accuracy of the probes, for in this section the fluid motion has no peripheral component and is very steady with respect to time. Conditions in the quadrant discharge are also favorable, that is, no curvature to the meridional streamlines, and small time-wise variations in the quantities measured. Therefore, the resulting agreement in flow rates lends substance to the values measured, and the methods employed in calculating these results.

As an overall check on the measurements, the energy balance given in the results shows good agreement with the measured mean total energy ; which is the most reliable information available. The discrepancies in the balance are within the previously stated accuracies of the measurements.

One item in the evaluation of results does not conform to expectations, that is the reduction in angular momentum occurring during passage of the fluid through the quadrant, Figure 20. As noted this amounted to a decrease of 11.8% of the entering fluid's angular momentum, an amount that cannot be accounted for by the action of wall shear. This section being a vane free space, some other explanation is necessary. Such an explanation can be supplied and leads one to believe that the reduction in the rate of flow of angular momentum is not a reality but only apparent and due to the methods of measurement in a fluctuating field. This same reasoning gives an explanation as to why the energy balance is not a contradiction in view of the loss in angular momentum.

The explanation referred to is the following:

Let V_A be the time mean of the axial velocity

V_θ be the time mean of the peripheral velocity

ΔV_A be the fluctuating component of the axial velocity

ΔV_θ be the fluctuating component of the peripheral velocity where all the values refer to a point. Then the angular momentum of a fluid particle possessing these values will be proportional to the product $(V_A \pm \Delta V_A)(V_\theta \mp \Delta V_\theta)$.

FIGURE 21

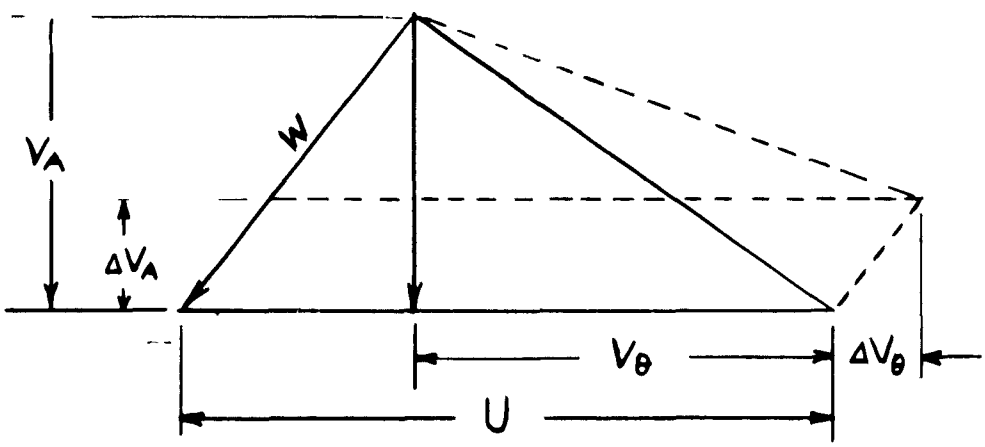

Figure 21 shows that for axial-flow pump runners, for which the circumferential velocity U is (as usual) larger than the circumferential component V_θ of the fluid velocity , a positive change in V_A is always associated with a negative change in V_θ, assuming only that the DIRECTION of the Relative flow remains approximately constant.

Now the measurements are time averaged, and if it is assumed that the probe reads a true time average value, then the angular momentum as it has been calculated in the evaluation of results is proportional to the product $V_A V_\theta$. It is suspected that this is the cause of the excessive reduction in angular momentum as recorded. The true time average value would be given by

$$\frac{1}{T}\int_0^T (V_A \pm \Delta V_A)(V_\theta \mp \Delta V_\theta)\, d\tau$$

where (τ) is an independent variable of time and (T) the period of the fluctuation. Now let the following relationship be the definition of K_M:

$$K_M = \frac{1}{(V_A V_\theta) \times T}\int_0^T (V_A \pm \Delta V_A)(V_\theta \mp \Delta V_\theta)\, d\tau$$

expanding the integrand gives

$$V_A V_\theta \pm \Delta V_A V_\theta \mp V_A \Delta V_\theta - \Delta V_A \Delta V_\theta$$

then taking time averages

$$K_M = \frac{1}{V_A V_\theta} (V_A V_\theta - \overline{\Delta V_A \Delta V_\theta})$$

or

$$K_M = 1 - \frac{\overline{\Delta V_A \Delta V_\theta}}{V_A V_\theta}$$

The conclusion is simply that K_M is always less than unity as the last term is always positive; therefore, the value of angular momentum, calculated at the pump discharge using time average values of V_A and V_θ, must be too large.

Similarly the effect of non-uniformities in V_A and V_θ on the evaluation of the kinetic energy of the peripheral motion can be found. As this energy is proportional to the product $V_A V_\theta^2$, let the definition of K_E be

$$K_E = \frac{1}{(V_A V_\theta^2) \times T} \int_0^T (V_A \pm \Delta V_A)(V_\theta \mp \Delta V_\theta)^2 \, d\tau$$

Then by expanding the integrand and taking a time average as indicated, and as previously done in the case of the angular momentum, the following expression for K_E is found:

$$K_E = 1 + \frac{\overline{\Delta V_\theta (V_A \Delta V_\theta - 2 V_\theta \Delta V_A)}}{V_A V_\theta^2}$$

Now the second term can be either positive or negative depending only upon the magnitude of V_A relative to V_θ, and of ΔV_θ relative to ΔV_A. Therefore, K_E can be greater than unity or less than unity.

An extension of this reasoning to allow an estimate of the magnitudes of K_E and K_M is carried out in the appendix I. Two specific relative velocity distributions are considered and K_E and K_M are evaluated for the particular pressure-rise coefficient ψ_0 and through-flow coefficient ϕ_0. with which the test results are concerned. This evaluation shows that K_M can readily assume values ranging from O. 9 to O. 8, and that its magnitude is mainly dependent upon the quality of the velocity distribution, that is its departure from a uniform distribution; and is not as sensitive to the form of the velocity distribution.

Values of K_M of this order of magnitude would readily account for the reduction in angular momentum encountered, which was approximately 12%. Relative velocity distributions with quality factors (defined in the appendix) that correspond to such values of K_M are commonly realized;and the conclusion that this reduction in angular momentum is only apparent seems to be a safe one. The effect on the evaluation of the kinetic energy, which gave good agreement in the experimental results for the same range

of quality factors as considered for the values of K_M just stated, is seen to be much less, K_E ranging from 0.97 to 1.04, than the effect on angular momentum. In fact, corrections of this magnitude are almost within the experimental accuracy.

The reason for basing the definitions of the efficiencies on the ratios of the pressure-rise coefficients is the necessity to differentiate between actual losses and apparent losses, attributable to the limited accuracy of the measurements. This limitation is, in part, avoided by employing the pressure-rise coefficients. These coefficients are derived from the most reliable quantity measured, the total pressure, and are insensitive to the inaccuracy of the volume flow measurements. This can be seen from their definition

$$(\overline{\gamma_0})_{SECTION} = \frac{1}{Q_{SECTION} \times \rho U_b^2/2} \int_0^{Q_{SECTION}} P_T \, dQ$$

The efficiencies as defined give a reliable result.

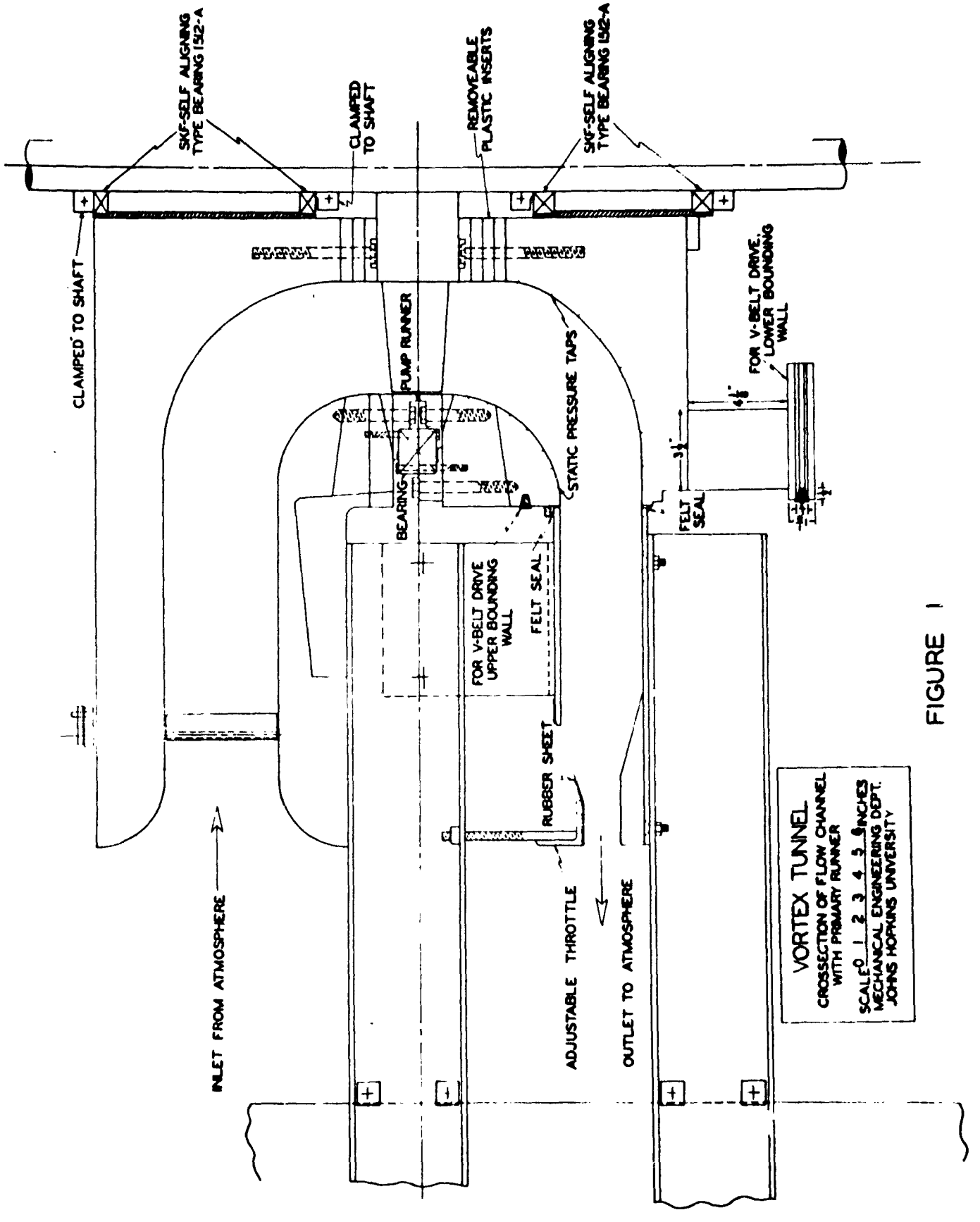
SKF-SELF ALIGNING TYPE BEARING 1312-A
CLAMPED TO SHAFT
REMOVEABLE PLASTIC INSERTS
SKF-SELF ALIGNING TYPE BEARING 1312-A
CLAMPED TO SHAFT
PUMP RUNNER
STATIC PRESSURE TAPS
FOR V-BELT DRIVE, LOWER BOUNDING WALL
BEARING
FELT SEAL
FOR V-BELT DRIVE UPPER BOUNDING WALL
FELT SEAL
RUBBER SHEET
INLET FROM ATMOSPHERE
ADJUSTABLE THROTTLE
OUTLET TO ATMOSPHERE
VORTEX TUNNEL
CROSSECTION OF FLOW CHANNEL WITH PRIMARY RUNNER
SCALE 0 1 2 3 4 5 6 INCHES
MECHANICAL ENGINEERING DEPT.
JOHNS HOPKINS UNIVERSITY

FIGURE 1

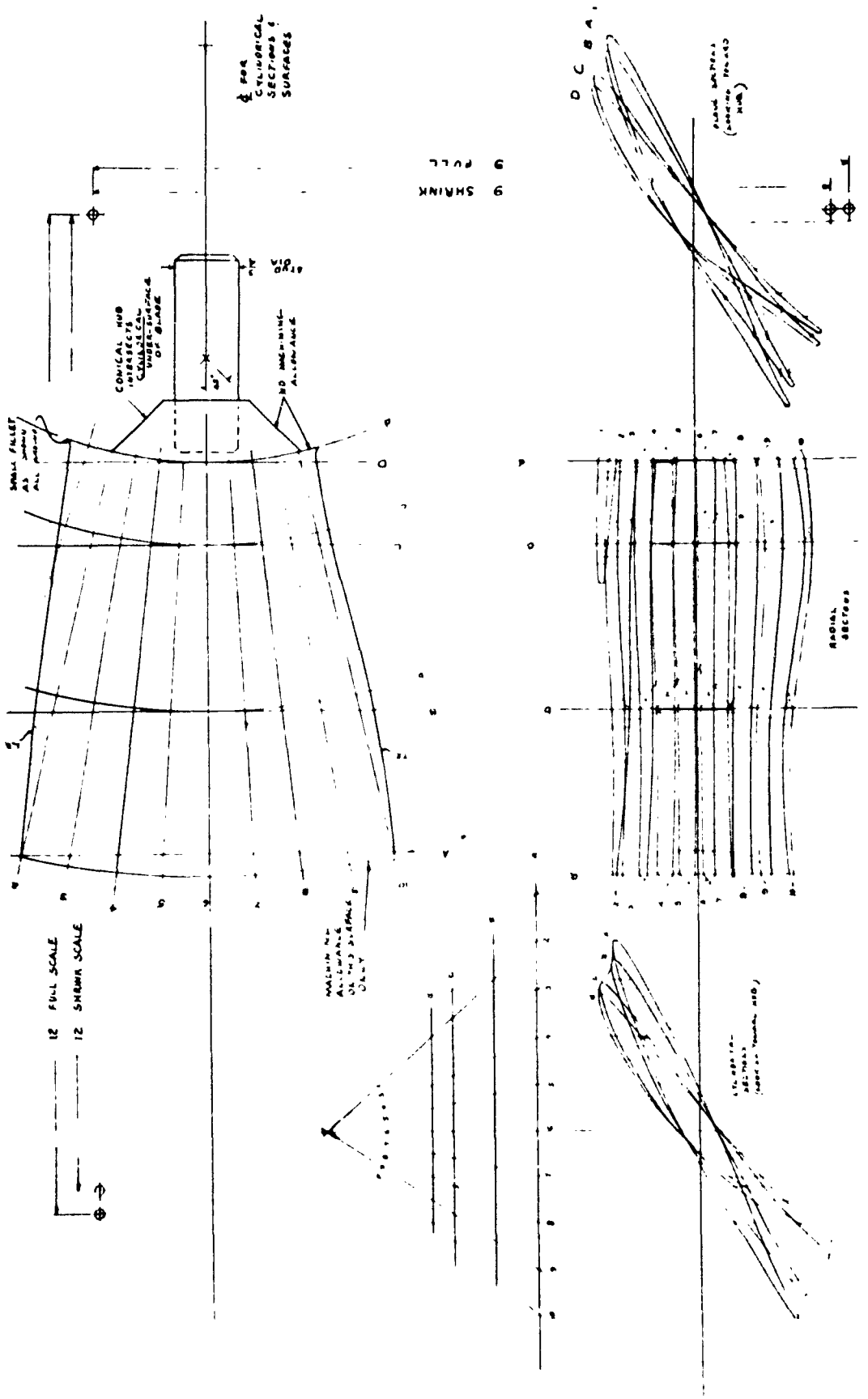

FIGURE 1A

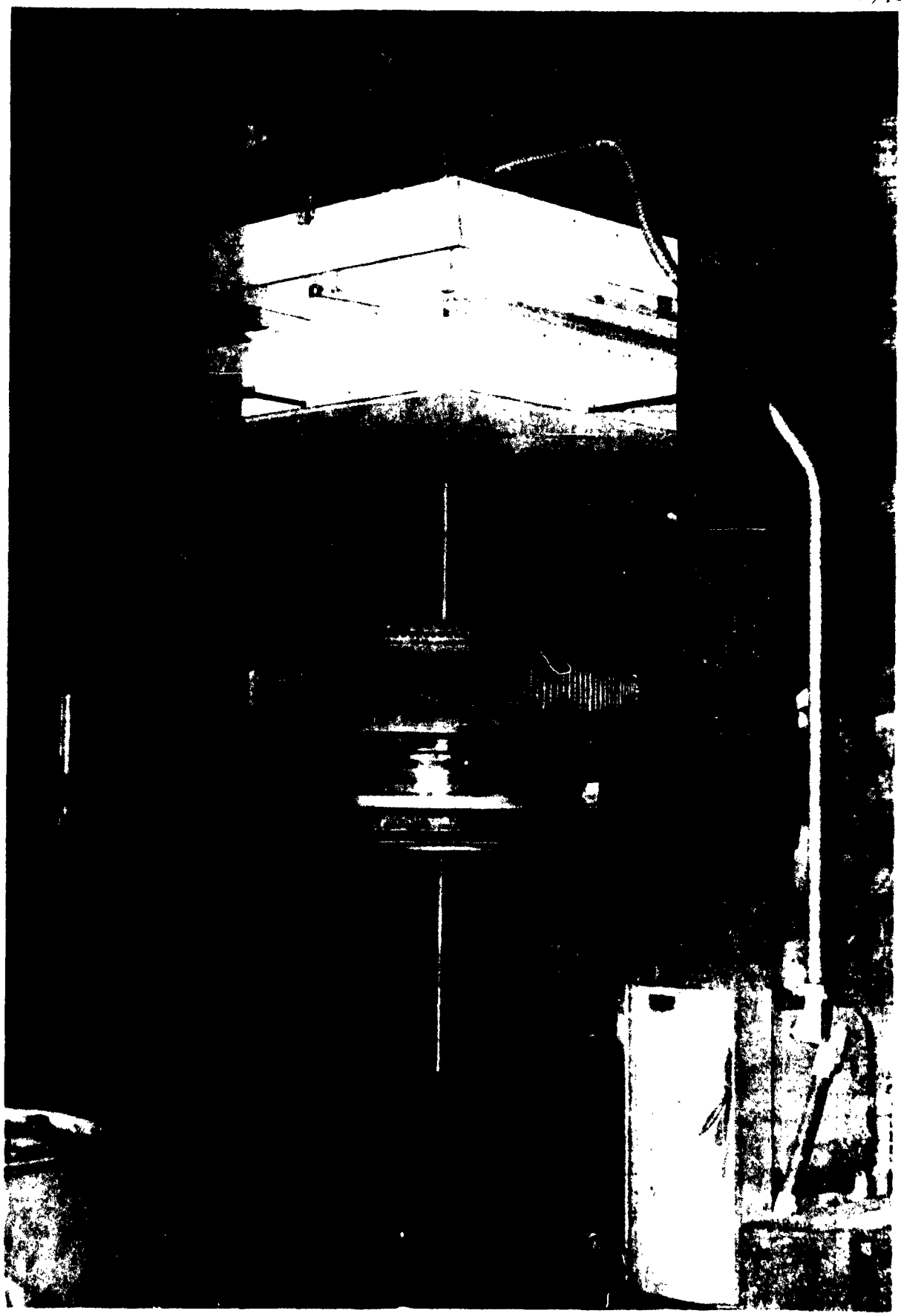

FIGURE 2

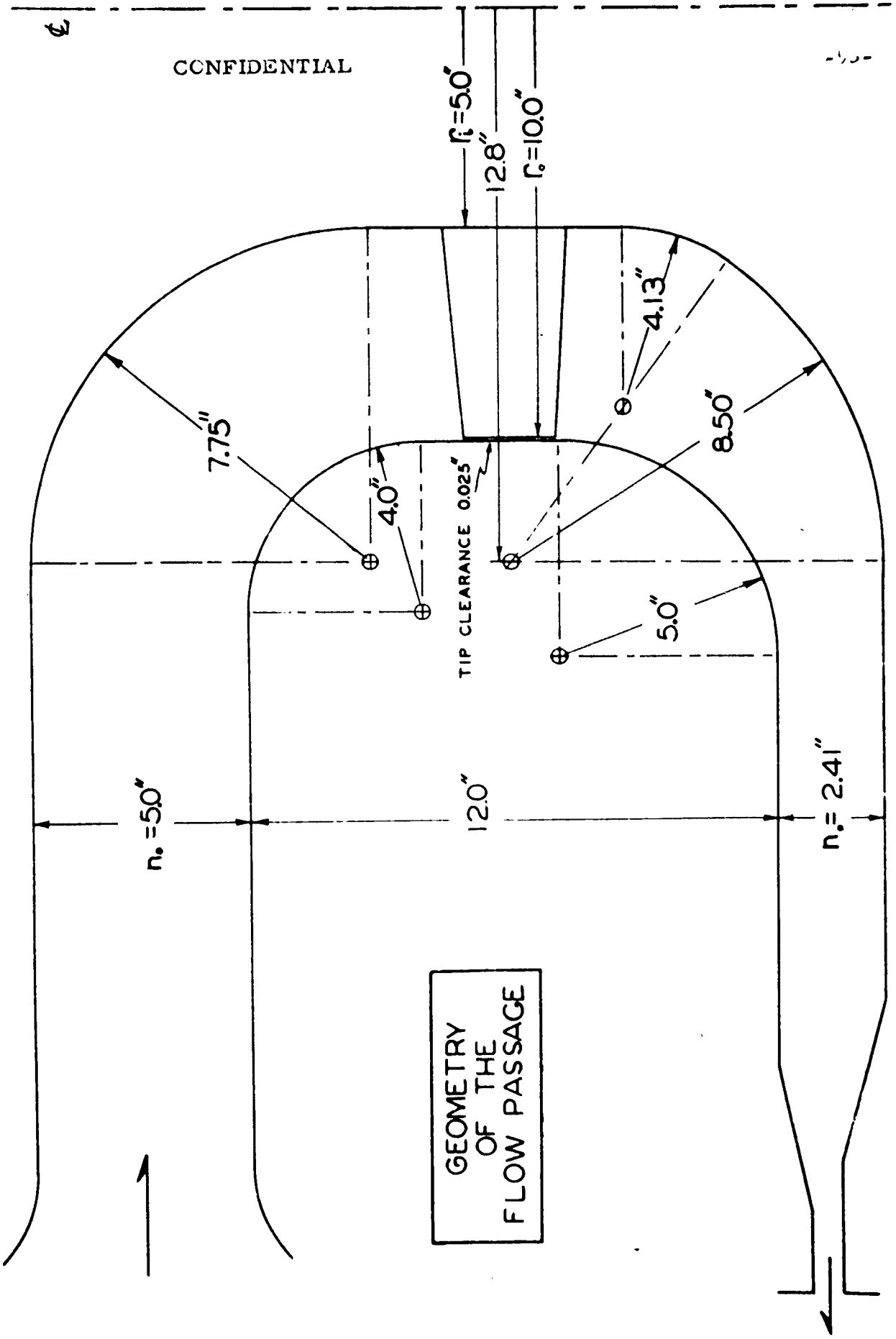
r_i=5.0"
12.8"
r_o=10.0"
4.13"
8.50"
7.75"
4.0"
TIP CLEARANCE 0.025"
5.0"
r_o=5.0"
12.0"
r_o=2.41"
GEOMETRY OF THE FLOW PASSAGE

FIGURE 3

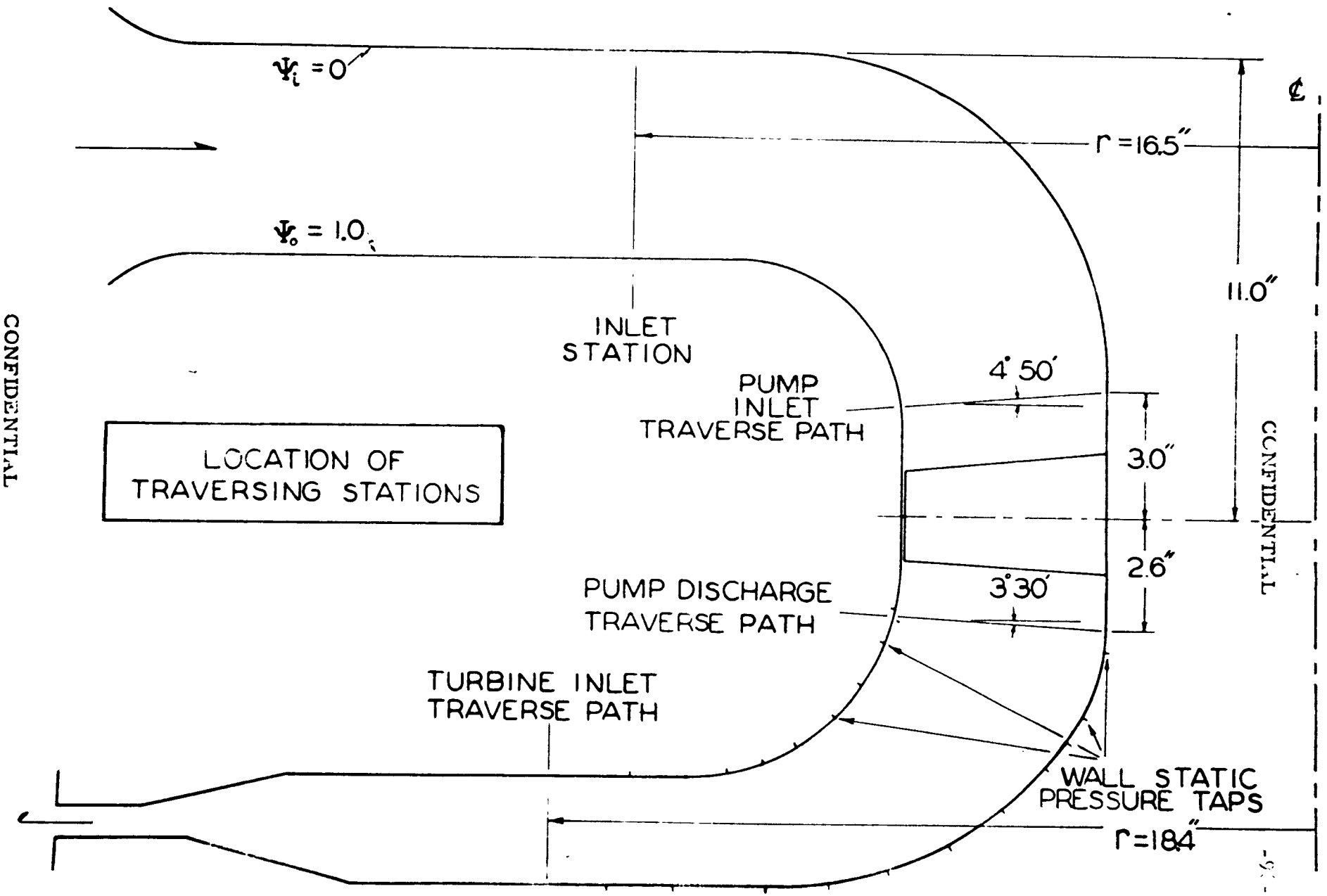

FIGURE 4

FIGURE 5

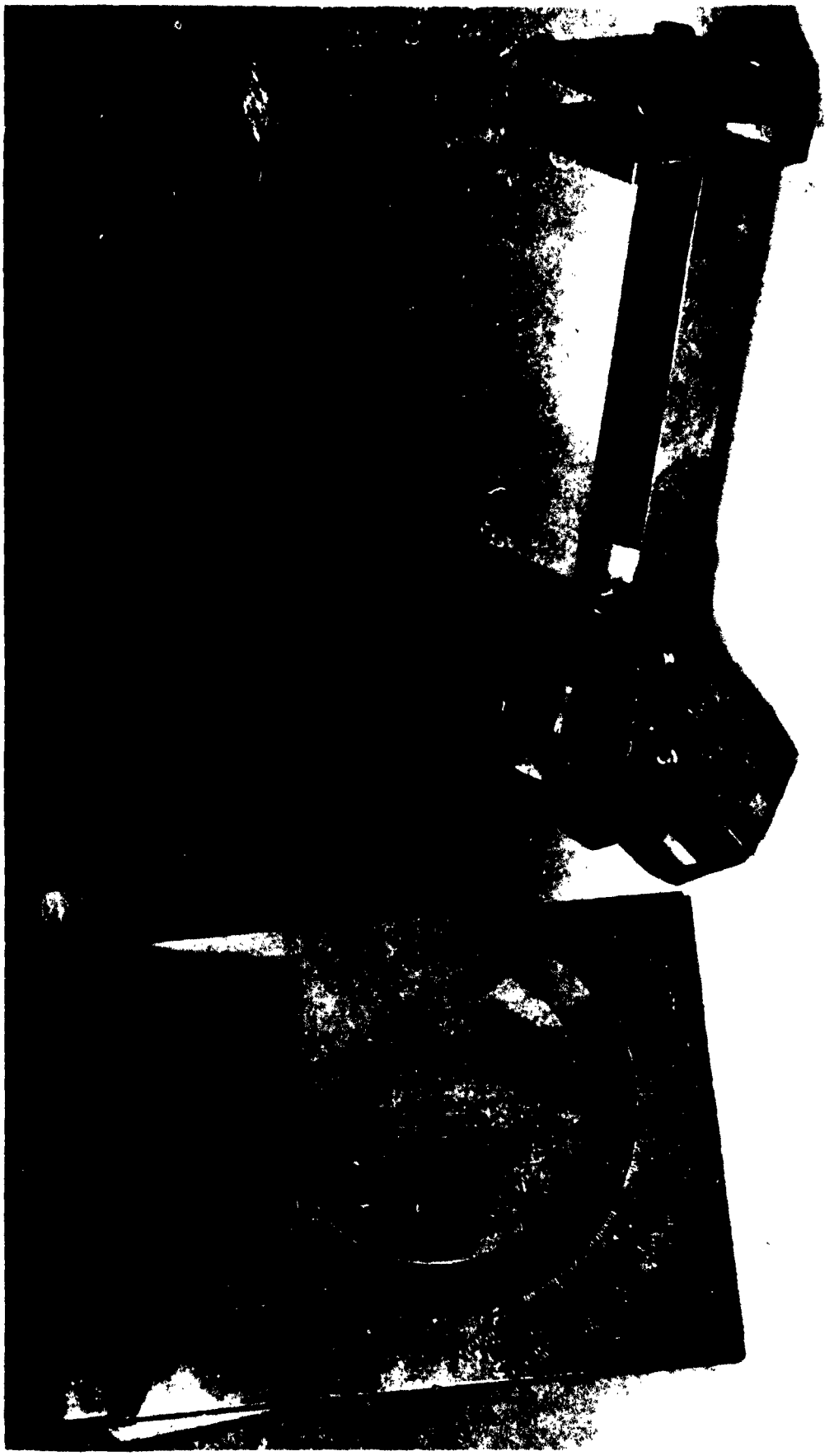

FIGURE 6

FIGURE 7

FIGURE 8

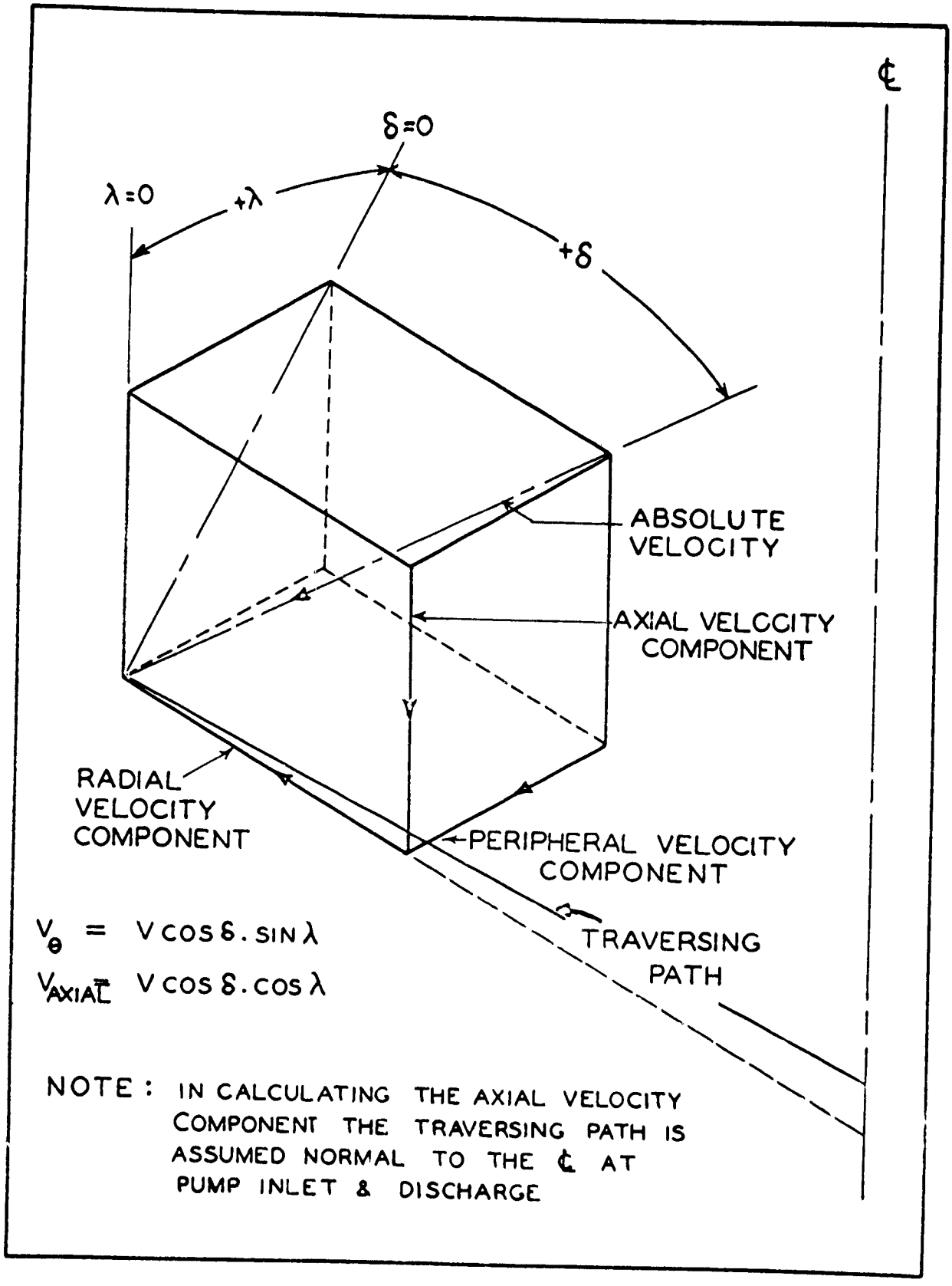

CONFIDENTIAL

FIGURE 9

FIGURE 10

FIGURE 11

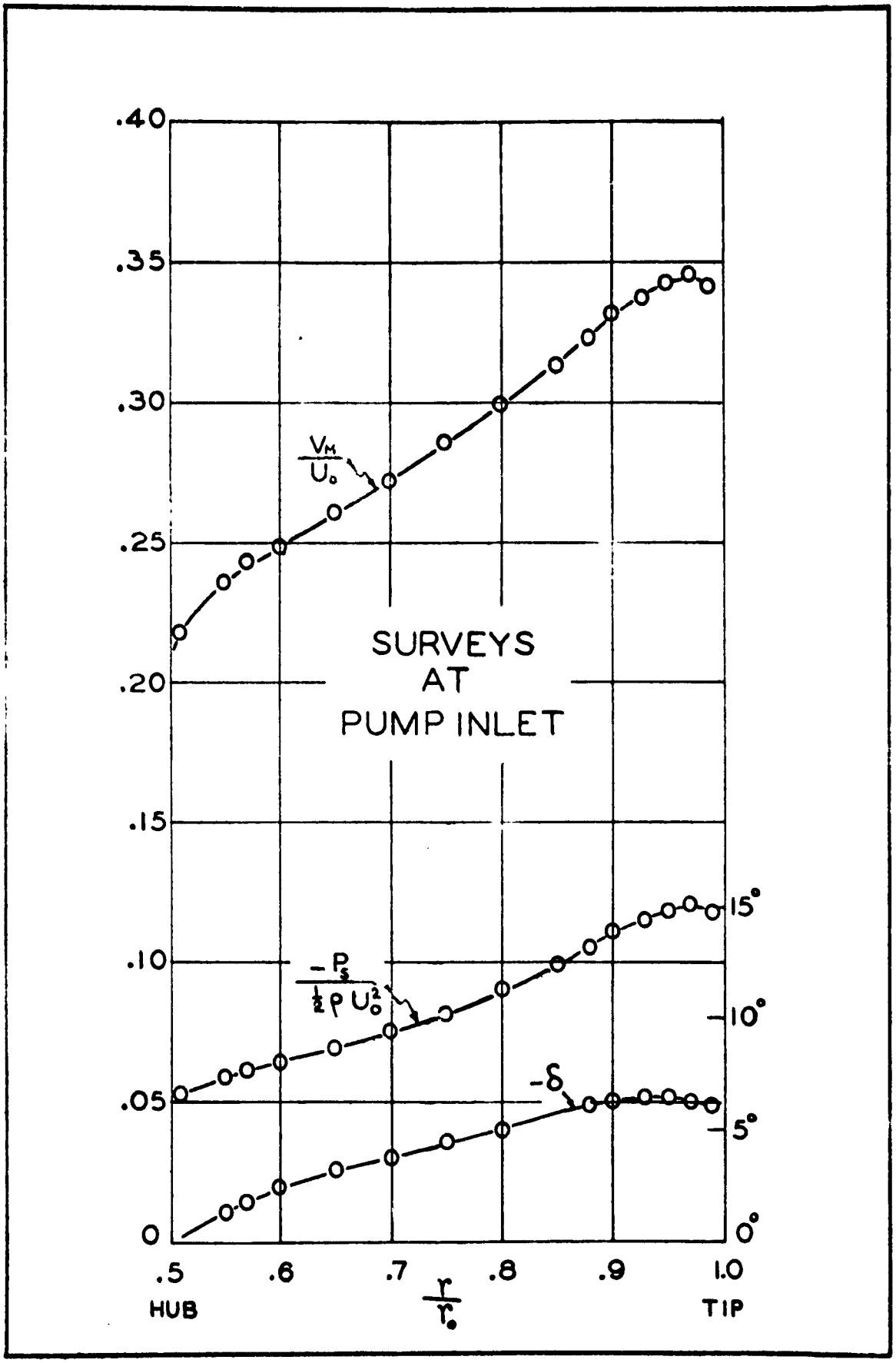
.40
.35
.30
.25
.20
.15
.10
.05
0
$\frac{V_M}{U_0}$
SURVEYS
AT
PUMP INLET
$\frac{-P_s}{\frac{1}{2}\rho U_0^2}$
$-\delta$
15°
10°
5°
0°
.5
.6
.7
.8
.9
1.0
HUB
$\frac{r}{r_0}$
TIP

FIGURE 12

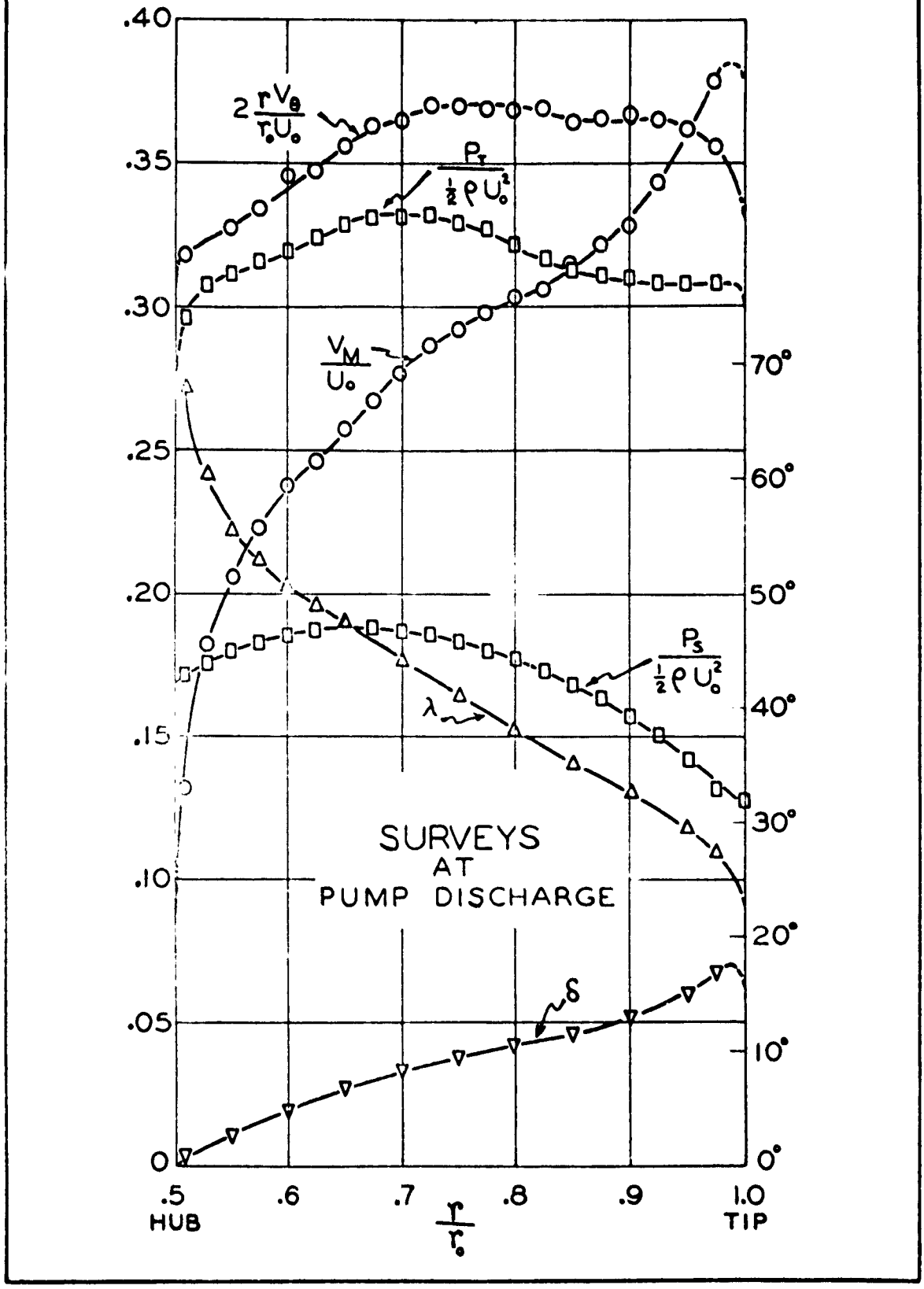
.40
.35
.30
.25
.20
.15
.10
.05
0
$2\frac{rV_\theta}{r_0U_0}$
$\frac{P_T}{\frac{1}{2}\rho U_0^2}$
$\frac{V_M}{U_0}$
$\frac{P_S}{\frac{1}{2}\rho U_0^2}$
λ
δ
70°
60°
50°
40°
30°
20°
10°
0°
SURVEYS
AT
PUMP DISCHARGE
.5
HUB
.6
.7
.8
.9
1.0
TIP
$\frac{r}{r_0}$

FIGURE 13

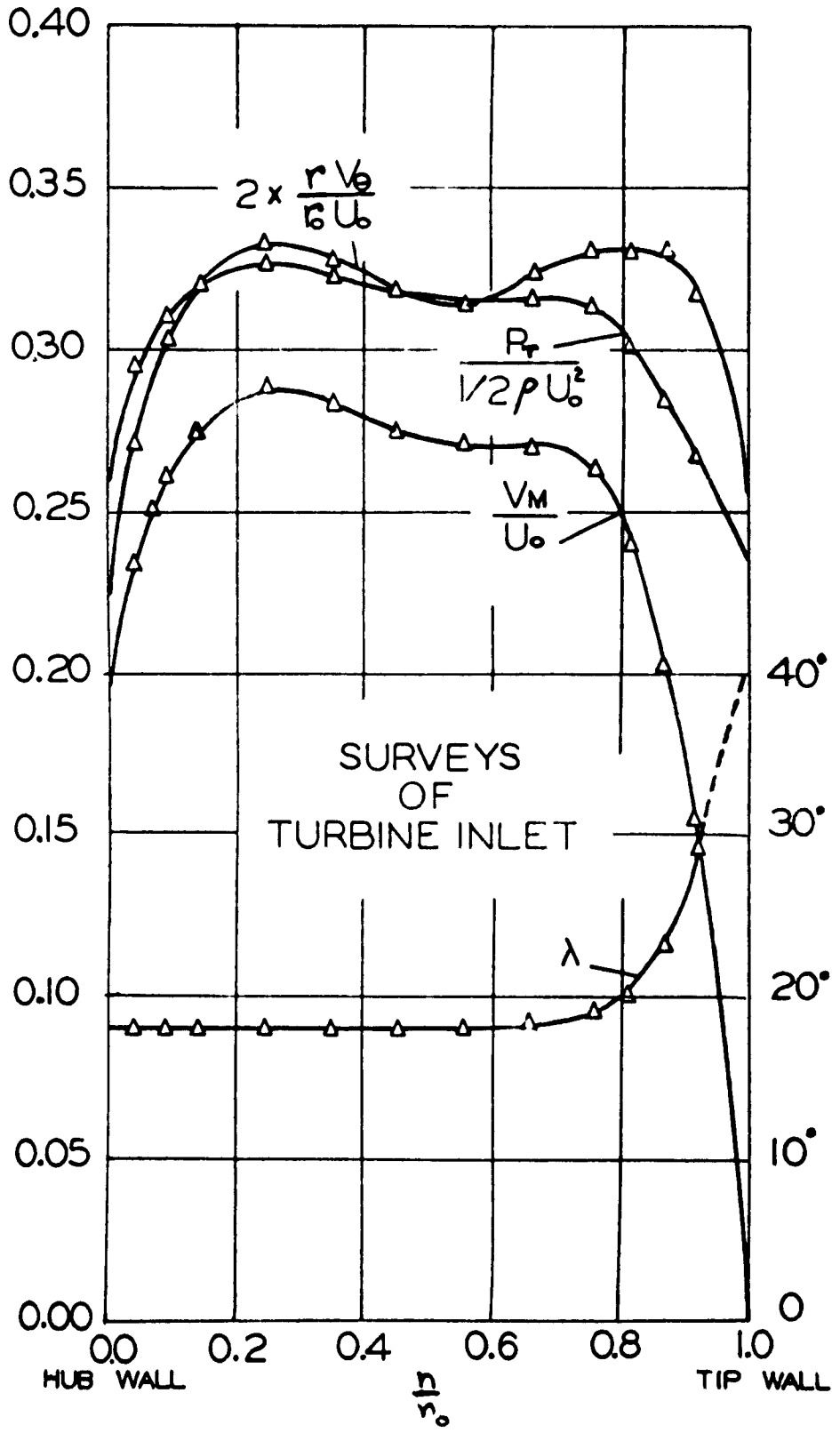

FIGURE 14

CONFIDENTIAL

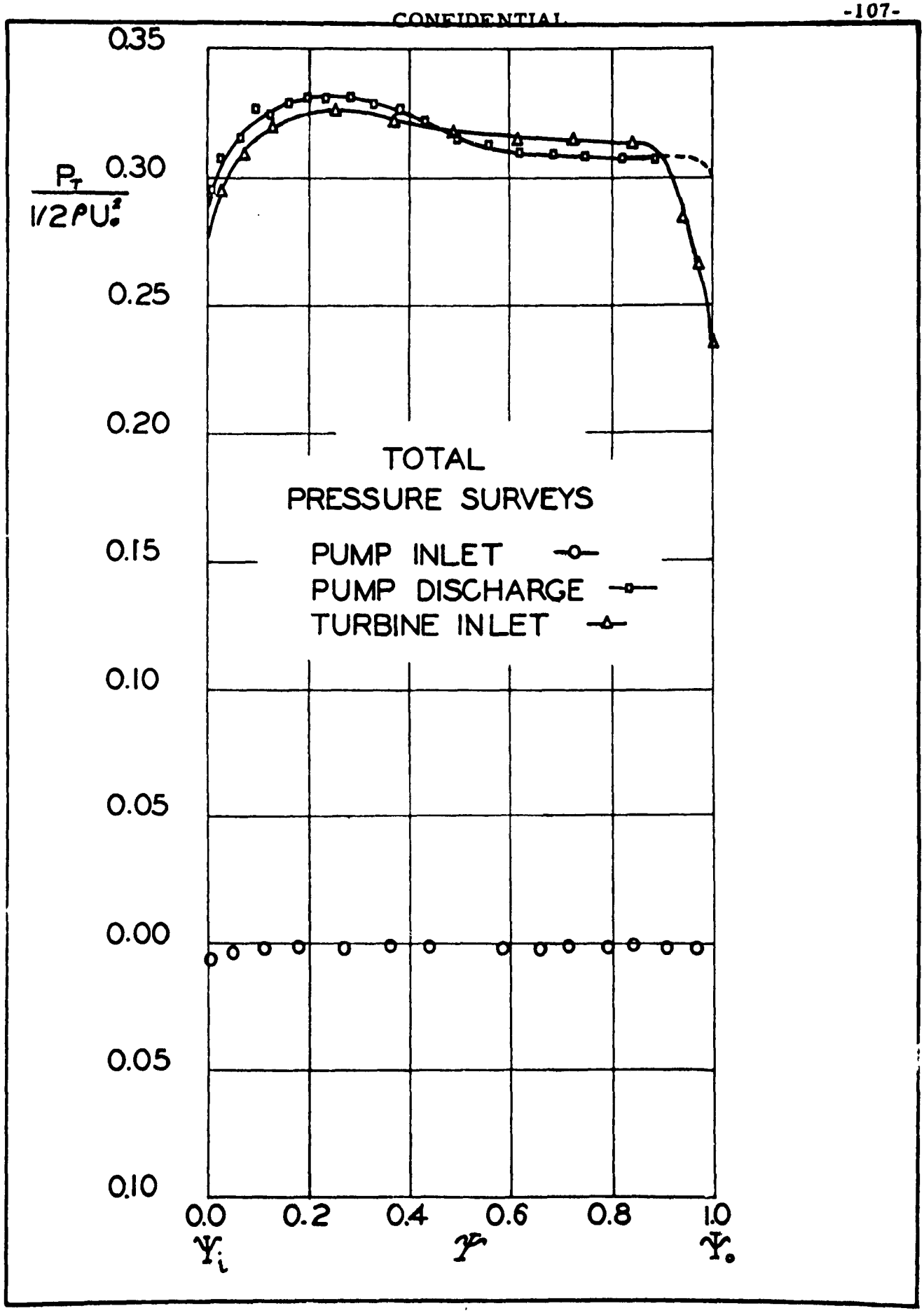
0.35
0.30
$\frac{P_T}{1/2 \rho U_\infty^2}$
0.25
0.20
0.15
0.10
0.05
0.00
0.05
0.10
TOTAL
PRESSURE SURVEYS
PUMP INLET
PUMP DISCHARGE
TURBINE INLET
0.0
0.2
0.4
0.6
0.8
1.0
Y_i
Y
Y_o

FIGURE 15

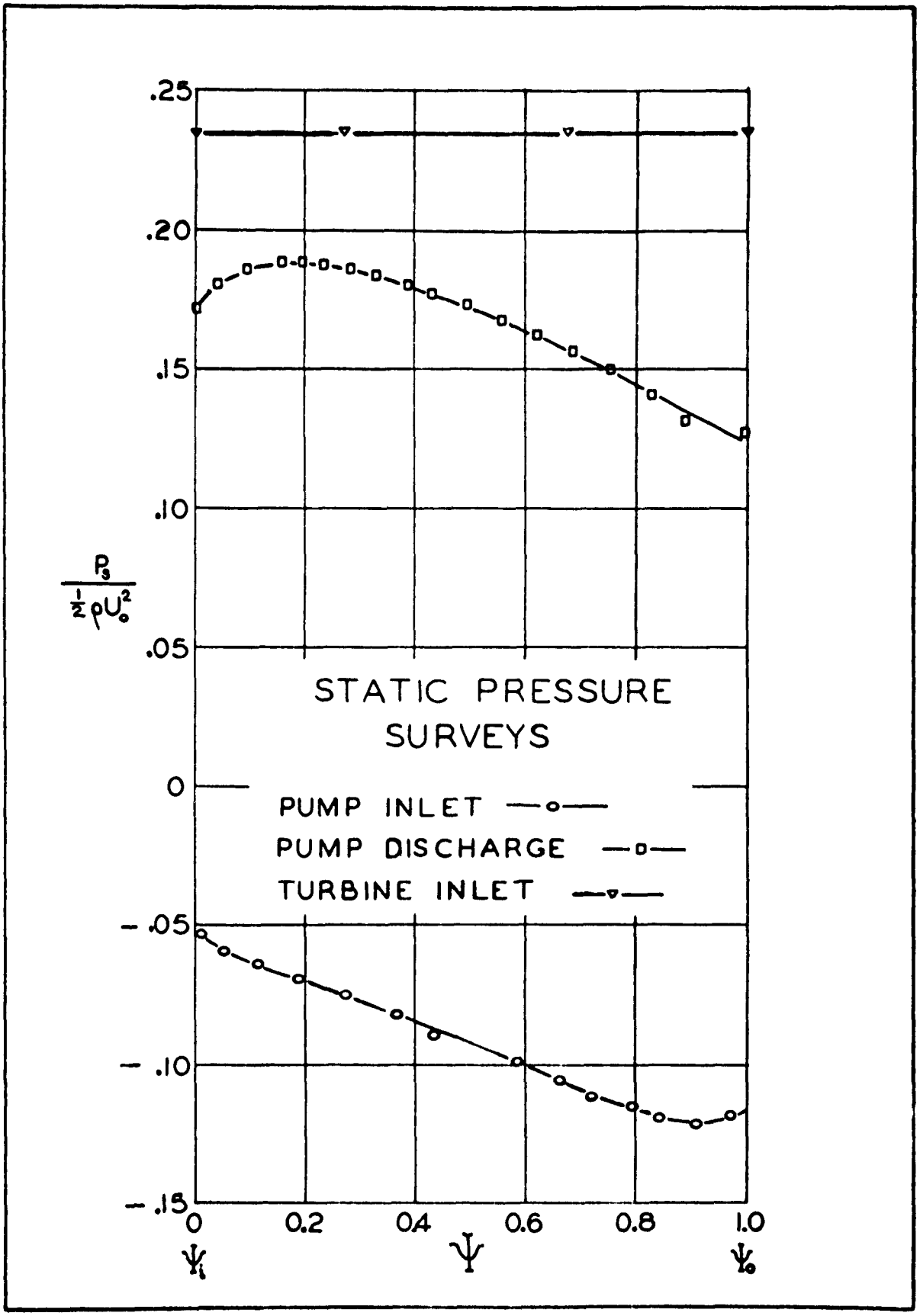
.25
.20
.15
.10
.05
0
-.05
-.10
-.15
$\frac{P_s}{\frac{1}{2}\rho U_o^2}$
STATIC PRESSURE SURVEYS
PUMP INLET
PUMP DISCHARGE
TURBINE INLET
0
0.2
0.4
0.6
0.8
1.0
Ψ_i
Ψ
Ψ_o

FIGURE 16

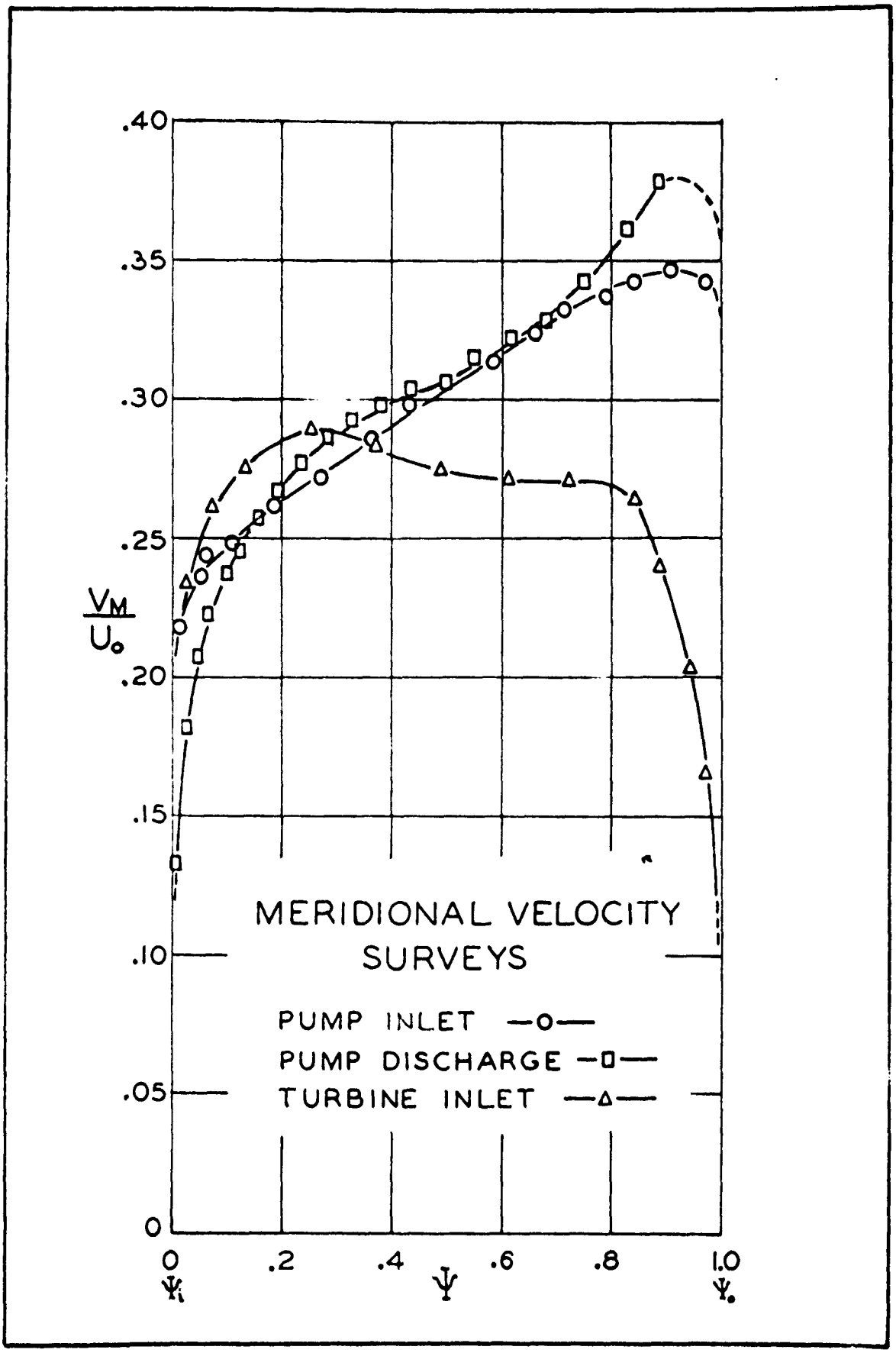
.40
.35
.30
.25
.20
.15
.10
.05
0
$\frac{V_M}{U_o}$
MERIDIONAL VELOCITY SURVEYS
PUMP INLET —o—
PUMP DISCHARGE —□—
TURBINE INLET —△—
0
.2
.4
.6
.8
1.0
Ψ_i
Ψ
Ψ_o

FIGURE 17

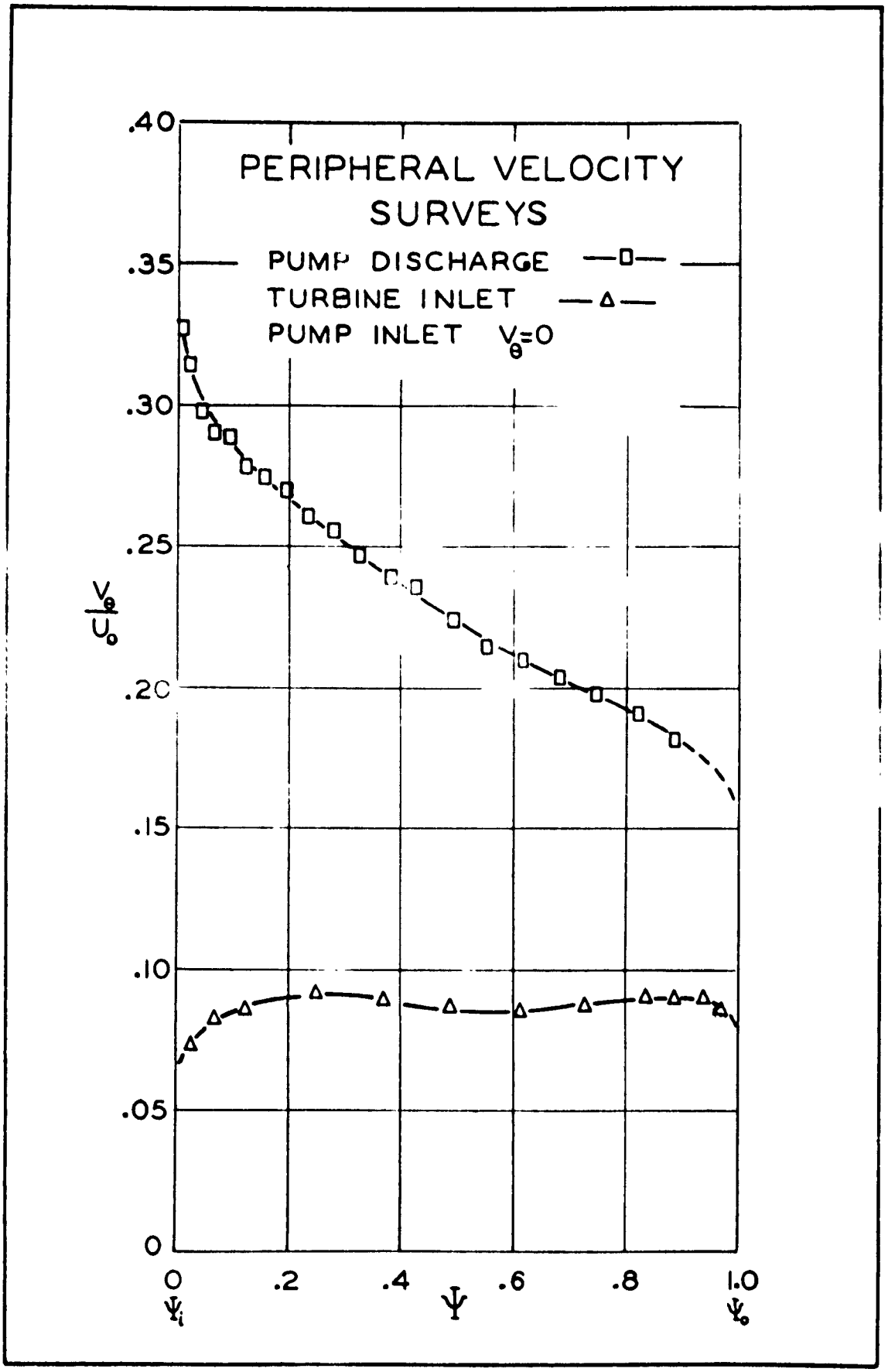
PERIPHERAL VELOCITY SURVEYS
PUMP DISCHARGE
TURBINE INLET
PUMP INLET $V_\theta = 0$
$\frac{V_\theta}{U_o}$
.40
.35
.30
.25
.20
.15
.10
.05
0
0
.2
.4
.6
.8
1.0
Ψ_i
Ψ
Ψ_o

FIGURE 18

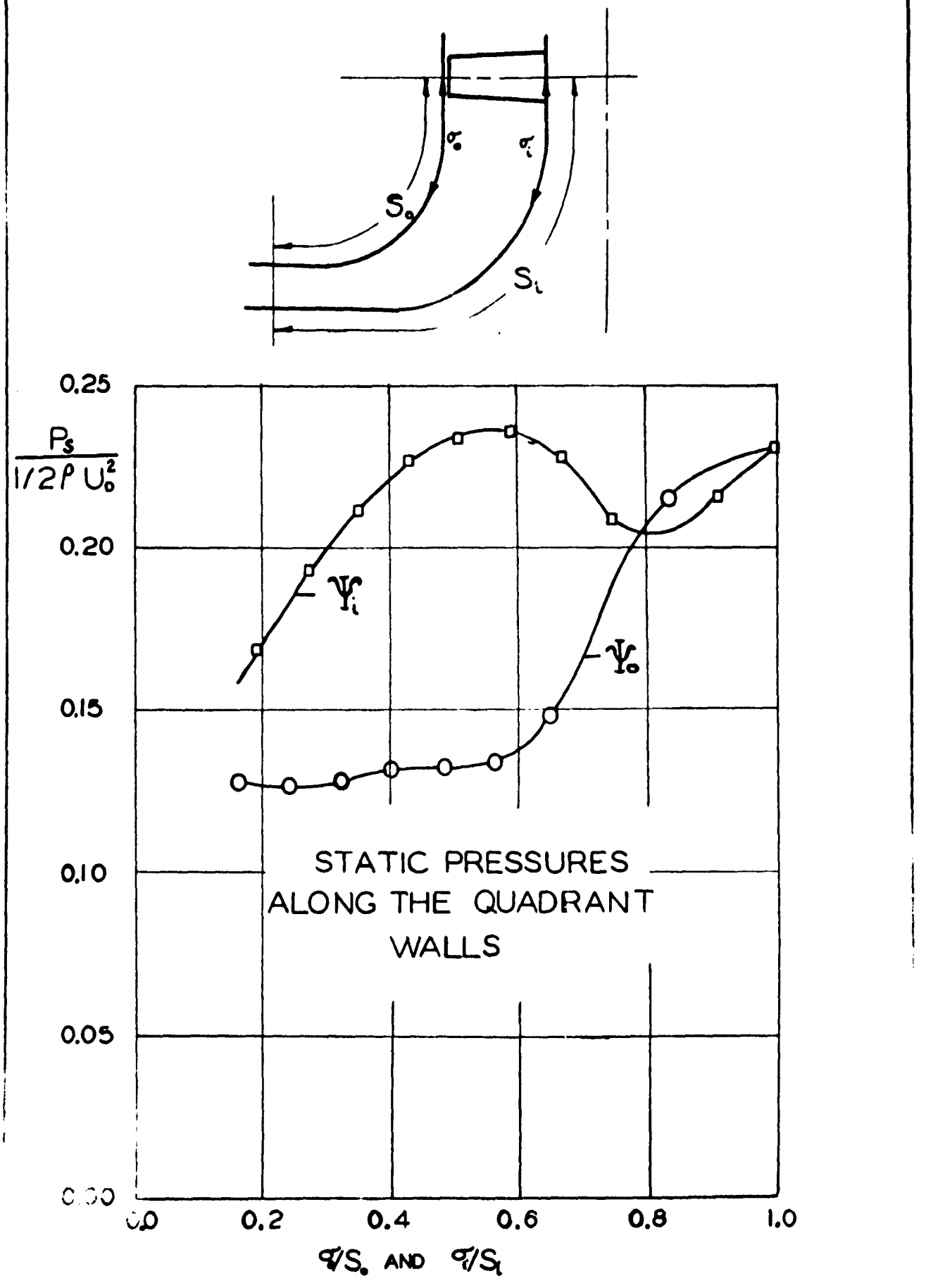
σ_o
σ_i
S_o
S_i
0.25
$\frac{P_s}{1/2 \rho U_o^2}$
0.20
0.15
0.10
0.05
0.00
Ψ_i
Ψ_o
STATIC PRESSURES ALONG THE QUADRANT WALLS
0.0
0.2
0.4
0.6
0.8
1.0
σ/S_o AND σ/S_i

FIGURE 19

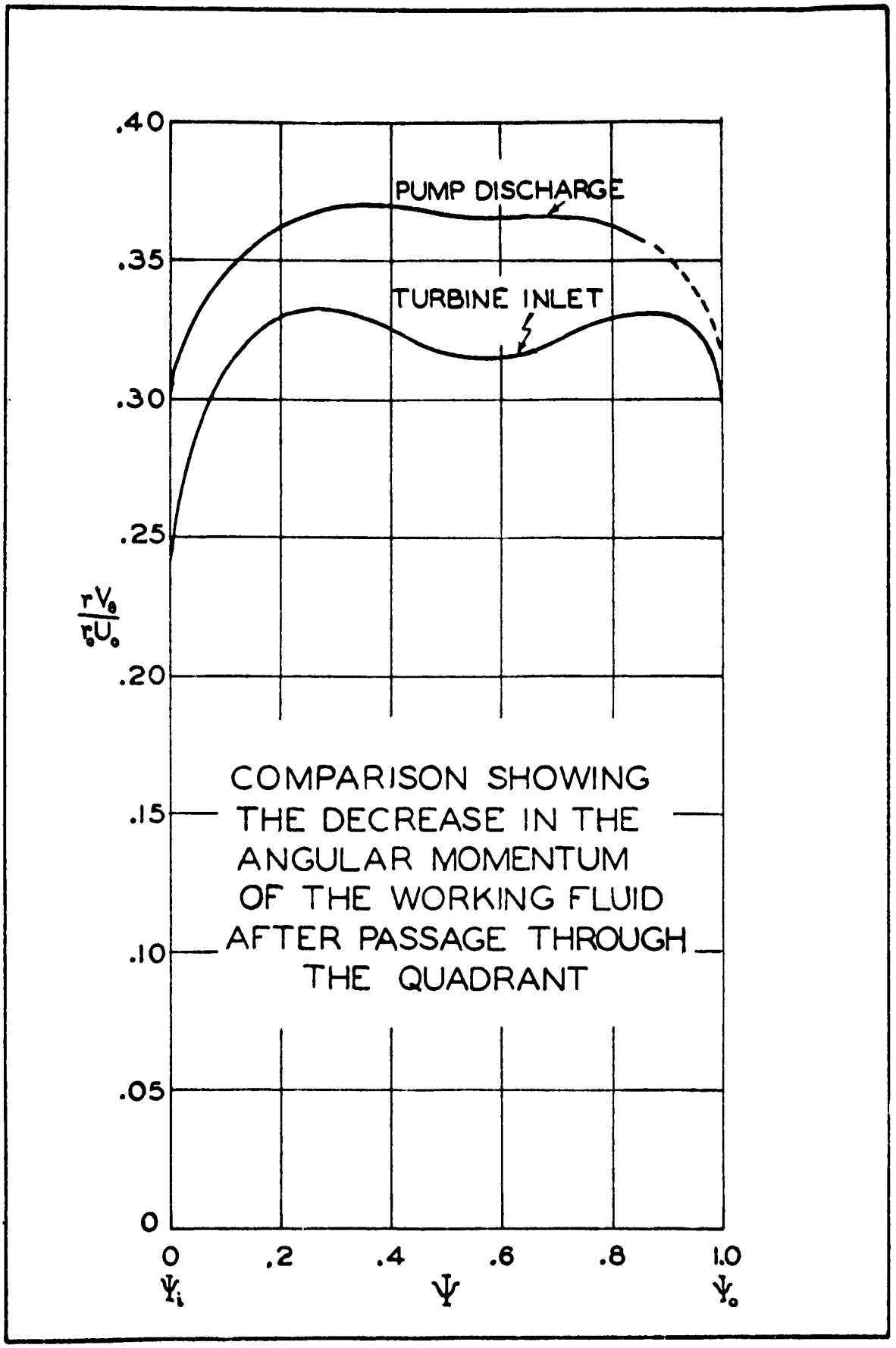
.40
.35
.30
.25
.20
.15
.10
.05
0
PUMP DISCHARGE
TURBINE INLET
$\frac{rV_\theta}{r_o U_o}$
COMPARISON SHOWING THE DECREASE IN THE ANGULAR MOMENTUM OF THE WORKING FLUID AFTER PASSAGE THROUGH THE QUADRANT
0
.2
.4
.6
.8
1.0
Ψ_i
Ψ
Ψ_o

FIGURE 20

Chapter II

A THEORETICAL ANALYSIS OF THE FLOW IN THE QUADRANT BETWEEN THE PRIMARY AND THE SECONDARY RUNNER VANE SYSTEMS

(1) INTRODUCTION

Theoretical work previously conducted in the Department of Mechanical Engineering at The Johns Hopkins University has evolved and demonstrated a means of predicting the complicated flow in a turbomachine, within the assumptions of an inviscid, incompressible fluid and rotational symmetry.(1)

Principally, this analysis will concern itself with providing a comparison between the real and the predicted flow fields. It is intended in making this comparison to accomplish the following: to ascertain the degree of agreement that is realized, between the actual flow and that predicted, by the assumptions and methods of solutions employed; and to point out which aspects of the real flow field, that are neglected by the solution, must be considered separately when employing such a solution. In addition, it is hoped to demonstrate a means by which information can be obtained to be used as a basis for solutions utilizing higher order approximations.

(2) THE THEORETICAL PROBLEM AND ITS SOLUTION

Given a curved space of revolution, with the entering flow and discharge conditions prescribed, compute the flow field throughout the system.

The analysis is conducted in two parts; and considers the system to be axially-symmetric, the working fluid to be incompressible and the motion to be steady. First, the fluid is assumed to be irrotational. Therefore, as the boundaries are completely specified the flow field can be determined. Second, the meridional streamlines obtained from the potential solution are then used as a basis for a higher order approximation to the real flow field.

---

(1) L. H Smith., S. C. Traugott., G. F. Wislicenus, "A Practical Solution of a Three-Dimensional Flow Problem of Axial-Flow Turbomachinery"., Trans: A. S. M. E., July 1953.

The second approximation considers a rotational fluid, but does not admit viscosity.

This solution is confined to that portion of the system extending from the discharge of the primary pump runner, section 6_A --- Figure 32 to the proposed turbine inlet, section 11. The flow entering the pump is for all practical purposes irrotational, excepting the immediate neighborhood of the walls. This is readily seen from the experimental total pressure distribution, Figure 15 -- Chapter 1.

In order to carry out the solution for a rotational fluid, the properties (velocity components, total pressures) of the fluid had to be specified at one section of the region analysed. To do this, the properties determined experimentally at the pump discharge were used. However, the traverse path at this section does not correspond to a normal to the meridional streamlines (in first approximation the potential streamlines); which is necessary to the solution. Therefore a normal (in first approximation) was assumed that coincided as closely as possible to the traverse path. The location of this normal with respect to the traversing path is shown in Figure 32. Then, the fluid properties along this normal section were calculated from those at the measured section. The meridional velocity distributions at the two sections were assumed to have the same shape; and the magnitudes of the meridional components at the normal section were chosen to satisfy continuity. The peripheral velocities at this new section Figure 33, were obtained by conservation of angular momentum. The total pressures were assumed to be the same for corresponding streamlines. The proximity of the two sections justifies these assumptions.

(3) REVIEW OF THE EQUATIONS TO BE EMPLOYED

The equation of motion for a homogeneous inviscid liquid and a conservative force field [2] is

$$\frac{d\vec{V}}{dt} = -\nabla\left(\frac{P}{\rho} + \Omega\right)$$ where Ω is the force potential.

Since $$\frac{d\vec{V}}{dt} = \frac{\partial\vec{V}}{\partial t} + (\vec{V}\cdot\nabla)\vec{V} = \frac{\partial\vec{V}}{\partial t} + \frac{\nabla V^2}{2} - \vec{V}\wedge(\nabla\wedge\vec{V})$$

then $$\frac{\partial\vec{V}}{\partial t} - \vec{V}\wedge\vec{\zeta} = -\nabla\left(\frac{P}{\rho} + \frac{V^2}{2} + \Omega\right)$$

and for steady motion $$\frac{\partial\vec{V}}{\partial t} = 0$$

---

[2] L. M. Milne-Thomson, "Theoretical Hydrodynamics", 2nd Edition, p. 74.

so

$$\vec{V}_\Lambda \vec{\zeta} = \nabla\left(\frac{P}{\rho} + \frac{V^2}{2} + \Omega\right) \qquad (1)$$

For the particular system to be analyzed, it is convenient to resolve the velocities and vorticities into their meridional (subscript M), normal (subscript n), and peripheral (subscript θ) components. Then,

$$\vec{\zeta} = \vec{i}_M \zeta_M + \vec{i}_n \zeta_n + \vec{i}_\theta \zeta_\theta$$

$$\vec{V} = \vec{i}_M V_M + \vec{i}_\theta V_\theta$$

and

$$\zeta_M = \frac{\partial V_\theta}{\partial n} + \frac{V_\theta}{r/\cos\Phi}$$

$$\zeta_\theta = -\left(\frac{\partial V_M}{\partial n} \pm \frac{V_M}{R_M}\right)$$

$$\zeta_n = 0$$

Where R_M represents the radii of curvature of the meridional streamlines.

The (+) sign applies when the forces due to the peripheral velocity and the meridional curvature act in the same direction. When they are opposed the (-) sign applies.

That $\zeta_n = 0$ can be shown by considering equation (1) where $\nabla\left(\frac{P}{\rho} + \frac{V^2}{2} + \Omega\right)$ must, by definition, be normal to the surfaces $\frac{P}{\rho} + \frac{V^2}{2} + \Omega = CONSTANT$ and as $\vec{V}$ and $\vec{\zeta}$ are both normal to $\vec{V}_\Lambda \vec{\zeta}$ and to $\nabla\left(\frac{P}{\rho} + \frac{V^2}{2} + \Omega\right)$, then the streamlines and vortex lines must lie in these stream surfaces, and $\zeta_n = 0$.

The equations used in carrying out the potential solution are

$$\frac{\partial V_M}{\partial n} \pm \frac{V_M}{R_M} = 0 \quad \text{as} \quad \vec{\zeta} = 0 \qquad (2)$$

and

$$V_\theta r = CONSTANT$$

Now if $\vec{\zeta} \neq 0$, and we consider points on two adjacent stream-surfaces, then as

$$\left|\nabla\left(\frac{P}{\rho} + \frac{V^2}{2} + \Omega\right)\right| = g\frac{\partial H}{\partial n}$$

$$\left|\vec{V}_\Lambda \vec{\zeta}\right| = g\frac{\partial H}{\partial n} \qquad (3)$$

Writing the equation of continuity between sections (1) and (2) see Figure 21

$$V_{M_1} \rho_1 r_1 dn_1 = V_{M_2} \rho_2 r_2 dn_2 \qquad (4)$$

and as $\Delta H_1 = \Delta H_2$ between the same two streamlines

then $(\vec{V}_1 \wedge \vec{S}_1) dn_1 = (\vec{V}_2 \wedge \vec{S}_2) dn_2$

or $$\frac{(\vec{V}_1 \wedge \vec{S}_1)}{\rho_1 r_1 V_{M_1}} = \frac{(\vec{V}_2 \wedge \vec{S}_2)}{\rho_2 r_2 V_{M_2}}$$

and as we are concerned with an incompressible fluid

$$\frac{(\vec{V}_1 \wedge \vec{S}_1)}{r_1 V_{M_1}} = \frac{(\vec{V}_2 \wedge \vec{S}_2)}{r_2 V_{M_2}} \qquad (5)$$

This is the basic equation employed in considering the flow with rotation. For ease of solution however a more convenient form of this equation can be derived. The derivation utilizes one additional bit of information. This results from the fact that the non-uniformity in energy addition, along the span of the primary pump vane system, is assumed to be only proportional to the variation in vane circulation across the span. Then as the energy of a fluid particle is constant, as it moves along a meridional stream-surface, the difference between the energy of particles on two such adjacent surfaces

FIGURE 22a

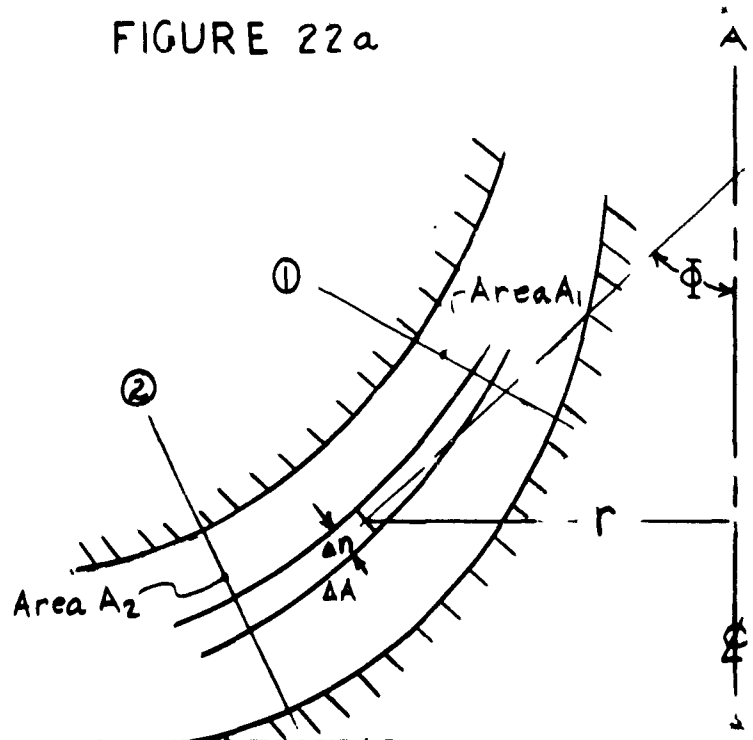

is proportional to the increment in circulation that exists between these stream-surfaces. Now

$$\Delta\Gamma = \int_C \vec{V}\cdot d\vec{S}$$

where the contour C refers to the boundary of a surface generated by rotating the line Δn (shown in Figure 21) through 360° about the axis A-A; where Δn is that portion of the normal terminating on the meridional section of the two adjacent stream-surfaces being considered. Then from Stokes' Theorem

$$\Delta\Gamma = \int_C \vec{V}\cdot d\vec{S} = \int_{\Delta A} (\nabla\times\vec{V})\cdot d\vec{A}$$

where ΔA is the surface generated by Δn, and $\vec{A}$ is an area vector normal to ΔA having that direction which is associated with Γ by the right hand screw rule.

Then

$$\Delta\Gamma = \int_{\Delta A} \vec{\zeta}\cdot d\vec{A}$$

For the present purpose $\Delta\Gamma = \zeta_M \Delta A$

and as $\Delta\Gamma_1 = \Delta\Gamma_2$ and $\Delta A = 2\pi r \Delta n$

then

$$\zeta_{M_1}\Delta A_1 = \zeta_{M_2}\Delta A_2$$

or

$$\zeta_{M_1} r_1 \Delta n_1 = \zeta_{M_2} r_2 \Delta n_2$$

Combining this with the equation of continuity

$$V_{M_1} r_1 \Delta n_1 = V_{M_2} r_2 \Delta n_2$$

the following relationship results

$$\zeta_{M_2} = \zeta_{M_1}\frac{V_{M_2}}{V_{M_1}} \qquad (6)$$

Now expanding equation (5) gives

$$\frac{V_{\theta_1}\zeta_{M_1} - V_{M_1}\zeta_{\theta_1}}{r_1 V_{M_1}} = \frac{V_{\theta_2}\zeta_{M_2} - V_{M_2}\zeta_{\theta_2}}{r_2 V_{M_2}}$$

and substituting into this, the following:

$$\zeta_{M_2} = \zeta_{M_1}\frac{V_{M_2}}{V_{M_1}}$$

results in the expression

$$\frac{V_{\theta_1}\zeta_{M_1} - V_{M_1}\zeta_{\theta_1}}{r_1} = \frac{V_{\theta_2}\zeta_{M_1} - V_{M_1}\zeta_{\theta_2}}{r_2}$$

Then solving this equation for ζ_{θ_2}

and employing the equation $V_{\theta_2} r_2 = V_{\theta_1} r_1$, we get:

$$\zeta_{\theta_2} = \left[\frac{r_1}{r_2} - \frac{r_2}{r_1}\right] \frac{V_{\theta_1}}{V_{M_1}} \zeta_{M_1} + \frac{r_2}{r_1} \zeta_{\theta_1}$$

which is the form used in calculating this solution.

(4) A DISCUSSION OF THE SOLUTIONS

The results of the potential solution to be presented in the following section were obtained from two approximations. The first approximation was based on the known curvatures of the bounding walls and the difference equation

$$\frac{\Delta V_M}{\Delta n} - \frac{V_M}{R_M} = 0 \quad \text{and} \quad V_\theta r = \text{constant.}$$

A velocity of unit magnitude was assumed at the outer boundary (Ψ_o) and from this a hyperbolic velocity distribution was constructed for the particular normal being considered. This hyperbolic distribution was modified near the opposite wall (Ψ_i) in keeping with the curvature of this wall. For example, if the (Ψ_o) boundary were curved and the (Ψ_i) boundary straight, then the velocity distribution, as the (Ψ_i) boundary is approached, would be made uniform. The magnitude of the velocities near (Ψ_i) were selected in such a manner that a smooth shape would be obtained for the velocity profile. This would seem to be a very inaccurate approach, but its accuracy is not important. The initial approximation is used as a time saver; in that it is a degree closer the final result than the assumption of a uniform velocity distribution. From this approximation new streamlines can be determined, and thereafter more reliable velocity distributions.

The results of the second approximation were judged to be sufficient for the present purposes; which are to supply information, upon which a solution for a rotational flow can be conducted. This essential information is the meridional streamline pattern. The change in the streamline spacing obtained between the first and second approximation to the potential solution was not sufficient to warrant a third approximation.

The potential velocity profiles presented in the results were based on the experimentally determined operating conditions. Each profile was adjusted so that the volume rate of flow be a constant, and equal to the operating flow rate found by experiment.

The solution of the rotational flow field was found from one approximation and based on the meridional streamlines obtained from the potential solution. Actually two approximations based on the same meridional streamlines were carried out at section 7, Figure 32. The streamlines corresponding to this first approximation are found to depart by a very small amount from those used to obtain them (potential streamlines), figure (22b) However, this is not the reason for attempting only one approximation to the rotational flow field.

The solution of the rotational flow at any normal section is begun by assuming the location on the normal of the mean velocity. The magnitude of this velocity can be assumed equal to that value defined by

$$\overline{V}_M = \frac{Q_{(section)}}{A}$$

where Q (section) has already been defined in Chapter 1, and A is the area of the normal section, figure (22a).

The location of this velocity on the normal is found by a series of successive iterations. The first iteration at section 7 was obtained by choosing this location as coincident with the (Ψ_i) streamline. This location was found to be too close to the outside casing wall (Ψ_o); when the results of this first approximation were evaluated. Therefore, a second approximation was evaluated for this same section by assuming the location of the mean to be the same as that just calculated in the first iteration. Let the streamline passing through this point be called ($\overline{\Psi}$). The mean velocity calculated for this second iteration was found to be less than 1% higher. Then, the location of the mean velocities for the other sections calculated was assumed to coincide with the intersection of the ($\overline{\Psi}$) streamline and the normal for the particular section being considered.

This assumption of the location of $\overline{V}_M$ for each normal section on the ($\overline{\Psi}$) streamline gave very good results, at section 8 the assumed mean velocity and its location agreed with the calculated values. The agreement at section 9 was also excellent; the assumed mean velocity was less than 1% higher than the calculated value. At section 11, the calculated velocity was only 1.3% higher than the assumed value.

5. THE RESULTS OF THE ANALYSIS

The Potential Solution.

The results of this solution are presented in the four illustrations, Figures 22, 23, 24 and 25. Figure 22 shows the derived meridional velocity distributions and meridional streamlines in relationship to the flow passage. Figure 23 shows the changes in velocity that a fluid particle undergoes as it moves along a meridional stream-surface. This graph was obtained by laying off points along the abscissa to represent the distances of the 10 equipotentials from the number one equipotential, these distances being measured along the Ψ_2 streamline. Then, an ordinate was constructed at each of these points on the abscissa; and the magnitudes of the meridional velocities, at the intersections of the streamlines and equipotential lines, were laid off along their respective ordinates. Figure 24 gives a comparison of the velocity profiles at section 5 that were found from experiment and from the potential solution. The fifth figure compares the static pressured distributions along the casing walls of the quadrant that are computed from the potential solution and from the solution with rotational flow with that determined by experiment. In order to obtain this potential flow static pressure distribution, the following procedure was used. As the flow is irrotational the constant in Bernoulli's Equation is fixed by the operating conditions as determined by experiment; that is, by the mean total energy measured at the pump discharge. The absolute velocity in this same equation can be evaluated for any point in the fluid stream. The meridional velocities are known; and the peripheral velocities can be calculated for any point from the mean runner head rise and conservation of angular momentum.

The Rotational Solution.

The results of the solution for a rotational flow (see Figures 26, 27, 28, 29 and 30) are presented as graphs showing the variation in the meridional velocities, given in dimensionless form V_M/U_o, as a function of position along the normal for the particular section. On these same graphs the meridional velocities derived from the potential solution are shown. The experimental velocities for the two sections 6A and 11 are also given for comparison.*

Two additional illustrations complete the presentation of results. One, Figure 30, is a composite graph of the meridional velocity profiles plotted against the variable Ψ, the stream function. The second, Figure 31, shows the relationship of these velocity profiles to the flow passage; and a comparison of the meridional streamlines obtained from the solution of the rotational flow with those of the potential flow.

*The experimental results in section 6A shown in Figures 26 and 33 determine the vorticity assumed for this solution.

The static pressure distributions along the quadrant walls, Figure 25, for a rotational flow were found by considering the energy of fluid particles along a streamline to be a constant. Then, employing Bernoulli's Equation and the equation rV_θ = constant, the static pressures were computed as the velocity field is known. The total energy, the Bernoulli Constant, was evaluated from the total energy of the fluid at section 6_A. However, the inaccuracy in choice of total pressures at the boundaries, resulting from fairing the total pressure distributions in these regions, gave a considerable difference between the experimental static pressures and those being calculated. This discrepancy was reduced, and a much more probable result obtained, by adjusting the calculated distribution. The adjustment was made by shifting the calculated static pressure distributions for each boundary; so that, at the values of $\frac{\eta}{\eta_i}$ and $\frac{\sigma_\theta}{\sigma_0}$ corresponding to the wall static pressures taps located nearest the blade center line ($\frac{\eta}{\eta_i} = \frac{\sigma_\theta}{\sigma_0} = 0$), the values of the static pressures, measured and calculated, are equal.

6. CONCLUSIONS

From the comparison of the measured and calculated peripheral velocity components (rotational flow) at section 11, Figure 33, it is seen that in the central portion of this section, the measured peripheral velocity distribution is concave. The magnitudes of these velocities, predicted by conservation of the angular momentum of the fluid particles at section 6, have a constant value in the same region. The neglect of viscosity in the solution accounts for the difference. The possibility of secondary motions tending to establish equilibrium is excluded from the results of the solution by the assumption of an inviscid fluid. The effect is small and does not detract from the usefulness of the solution.

The solution of the rotational flow field gives results that are satisfactory if the application of these results allows the boundary layers to be either disregarded or corrected for. Such an application would be the design of the proposed turbine stage, where the magnitudes of the predicted velocities could be increased to compensate for the boundary layer growth. The manner in which this increase or correction is estimated is outside the scope of this analysis.

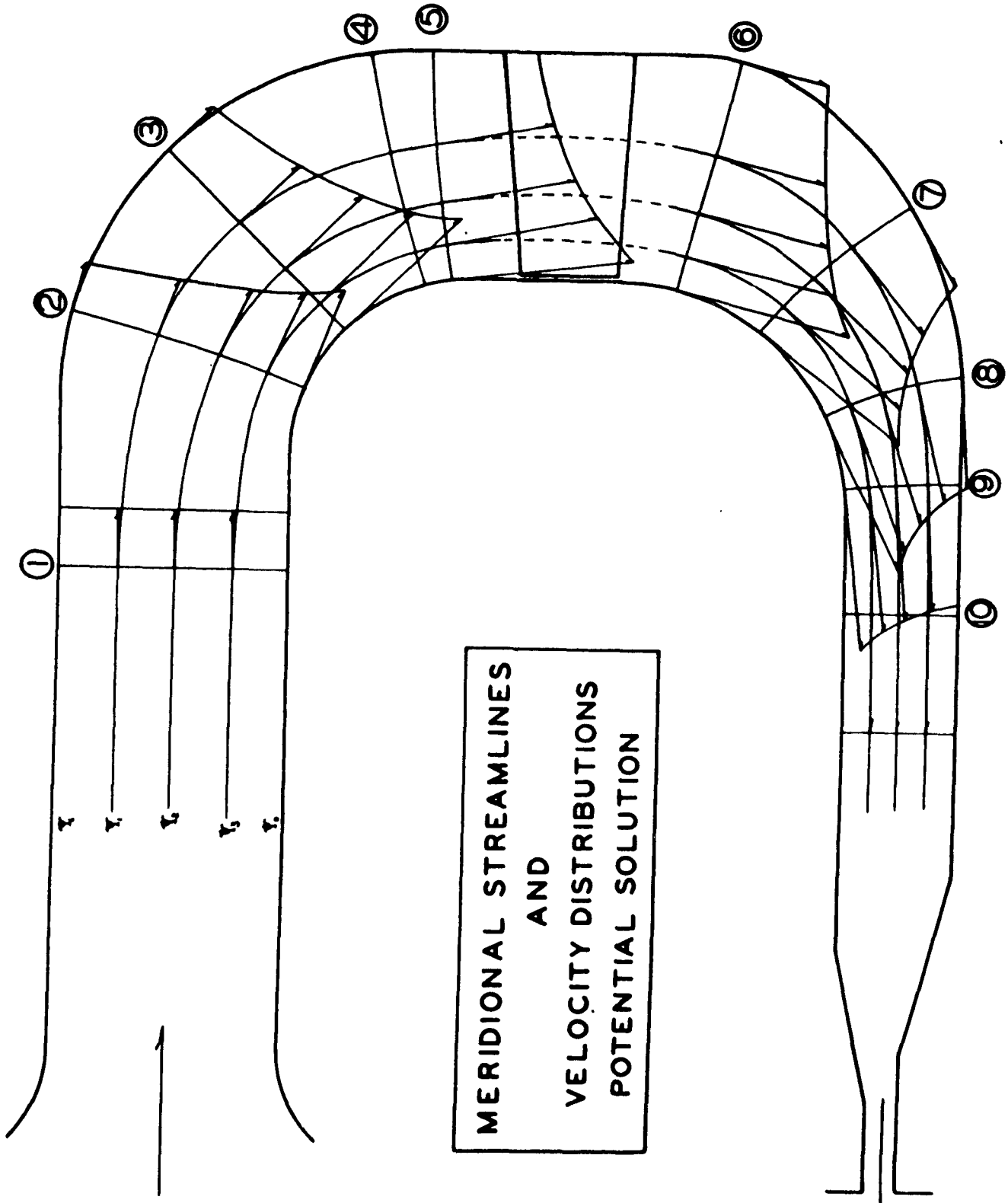
MERIDIONAL STREAMLINES
AND
VELOCITY DISTRIBUTIONS
POTENTIAL SOLUTION

FIGURE 22b

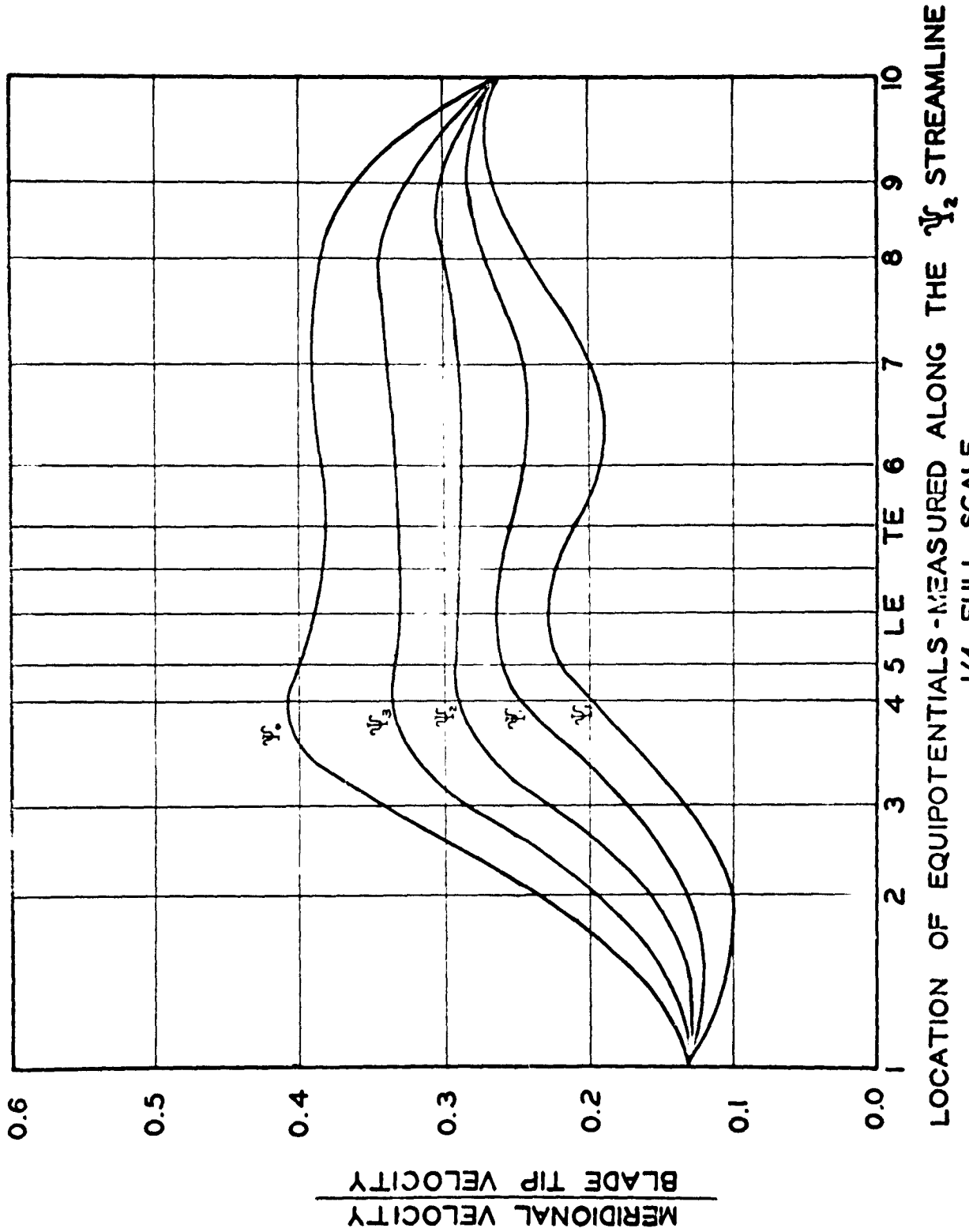
MERIDIONAL VELOCITY / BLADE TIP VELOCITY
0.6
0.5
0.4
0.3
0.2
0.1
0.0
1
2
3
4
5 LE
TE 6
7
8
9
10
LOCATION OF EQUIPOTENTIALS - MEASURED ALONG THE Ψ2 STREAMLINE
1/4 FULL SCALE
Ψ1
Ψ2
Ψ3
Ψ4
Ψ5

FIGURE 23

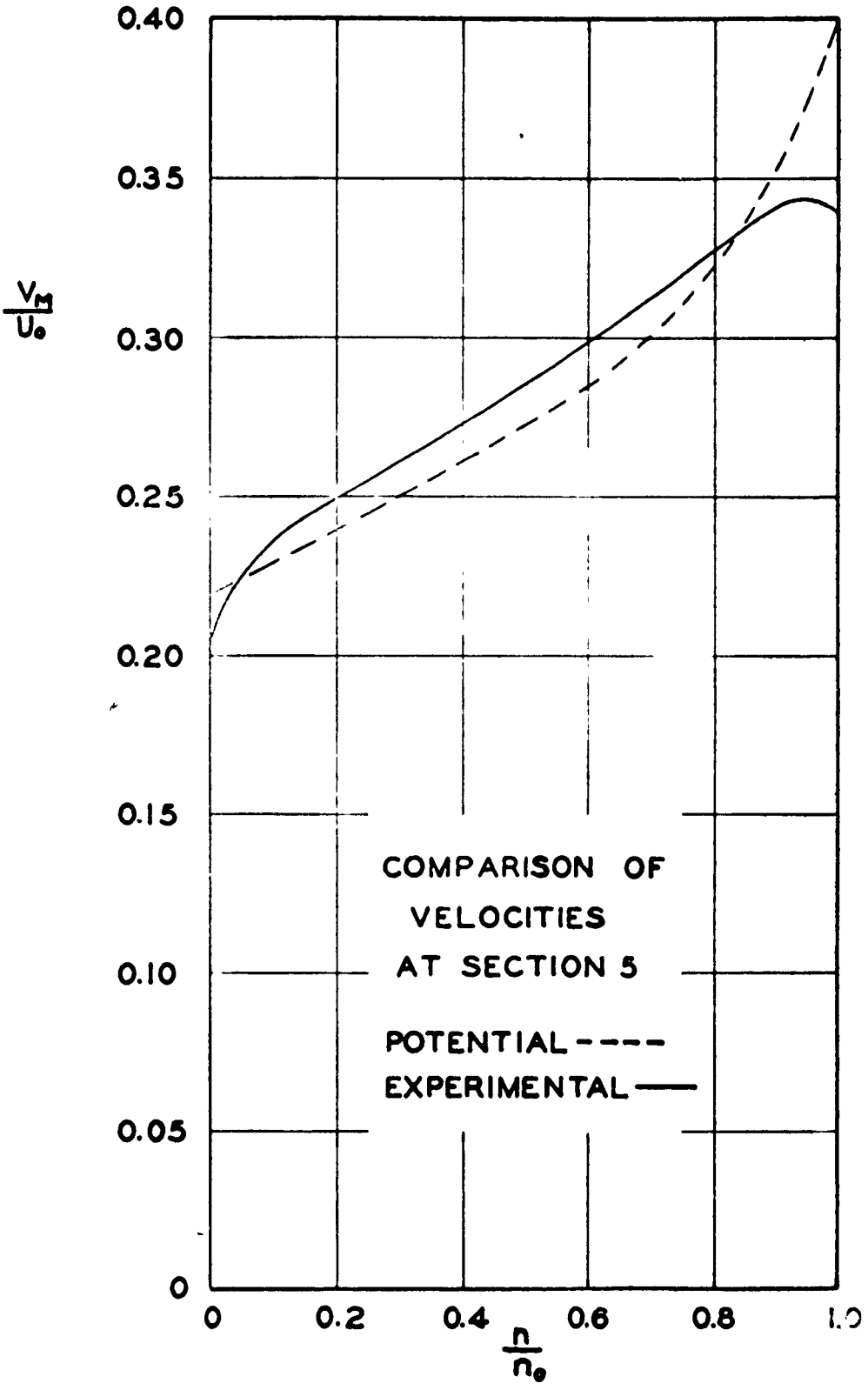
0.40
0.35
0.30
0.25
0.20
0.15
0.10
0.05
0
$\frac{V_M}{U_0}$
0
0.2
0.4
0.6
0.8
1.0
$\frac{n}{n_0}$
COMPARISON OF
VELOCITIES
AT SECTION 5
POTENTIAL - - - -
EXPERIMENTAL ——

FIGURE 24

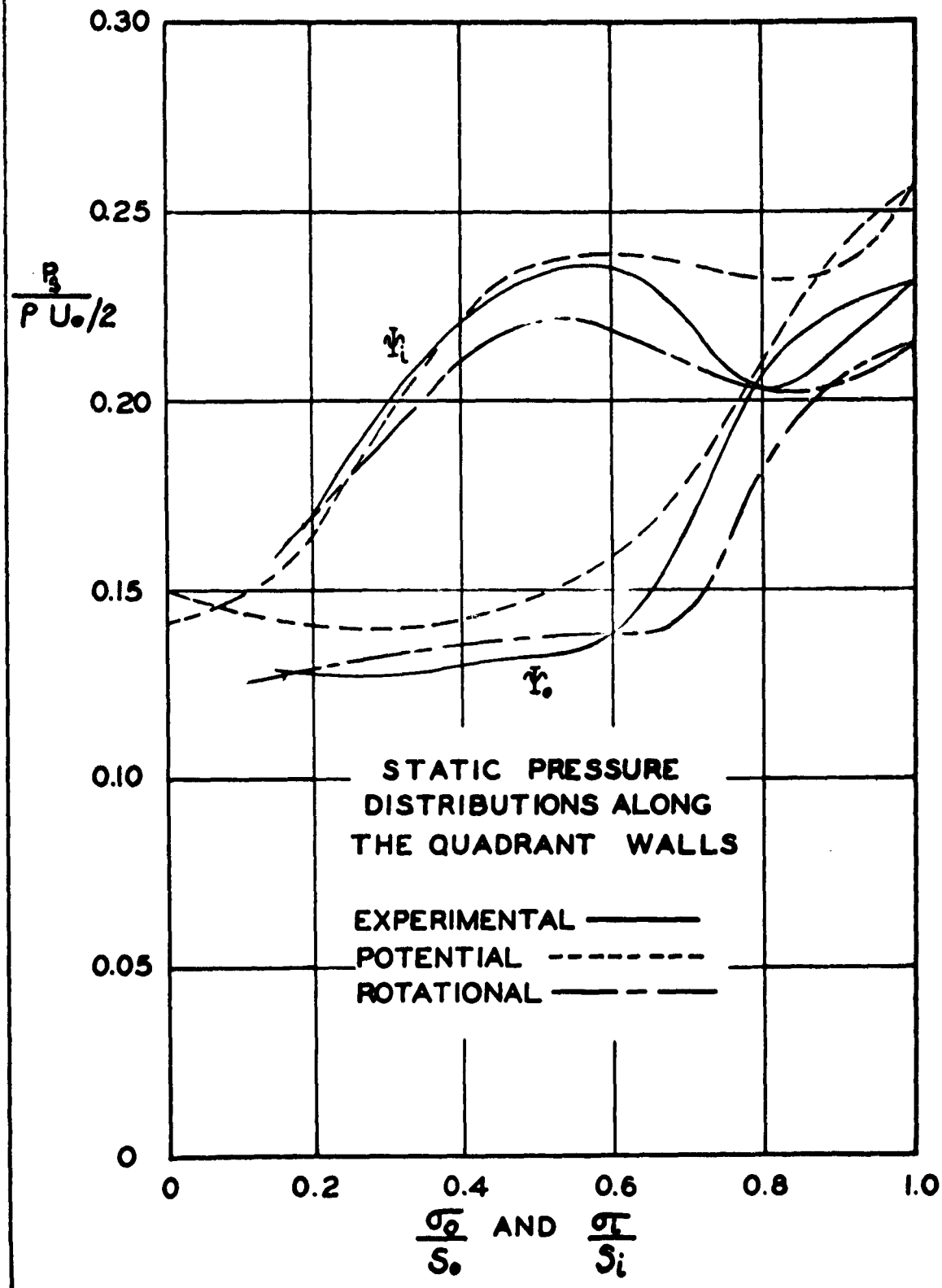
0.30
0.25
0.20
0.15
0.10
0.05
0
$\frac{P_3}{P U_0/2}$
Ψ_i
Ψ_0
STATIC PRESSURE
DISTRIBUTIONS ALONG
THE QUADRANT WALLS
EXPERIMENTAL
POTENTIAL
ROTATIONAL
0
0.2
0.4
0.6
0.8
1.0
$\frac{\sigma_0}{S_0}$ AND $\frac{\sigma_i}{S_i}$

FIGURE 25

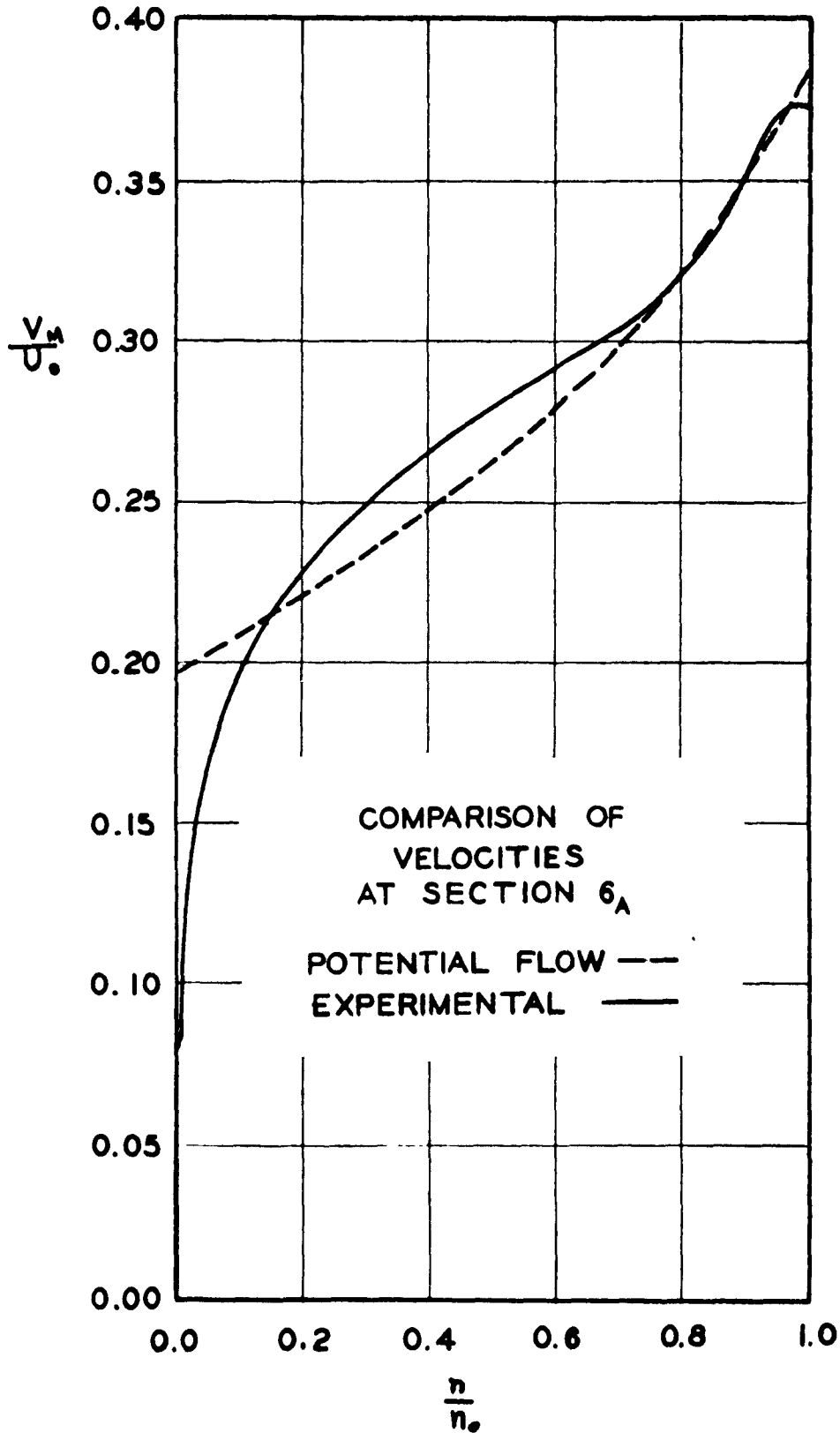
0.40
0.35
0.30
0.25
0.20
0.15
0.10
0.05
0.00
$\frac{V_M}{U_\infty}$
COMPARISON OF
VELOCITIES
AT SECTION 6_A
POTENTIAL FLOW
EXPERIMENTAL
0.0
0.2
0.4
0.6
0.8
1.0
$\frac{n}{n_\infty}$

FIGURE 26

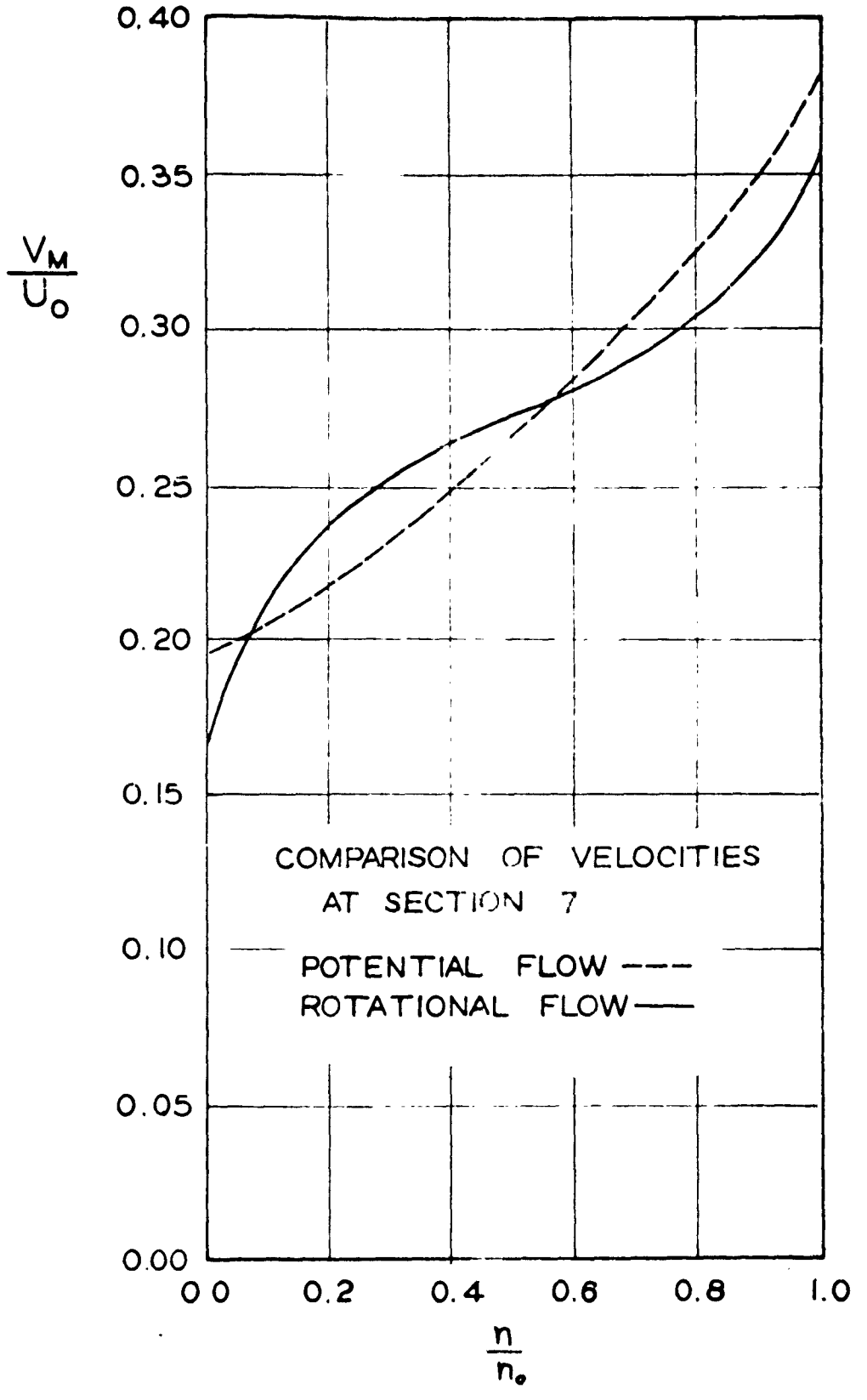
0.40
0.35
0.30
0.25
0.20
0.15
0.10
0.05
0.00
$\frac{V_M}{U_o}$
0 0
0.2
0.4
0.6
0.8
1.0
$\frac{n}{n_o}$
COMPARISON OF VELOCITIES
AT SECTION 7
POTENTIAL FLOW ---
ROTATIONAL FLOW ——

FIGURE 27

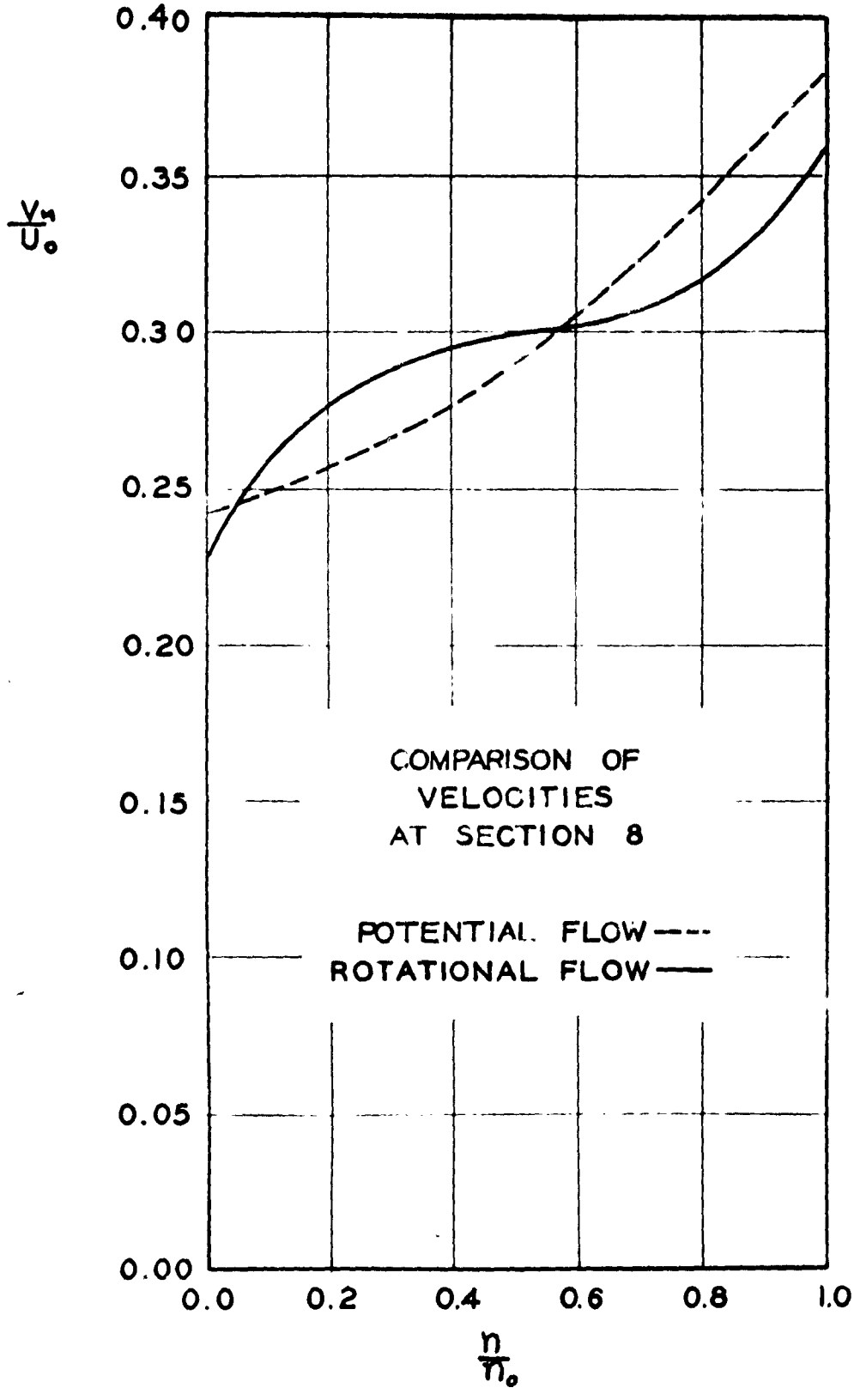
0.40
0.35
0.30
0.25
0.20
0.15
0.10
0.05
0.00
$\frac{V_n}{U_o}$
COMPARISON OF
VELOCITIES
AT SECTION 8
POTENTIAL FLOW ---
ROTATIONAL FLOW ——
0.0
0.2
0.4
0.6
0.8
1.0
$\frac{n}{n_o}$

FIGURE 28

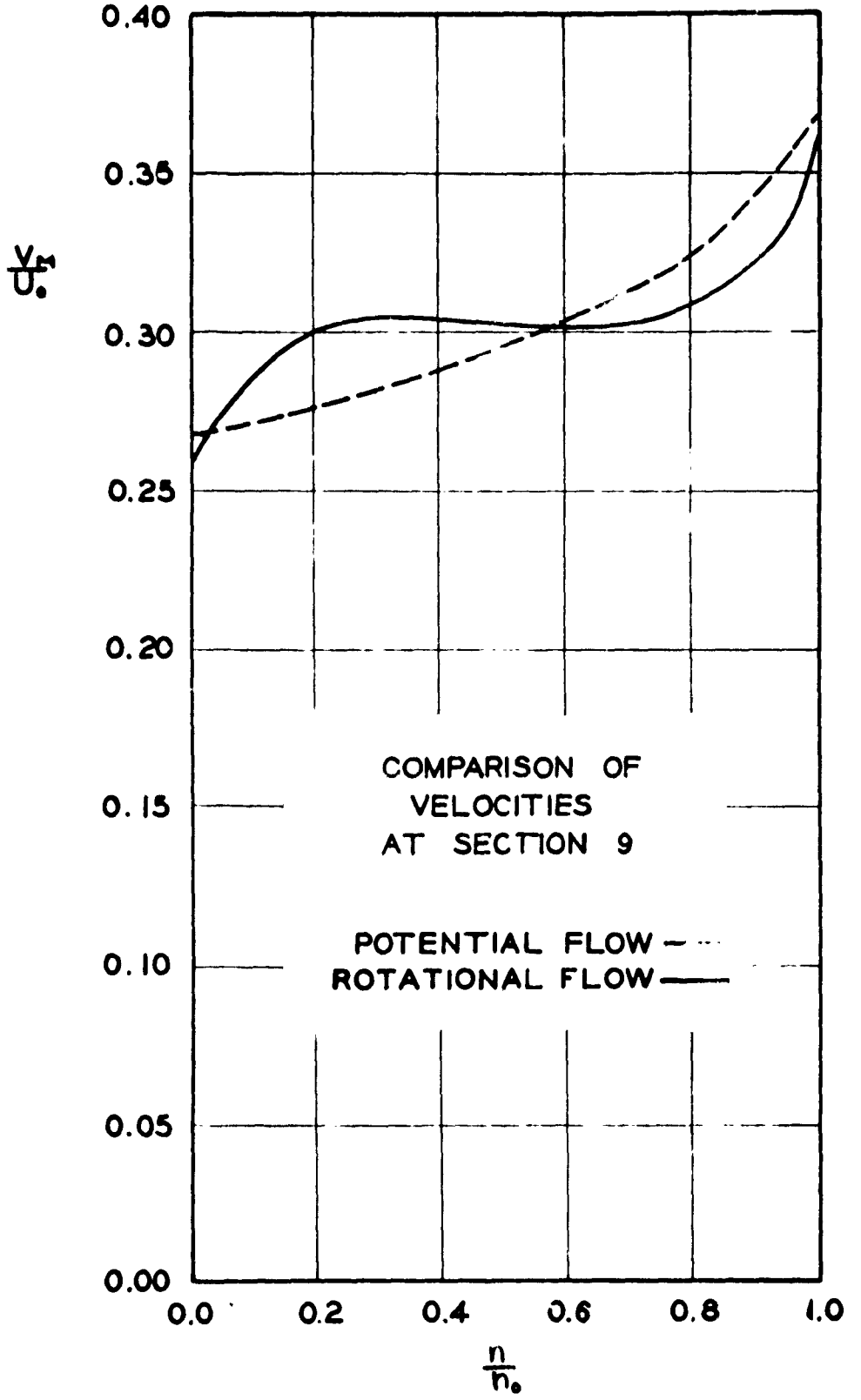
0.40
0.35
0.30
0.25
0.20
0.15
0.10
0.05
0.00
$\frac{V_r}{U_\infty}$
COMPARISON OF
VELOCITIES
AT SECTION 9
POTENTIAL FLOW
ROTATIONAL FLOW
0.0
0.2
0.4
0.6
0.8
1.0
$\frac{n}{n_\infty}$

FIGURE 29

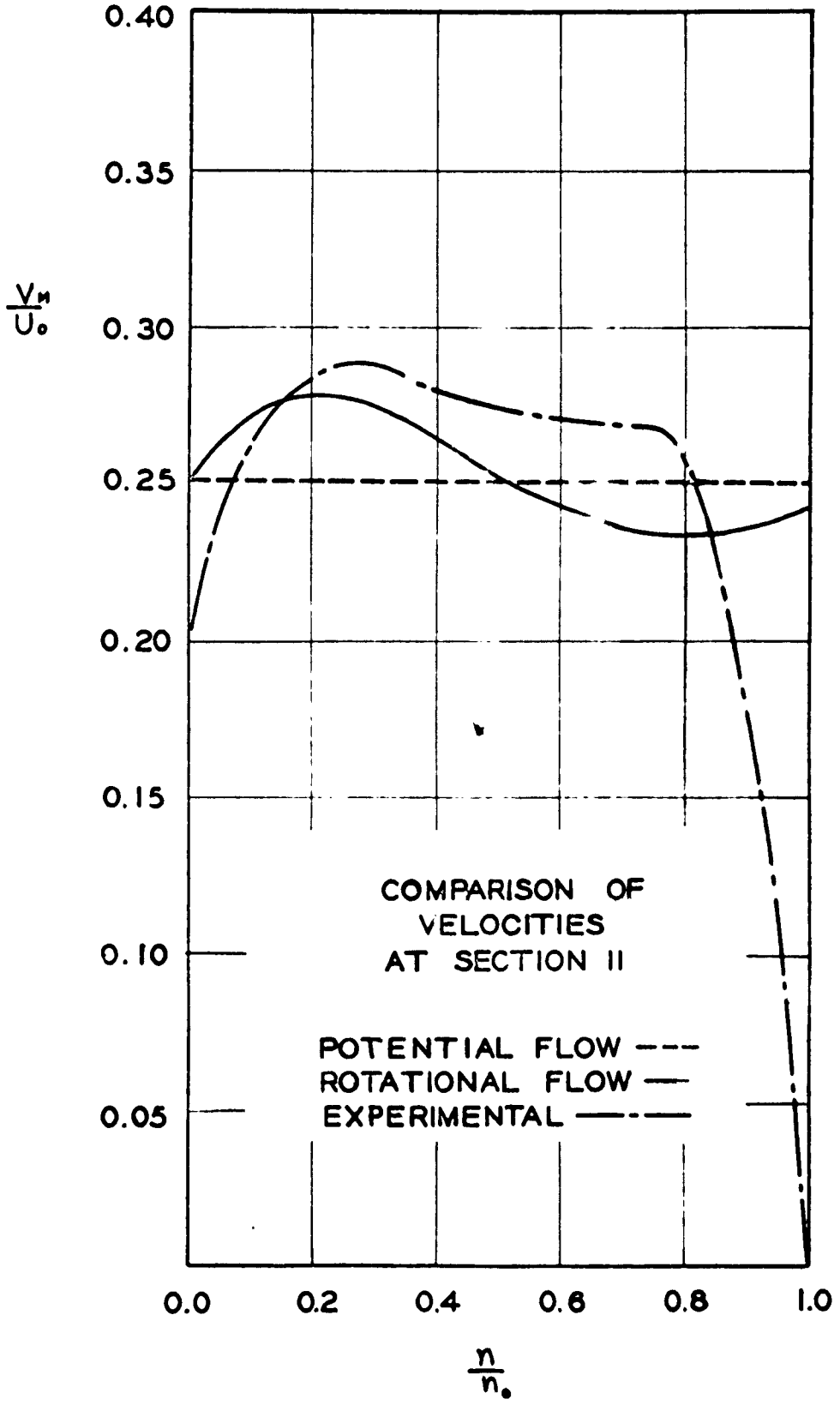
0.40
0.35
$\frac{V_M}{U_o}$
0.30
0.25
0.20
0.15
0.10
0.05
COMPARISON OF
VELOCITIES
AT SECTION II
POTENTIAL FLOW ---
ROTATIONAL FLOW —
EXPERIMENTAL —·—
0.0
0.2
0.4
0.6
0.8
1.0
$\frac{n}{n_o}$

FIGURE 30

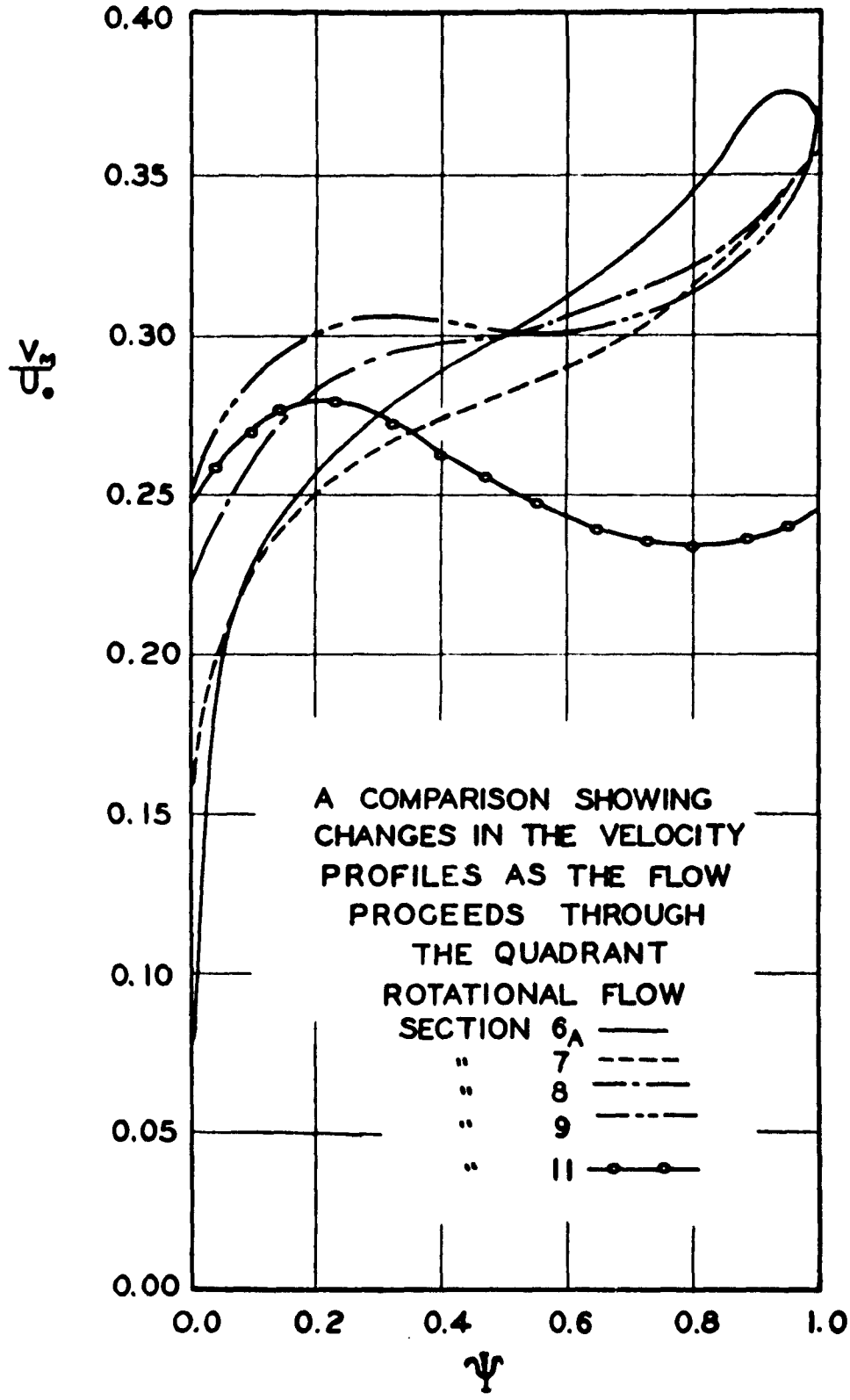
0.40
0.35
0.30
0.25
0.20
0.15
0.10
0.05
0.00
$\frac{V_m}{U_\infty}$
0.0
0.2
0.4
0.6
0.8
1.0
Ψ
A COMPARISON SHOWING CHANGES IN THE VELOCITY PROFILES AS THE FLOW PROCEEDS THROUGH THE QUADRANT ROTATIONAL FLOW
SECTION 6_A
" 7
" 8
" 9
" 11

FIGURE 31

MERIDIONAL STREAMLINES AND VELOCITY DISTRIBUTIONS FOR A ROTATIONAL FLOW

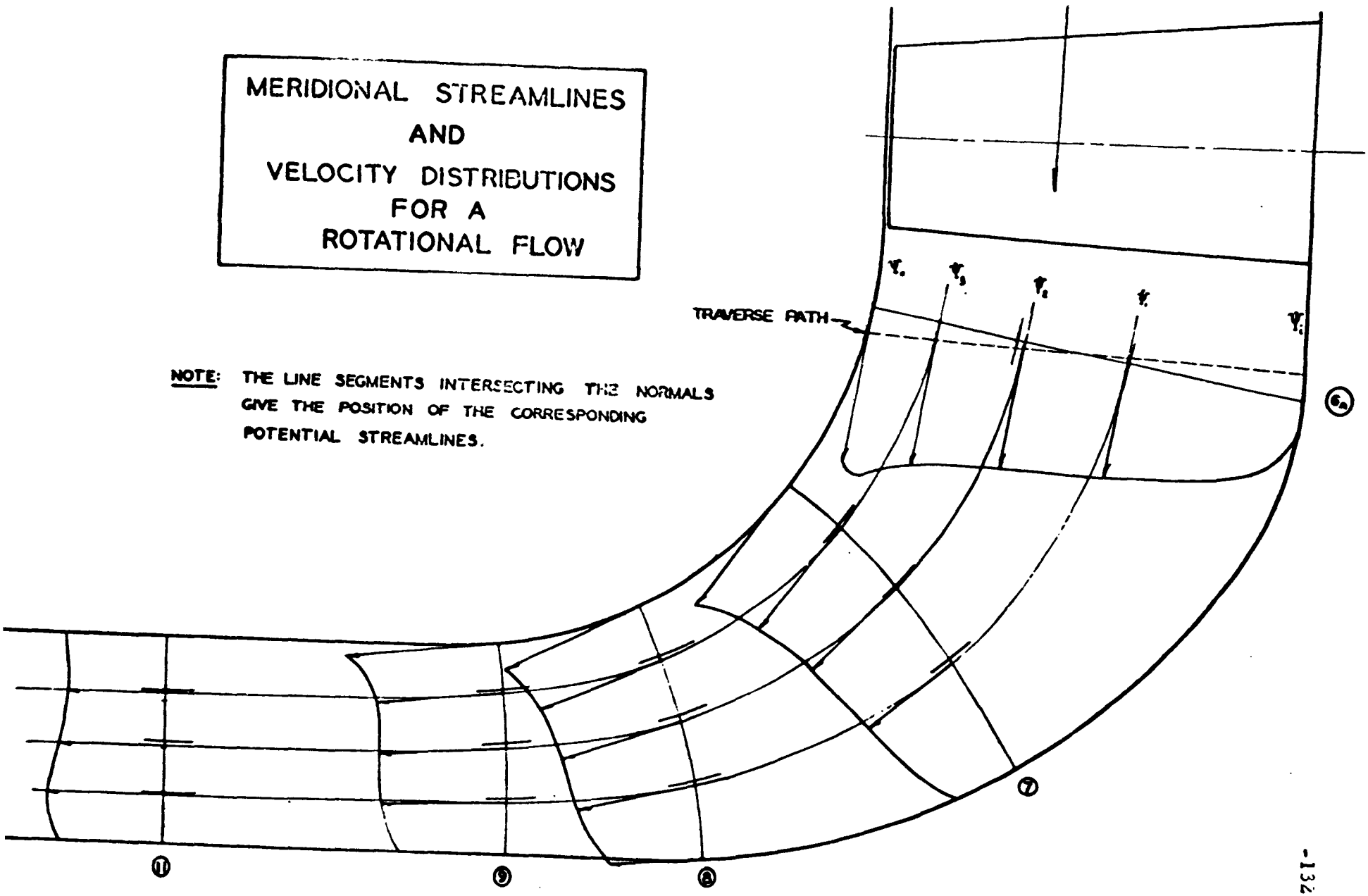

NOTE: THE LINE SEGMENTS INTERSECTING THE NORMALS GIVE THE POSITION OF THE CORRESPONDING POTENTIAL STREAMLINES.

FIGURE 32

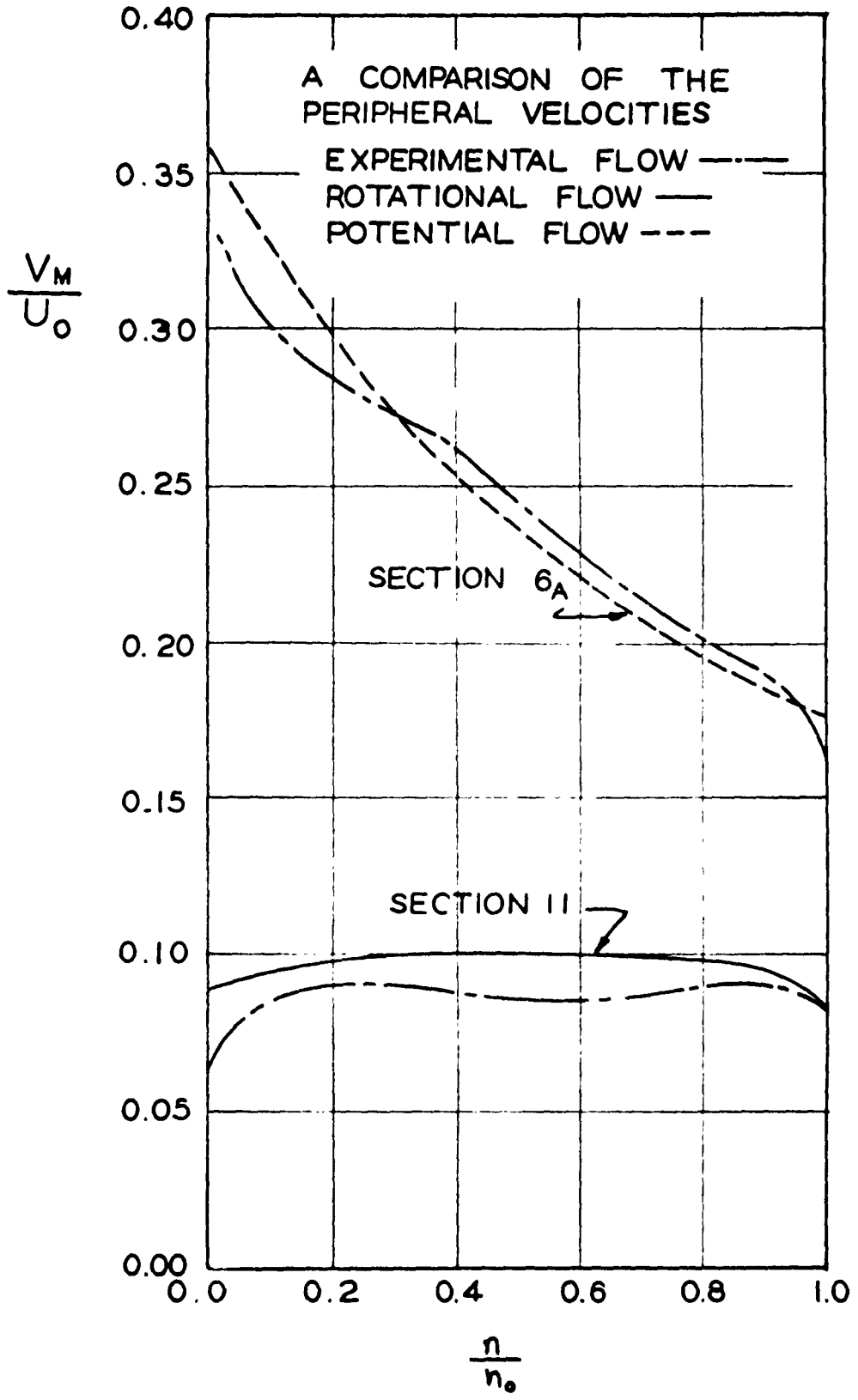
A COMPARISON OF THE
PERIPHERAL VELOCITIES
EXPERIMENTAL FLOW
ROTATIONAL FLOW
POTENTIAL FLOW
SECTION 6A
SECTION 11
0.40
0.35
0.30
0.25
0.20
0.15
0.10
0.05
0.00
0.0
0.2
0.4
0.6
0.8
1.0
VM/U0
n/n0

FIGURE 33

APPENDIX I

Analysis of the Effect of Some Predictable Velocity Fluctuations at the Discharge of the Primary Runner

Presented here is an evaluation concerning the magnitudes of the effects of non-uniformities, in the velocity distribution relative to the vane system, on the values of angular momentum and kinetic energy of the peripheral motion calculated using mean values of V_M and V_θ .

Notation:

$V_A = V_A(\tau)$ the axial velocity components

$V_\theta = V_\theta(\tau)$ the peripheral velocity components

$W = W(\tau)$ the relative velocity components

U_o equals the tip velocity of the blade.

Where t is the time $q_w(t)$ is a periodic function of the time with a maximum value of unity.

In the dimensionless form, let

$$q_A = \frac{V_A}{U_o}$$

$$q_\theta = \frac{V_\theta}{U_o}$$

$$q_W = \frac{W}{U_o}$$

$$q_{W_1} = \frac{W_1}{U_o} = 1$$

$$\tau = \frac{t}{T}$$

where T is the period of the relative velocity fluctuations. $0 \leq \tau \leq 1$
Also define the quantitites

$$\phi_o = \frac{\overline{V_A}}{U} = \overline{q_A} \quad , \qquad \psi_r = 2\frac{r}{r_o}\frac{\overline{V_\theta}}{U_\theta} = 2\frac{r}{r_o}\overline{q_\theta}$$

Note: The bar over a quantity is used to represent a time average of that quantity.

This analysis is not concerned with the stream properties as functions of the radius (r). The results of the analysis will be correlated to the experimental test operating conditions by the mean values (averaged along the radius) of the operating values of ϕ_o and ψ_r. An additional assumption is made that the direction of the relative velocities is a constant.

Consider the following relative velocity distribution and the corresponding vector diagram, in which vectors marked with subscript 1 denote design velocities.

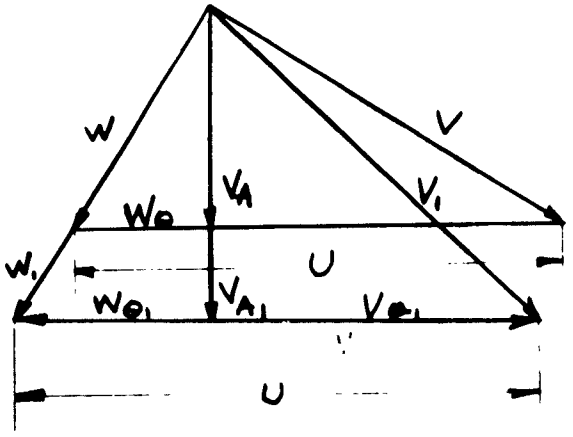

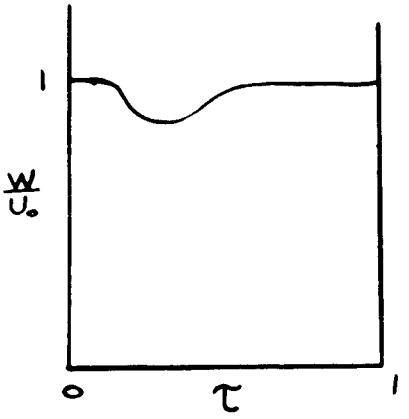

Let the ratio of the integrated product of axial and tangential velocities to the product of the averages of these velocities be denoted as K_M

$$K_M = \frac{\int_0^1 q_A q_\theta \, d\tau}{\overline{q}_A \overline{q}_\theta} \qquad (1)$$

The fluctuating velocities can be expressed in terms of the design velocities and the fluctuating relative velocity as follows:

$$q_\theta = \frac{U}{U_o} - \left[\frac{U}{U_o} - q_{\theta_1}\right] q_W$$

$$q_A = q_{A_1} q_W$$

The time averages become

$$\bar{q}_\theta = {}_0\int^1 q_\theta(\tau)\,d\tau$$

$$\bar{q}_A = {}_0\int^1 q_A(\tau)\,d\tau$$

Now define the following quantity

$$K_M = \frac{1}{\bar{q}_A \bar{q}_\theta} {}_0\int^1 q_A q_\theta \, d\tau \qquad (1)$$

Assuming that V_A and W_θ fluctuate proportionally to w, it follows from the vector diagram that

$$q_\theta = \frac{U}{U_0} - \left[\frac{U}{U_0} - q_{\theta_1}\right] q_w$$

$$q_A = q_{A_1} q_w$$

Also

$$\bar{q}_\theta = {}_0\int^1 q_\theta(\tau)\,d\tau$$

$$\bar{q}_A = {}_0\int^1 q_A(\tau)\,d\tau$$

Then by substituting these four relationships into equation (1), the following results

$$K_M = \frac{{}_0\int^1 q_{A_1} q_w \left[\frac{U}{U_0} - \left(\frac{U}{U_0} - q_{\theta_1}\right) q_w\right] d\tau}{q_{A_1}\left[\frac{U}{U_0} - \left(\frac{U}{U_0} - q_{\theta_1}\right) {}_0\int^1 q_w\,d\tau\right] {}_0\int^1 q_w\,d\tau}$$

or

$$K_M = \frac{1 - \left(1 - q_{\theta_1}\frac{U_0}{U}\right) \frac{{}_0\int^1 q_w^2\,d\tau}{{}_0\int^1 q_w\,d\tau}}{1 - \left(1 - q_{\theta_1}\frac{U_0}{U}\right) \int_0^1 q_w\,d\tau}$$

as

$$\psi_r = 2\frac{r}{r_0}\bar{q}_\theta = 2\frac{r}{r_0} {}_0\int^1 \left[\frac{U}{U_0} - \left(\frac{U}{U_0} - q_{\theta_1}\right) q_w\right] d\tau$$

it can be shown that

$$\psi_r = 2\left(\frac{r}{r_o}\right)^2 \left\{1 - \left[1 - q_{o_1}\frac{U_o}{U}\right]\int_0^1 q_w \, d\tau\right\}$$

or that

$$K_M = \frac{1 + \dfrac{\frac{\psi_r}{2}\left(\frac{r_o}{r}\right)^2 - 1}{\left[\int_0^1 q_w \, d\tau\right]^2}\int_0^1 q_w^2 \, d\tau}{\frac{1}{2}\left(\frac{r_o}{r}\right)^2 \psi_r} \qquad (2)$$

Now define the quantity

$$K_E = \frac{1}{\bar{q}_A (\bar{q}_o)^2}\int_0^1 q_A (q_o)^2 \, d\tau \qquad (3)$$

and by the same substitutions as in the case of K_M the following equation results

$$K_E = \frac{1 + 2\left[\frac{\psi_r}{2}\left(\frac{r_o}{r}\right)^2 - 1\right]\frac{\int_0^1 q_w^2 \, d\tau}{\left[\int_0^1 q_w \, d\tau\right]^2} + \left[\frac{\psi_r}{2}\left(\frac{r_o}{r}\right)^2 - 1\right]^2 \frac{\int_0^1 q_w^3 \, d\tau}{\left[\int_0^1 q_w \, d\tau\right]^3}}{\left(\frac{\psi_r}{2}\right)^2\left(\frac{r_o}{r}\right)^4}$$

or by letting $h = \frac{\psi_r}{2}\left(\frac{r_o}{r}\right)^2$ and $\alpha = \int_0^1 q_w \, d\tau$ then

$$K_E = \frac{K_M}{\eta} + \frac{\eta - 1}{\eta^2}\frac{\int_0^1 q_w^2 \, d\tau}{\alpha^2} - \frac{(\eta - 1)^2}{\eta^2}\frac{\int_0^1 q_w^3 \, d\tau}{\alpha} \qquad (4)$$

and

$$K_M = \frac{1}{\eta} + \frac{\eta - 1}{\eta}\frac{\int_0^1 q_w^2 \, d\tau}{\alpha^2} \qquad (5)$$

For the operating conditions tested and $\frac{r_o}{r} = \frac{4}{3}$ then $\eta = 0.32$

Now assuming the following relative velocity distribution, a step function

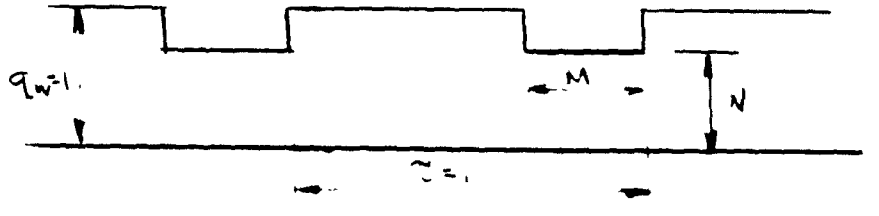

then

$$q_w(\tau) = 1 \quad \text{FOR} \quad 0 \le \tau \le 1 - M$$

$$q_w(\tau) = N \quad \text{FOR} \quad -M \le \tau \le 1$$

therefore

$$\alpha = \int_0^1 q_w(\tau) \, d\tau = (1)(1 - M) + \ldots$$

$$\alpha = 1 - (1 - N)M$$

M can be eliminated as

$$M = \frac{\alpha - 1}{N - 1}$$

and

$$\int_0^1 q_w^2 \, d\tau = 1 + (N+1)(\alpha - 1)$$

$$\int_0^1 q_w^3 \, d\tau = 1 + (N^3 - 1) M = 1 + \frac{(N^3 - 1)}{(N-1)}(\alpha - 1)$$

Then by substitution into equations (4) and (5)

$$K_M = \frac{1}{\eta} + \frac{\eta - 1}{\eta}\left[\frac{1 + (N+1)(\alpha - 1)}{\alpha^2}\right] \qquad (6)$$

$$K_E = \frac{2K_M}{\eta} - \frac{1}{\eta^2} + \left(\frac{\eta - 1}{\eta}\right)^2\left[\frac{1 + \frac{(N^3 - 1)}{(N-1)}(\alpha - 1)}{\alpha^3}\right] \qquad (7)$$

Therefore, with the two variables α and N describing the relative velocity pattern and the value of η given, we can determine the K factors as a function of α with N as a parameter.

The results of this evaluation are shown in the figures (34) and (35).

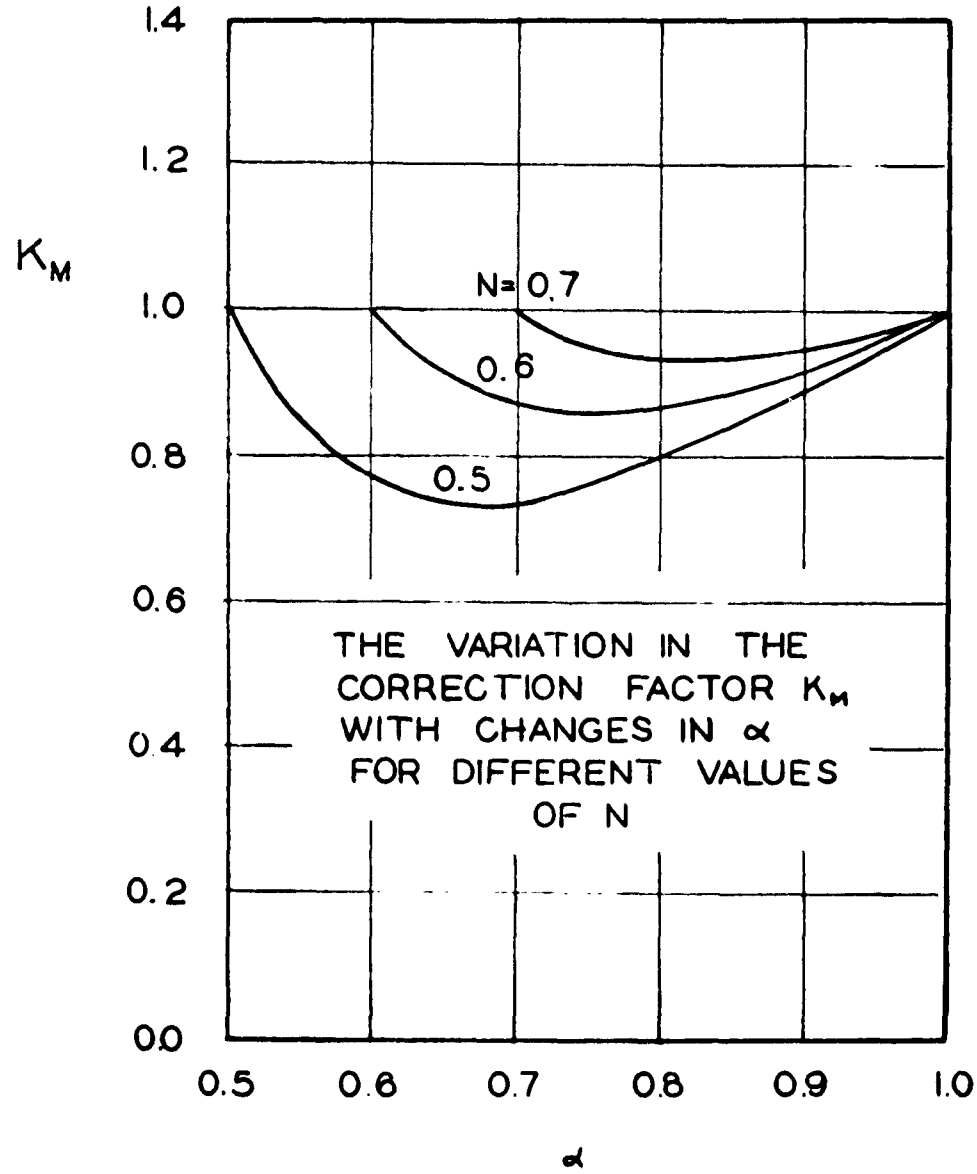

THE VARIATION IN THE CORRECTION FACTOR K_M WITH CHANGES IN α FOR DIFFERENT VALUES OF N

FIGURE 34

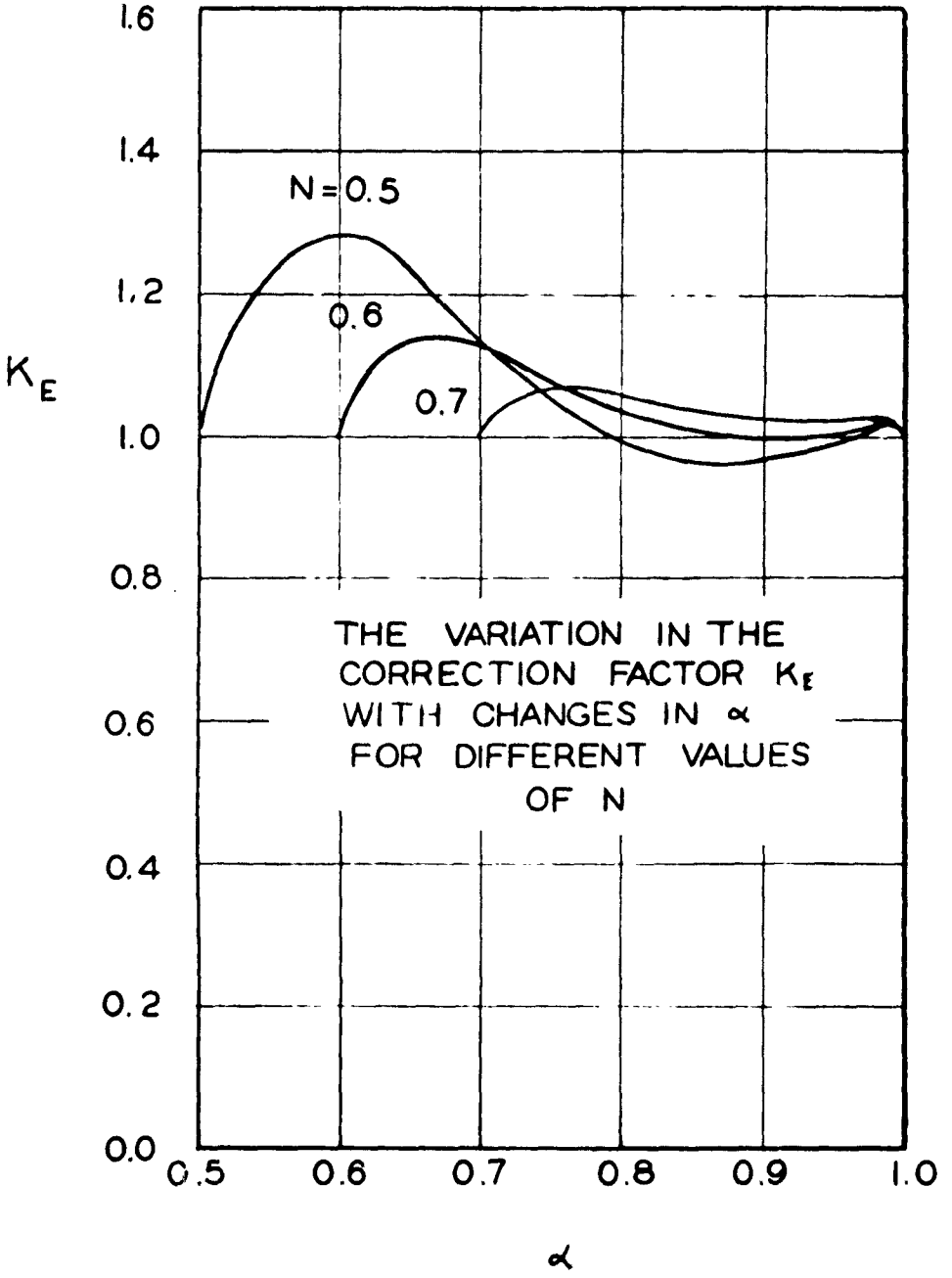

THE VARIATION IN THE CORRECTION FACTOR K_E WITH CHANGES IN α FOR DIFFERENT VALUES OF N

FIGURE 35

NOMENCLATURE

U	Blade Velocity (ft/sec)
V	Total Velocity (ft/sec)
A	Area (ft^2)
Q	Volume Rate of Flow (cfs)
r	Radial Distance from Center Line (ft)
n	Distance Measured Along Normal to the Meridional Streamlines (ft)
n	Channel Width Measured Along Normal to the Meridional Streamlines (ft)
P	Pressure (lb/ft^2)
HP	Horsepower
T	Period of a Cycle (sec)
g	Gravitational Acceleration (ft/sec^2)
H	Total Pressure Head (ft-lb/lb)
R	Radius of Curvature (ft)
t	Time (sec)
Ψ	Streamfunction $\Psi = \frac{\rho \int^n dQ}{Q_{TOTAL}}$
ψ	Pressure Rise Coefficient $\psi = \frac{2gH}{U^2}$
η	Efficiency
ρ	Mass Density of the Working Fluid
ϕ	Through Flow Coefficient $\phi = \frac{\rho \int^n dQ}{A \times U} = \frac{\bar{V}_m}{U}$

τ Dimensionless Time Variable = $\frac{t}{T}$

ζ Vorticity (ft/sec^2)

Φ Angle of Inclination to the Center Line Tangent to a Meridional Streamline

Subscripts

o Refers to Tip of Pump Blade

m Meridional Component

n Normal Component

θ Peripheral Component

T Total Pressure

S Static Pressure

A Axial Velocity Component

r Radial Velocity Component

DISTRIBUTION LIST FOR FINAL REPORT

Contract Nonr-248(32)

		Copies
Office of Naval Research Navy Department Washington 25, D. C.	Code 466 Code 429 Code 438	10 1 1
Chief, Bureau of Ships Navy Department Washington 25, D. C.	Code 300 Code 327 (Library) Code 371 Code 430 Code 503B Code 515 Code 541	1 2 1 1 1 1 1
Office of Naval Research Contract Administrator Southeastern Area 2110 G Street, N. W. Washington 7, D. C.		1
Officer-in-Charge Office of Naval Research Navy #100 Fleet Post Office New York, New York		1
Office of Naval Research Branch Office Tenth Floor The John Crerar Library Building 86 East Randolph Street Chicago 1, Illinois		1
Office of Naval Research Branch Office 346 Broadway New York 13, New York		1
Office of Naval Research Branch Office 1030 E. Green Street Pasadena 1, California		1
Office of Naval Research Branch Office 1000 Geary Street San Francisco 9, California		1

	Copies
Office of Naval Research Branch Office 150 Causeway Street Boston, Massachusetts	1
Commanding Officer and Director U. S. Naval Boiler and Turbine Laboratory Naval Base Philadelphia, Pennsylvania	1
Commanding Officer and Director David Taylor Model Basin Washington 7, D. C.	1
Director Naval Research Laboratory Washington, D. C. Attn: Technical Information Officer	1
Commanding Officer and Director U. S. Naval Engineering Experiment Station Annapolis, Maryland	1
Commanding General Air Research and Development Command P. O. Box 1395 Baltimore 3, Maryland Attn: RDRRF	1
Gibbs and Cox, Inc. 21 West Street New York, New York Attn: Mr. B. O. Smith VIA: Supervisor of Shipbuilding USN and Naval Inspector of Ordnance New York Shipbuilding Corp. Camden, New Jersey	1
General Dynamics Corporation Electric Boat Division Groton, Connecticut VIA: Supervisor of Shipbuilding USN and Naval Inspector of Ordnance General Dynamics Corp. Electric Boat Division Groton, Connecticut	1

	Copies
Engineering Research Institute University of Michigan Ann Arbor, Michigan Attn: Dr. Paul H. Geiger	1
VIA: Office of Naval Research Branch Office Tenth Floor The John Crerar Library Building 86 East Randolph Street Chicago 1, Illinois	